

CHEMISTRY OF COMET ATMOSPHERES

N. Biver

LESIA, Observatoire de Paris, PSL Research University, CNRS, Sorbonne Université, Université de Paris, Meudon, France

N. Dello Russo

Johns Hopkins University Applied Physics Laboratory, Laurel, MD 20723, USA

C. Opitom

Institute for Astronomy, University of Edinburgh, Royal Observatory, Edinburgh, EH9 3HJ, UK

M. Rubin

Physics Institute, Space Research and Planetary Sciences, University of Bern, Bern, Switzerland

The composition of cometary ices provides key information on the thermal and chemical properties of the outer parts of the protoplanetary disk where they formed 4.6 Gy ago. This chapter reviews our knowledge of composition of cometary comae based on remote spectroscopy and in-situ investigations techniques. Cometary comae can be dominated by water vapour, CO or CO₂. The abundances of several dozen of molecules, with a growing number of complex organics, have been measured in comets. Many species that are not directly sublimating from the nucleus ices have also been observed and traced out into the coma in order to determine their production mechanisms. Chemical diversity in the comet population and compositional heterogeneity of the coma are discussed. With the completion of the Rosetta mission, isotopic ratios, which hold additional clues on the origin of cometary material, have been measured in several species. Finally, important pending questions (e.g., the nitrogen deficiency in comets) and the need for further work in certain critical areas are discussed in order to answer questions and resolve discrepancies between techniques.

1. INTRODUCTION

We discuss the current knowledge of the composition of comets as derived from observations of molecular species in their comae. These species either sublimate directly into the coma from the nucleus ices (parent molecules) or they are secondary products. These secondary products can arrive in the coma from either the dissociation of a parent molecule or as a distributed source contained in released ice and dust. We review the investigative techniques which have made considerable progress in determining the composition of cometary comae over the last two decades including remote spectroscopic observation (from UV to Radio wavelengths) and in-situ mass spectrometry (*Giotto* and *Rosetta* missions). The measured column density (remote observation) or local density (mass spectrometry) of the given molecule characterizes the local state of the cometary coma at a given time. Observational techniques with a range of spatial coverage and resolution provide information on how molecules are distributed in the coma. The basic assumption of steady state continuous production of gas or dust from the nucleus is generally used to retrieve the molecular production rates Q_{molec} . We discuss the molecules that dominate the gas flow of the nucleus and drive cometary activity. We then present our current knowledge of all molecules that have been detected in the coma and their abundances relative to

other volatiles, most often water (Q_{molec}/Q_{H_2O}), and the source of possible discrepancies between various measurements. Composition can vary significantly from one comet to another, and we review this variability and link it to possible comet origins. Spatial, short, and long term monitoring of comets, especially as undertaken by the *Rosetta* mission to comet 67P/Churyumov-Gerasimenko (hereafter 67P), have also shown that the composition of the coma can vary both locally and with time or heliocentric distance. Isotopic abundances also provide important insights into the origin of cometary matter. Several key isotopic measurements, such as the D-to-H and ¹⁴N/¹⁵N ratios, which are fundamental to understanding the delivery of cometary material to planets are presented here. We conclude with needs and perspectives that should improve our current understanding of comet composition.

1.1. Radio spectroscopy of rotational lines

Radio spectroscopy is a powerful technique to probe the composition of cometary atmospheres. All asymmetric molecules have a dipole moment and can be observed in the millimeter to the submillimeter domain via their rotational lines. At the temperature of coma gas (typically 5 - 200 K), most molecules have their peak rotational emission in the 80–800 GHz frequency domain, probed by ground-

and space-based radio telescopes. In addition, the excitation process is mostly spontaneous emission due to radiative decay of the low energy rotational levels and can be efficient up to large heliocentric distances, such as in the case of CO detected in at least three comets (C/1995 O1 (Hale-Bopp), 29P, and C/2016 R2 (PanSTARRS)) beyond 5 au from the Sun. Of the ~ 30 molecular species detected by remote spectroscopy in comets, 80% have been detected in the radio (Bockelée-Morvan *et al.* 2004; Biver *et al.* 2015). Radio spectroscopy of comets has the additional unique capability of resolving the line Doppler velocity profile due to its very high spectral resolution ($\nu/\delta\nu = 10^6$ to 10^8). Cometary lines are typically 1–4 km s⁻¹ wide due to Doppler broadening (see example in Fig. 1) and resolving the line enables measurement of the gas expansion velocity, asymmetry in outgassing, and characterization of opacity effects, such as in comet 67P with *Rosetta*/MIRO (Biver *et al.* 2019).

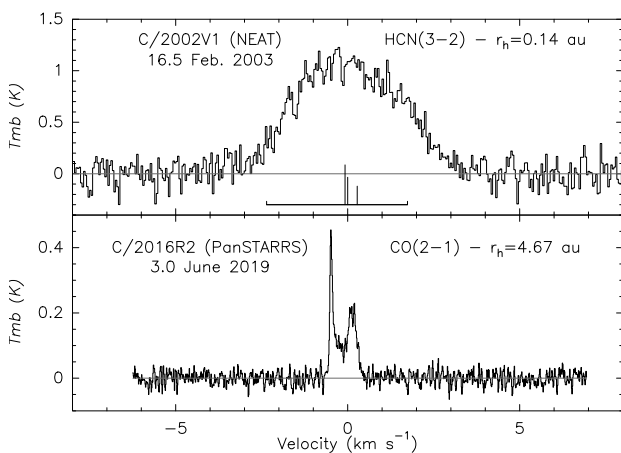


Fig. 1.— Cometary lines observed at 1 mm wavelength at high spectral resolution (10–40 kHz). The horizontal axis is the Doppler velocity relative to the comet reference frame. The vertical axis is the line intensity in unit of K in the main beam antenna temperature scale. The top spectrum is the HCN(3–2) line at 265886.434 MHz showing a broad line width due to the large expansion velocity (2.0 km s⁻¹) at a very small heliocentric distance (r_h), (Biver *et al.* 2011). The positions and intensities of the hyperfine components are indicated below the line. The bottom spectrum is the CO(2–1) line at 230538.000 MHz showing a narrow line in comet C/2016 R2 far from the Sun. It also exhibits a very narrow blue-shifted component (Full width at half maximum = 0.08 km s⁻¹) indicative of a very cold (~ 3 K) sunward jet.

1.1.1. Wide band high resolution spectroscopy

Since the advent of millimeter and submillimeter astronomy in the late 1980’s there has been steady progress in receiver and spectrometer performance. For the last ten years, new wide band receivers (typically 4 to 16 GHz instantaneous bandwidth) have equipped many facilities such as IRAM (i.e., EMIR, Carter *et al.* 2012), NOEMA or ALMA.

High spectral resolution ($\nu/\delta\nu > 10^6$) is also necessary to resolve cometary lines in spectra, and benefit from the full sensitivity of the receiver. This has become possible with the most recent correlators or Fourier Transform Spectrometers (FTS) (Klein *et al.* 2012) which can offer a spectral resolution better than 200 kHz over several GHz of bandwidth. An example of the combined (instantaneous) frequency coverage (2×8 GHz) and high resolution (200 kHz) spectrum of comet 46P is shown in Fig. 2 (Biver *et al.* 2021a).

1.1.2. Using a large number of lines to detect molecules

Another advantage of the wide frequency coverage of radio receivers and spectrometers is the ability to detect more complex molecules, which have line emission spectra that encompass a large number of lines with similar intensities. The number of lines increases rapidly with molecular complexity; for example, in the 210–270 GHz domain, CO has one line, H₂CO three lines, and CH₃CHO 64 lines, with intensities comparable within a factor three. Averaging many lines of similar expected intensity (weighted according to their S/N) for a given species increases its detectability; for example, the ability to average 100 lines of similar strength (and S/N) improves detection sensitivity by a factor of ten over a single line. This method has been applied recently in the detection of complex organics in comets even when individual lines are too weak by themselves to be seen in spectra (e.g., Biver *et al.* 2015). This technique is also applied to infrared echelle spectra that sample many ro-vibrational transitions of a given molecule (Paganini *et al.* 2017). The high spectral resolution of radio spectroscopy and the relatively narrow width of cometary lines also limits confusion between lines of different molecules.

1.2. Infrared spectroscopy of vibrational bands

Many parent molecules have strong vibrational bands in the near-infrared (IR) in the 2 – 5 μ m spectral region. Because there are several windows of high atmospheric transmittance in the near-IR, ground-based observations have been the primary driver of molecular identifications in this spectral region in comets. Since many species have IR vibrational bands in overlapping spectral regions, high spectral resolving power ($\lambda/\delta\lambda > 10^4$) is needed to detect ro-vibrational lines within vibrational bands (Fig. 3). Even relatively simple molecules can have complex ro-vibrational spectra creating a “forest” of lines with multiple contributing species, making high-resolution necessary in order to disentangle these highly diagnostic emissions in IR spectra (Fig. 3).

The IR spectral region provides the only means to detect certain species. For example, symmetric hydrocarbons (e.g., CH₄, C₂H₆, C₂H₄, and C₂H₂) can only be investigated in comets with remote sensing techniques at IR wavelengths. This is also the case for CO₂, one of the main cometary volatiles that under many circumstances drives activity, but can only be directly detected from space-based

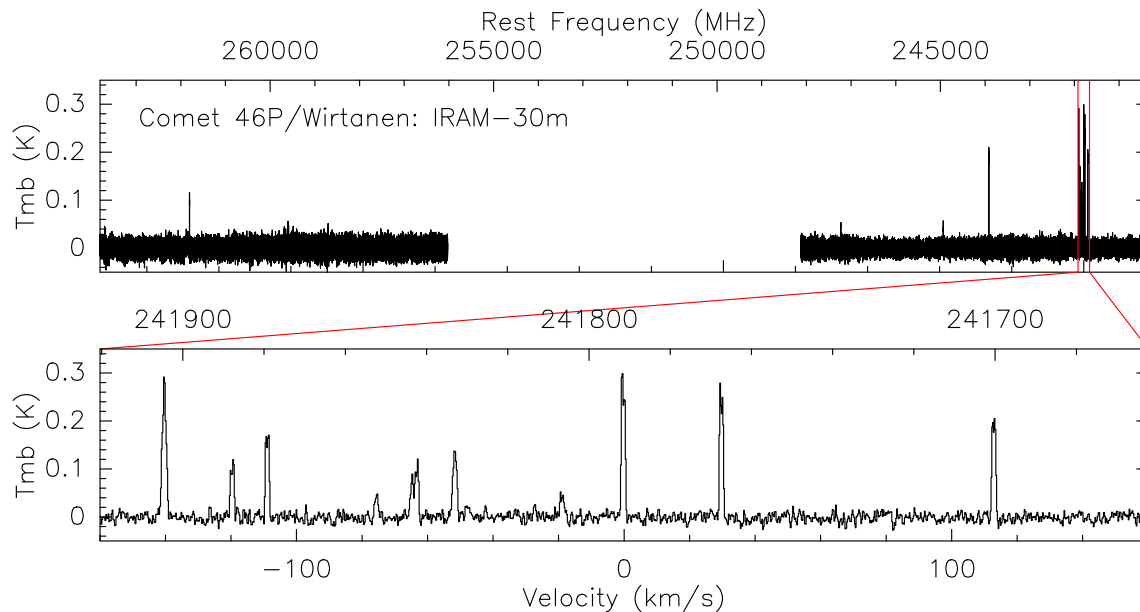


Fig. 2.— Spectrum of comet 46P/Wirtanen observed in December 2018 with the IRAM EMIR230 receiver coupled to the FTS spectrometer. With such a setup 2×8 GHz, on each vertical and horizontal polarization (averaged here), is instantaneously covered, with a 200 kHz resolution (zoom on one series of methanol lines at 242 GHz which are resolved).

platforms. Additionally, IR wavelengths provide the most efficient and straightforward method of studying H_2O , the most abundant volatile in comets, through multiple non-resonance fluorescence emissions from ground-based observatories or through its strong fundamental vibrational bands from space. Other molecules typically sampled at IR wavelengths (HCN , CH_3OH , H_2CO , NH_3 , CO , and OCS) can also be detected at radio wavelengths (and in the case of CO both radio and UV wavelengths), providing additional independent methods for studying these volatiles in comets.

1.2.1. Factors that affect detectability of molecules

Derived volatile production rates are determined by temperature-dependent fluorescence efficiencies (g-factors) for individual ro-vibrational emissions for the given species. Over the years IR fluorescence models have been developed and improved for all molecules that have been detected in comets as well as additional molecules with potentially detectable IR bands (e.g., Villanueva *et al.* 2018). The temperature-dependent strengths and positions of ro-vibrational emissions for H_2O , OH , CO , OCS , CH_4 , C_2H_6 , C_2H_2 , CH_3OH , H_2CO , HCN , NH_3 , and NH_2 are well enough understood to enable spectral blends to be interpreted and corrected for and production rates to be accurately determined with uniform methodology.

Many additional more complex molecules have strong IR bands that are theoretically detectable even at their lower abundances with the sensitivities of modern ground-based high-resolution IR spectrometers, but are in practice largely inaccessible. The reasons for this are related to spectral complexity, which increases fast for larger molecules. First, many parameters needed for developing accurate fluores-

cence models are unavailable for these complex molecules. Second, spectral confusion from many lines of simpler but more abundant molecules makes definitive identification of more complex but less abundant molecules very difficult. For example, spectral complexity in the $3.35 \mu\text{m}$ region of comets even at high spectral resolution is dominated by multiple dense emissions of primarily C_2H_6 and CH_3OH (Fig. 3), which interferes with the detection of more complex hydrocarbons (e.g., C_3H_8 , C_4H_{10}). The spectral complexity near $3.0 \mu\text{m}$ is dominated by the presence of many simple molecules (e.g., H_2O , OH , NH_3 , NH_2 , HCN , C_2H_2), which makes detection of more complex long-chain molecules such as HC_3N and C_4H_2 problematic.

Detection of species from ground-based IR observations can also be hindered by extinction from the terrestrial atmosphere. An example of this is CO_2 , an abundant species in comets that has a very strong band near $4.26 \mu\text{m}$, but is completely obscured in ground-based observations by terrestrial CO_2 . Detection of CO and CH_4 in comets depends on a sufficient large relative geocentric velocity to shift cometary lines from their terrestrial counterparts. Strong lines from other species (e.g., C_2H_2 , C_2H_4 , and NH_3) can coincidentally be in spectral regions of poor transmittance making their detection difficult unless atmospheric water vapor is low.

Ground-based observations of comets at mid- to far-IR wavelengths ($\sim 5 - 100 \mu\text{m}$) are similarly hindered by terrestrial atmospheric extinction in addition to increasing and rapidly changing thermal emission from telescope and atmosphere. Thus, studies in this wavelength region are mostly done from airborne observatories (e.g., SOFIA) or

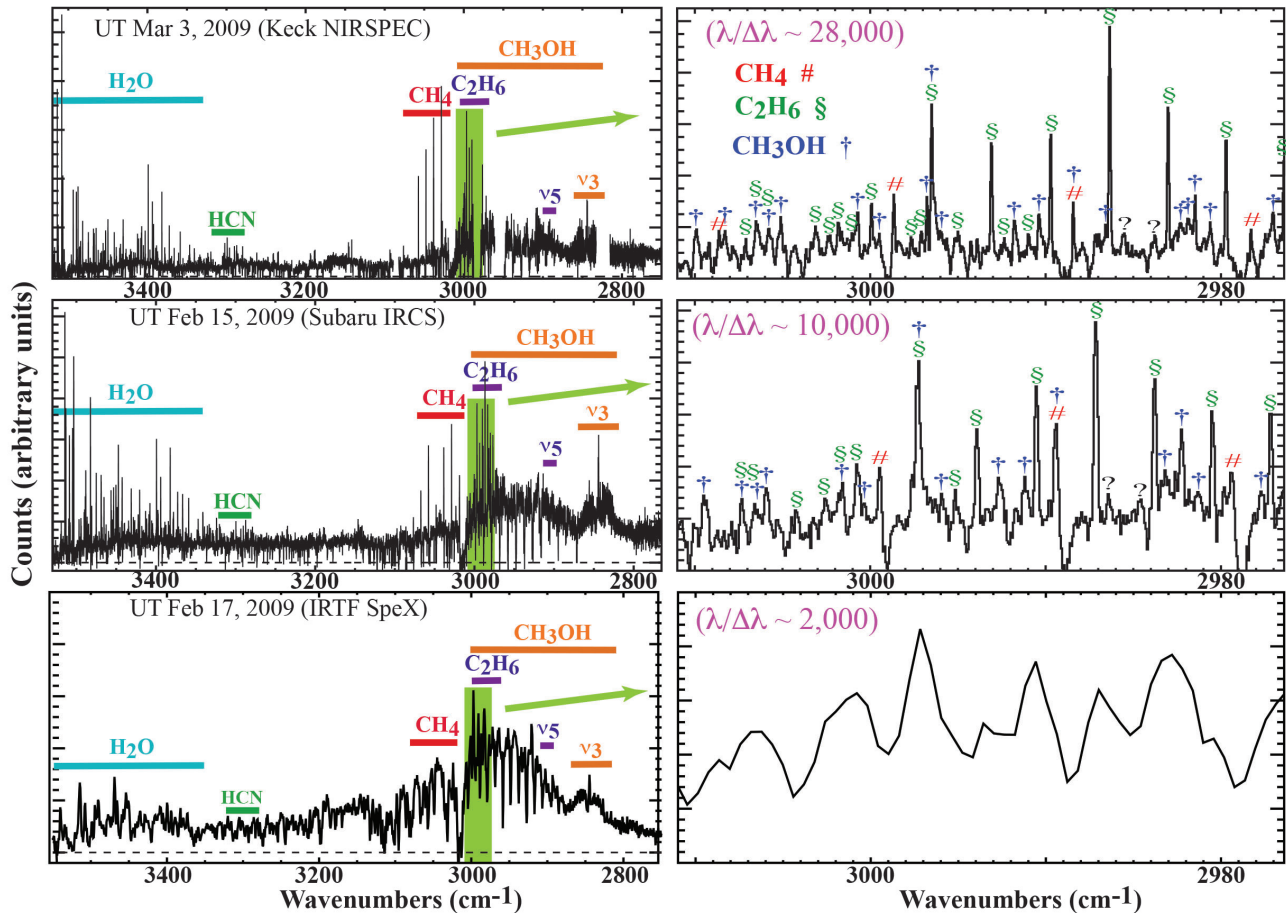


Fig. 3.— Near-IR spectra of comet C/2007 N3 Lulin obtained at different spectral resolving powers. This illustrates the density of ro-vibrational emissions from multiple species with overlapping vibrational bands in some spectral regions. High spectral resolving power is essential for disentangling and interpreting molecular contributions at IR wavelengths.

space-based telescopes (e.g., Spitzer). While most volatile coma molecules are best detected at near-IR and radio wavelengths, the mid- to far-IR can provide information on the composition of the less-volatile dusty coma components (e.g., Lisse *et al.* 2020).

1.3. UV-Visible spectroscopy of electronic transitions

Spectroscopic observations of cometary atmospheres at UV and visible wavelengths sample mostly electronic transitions from secondary products such as OH, NH, CH, CN, C₂, C₃, or NH₂, as illustrated in Fig. 4. Some parent species such as CO or S₂ can also be probed at UV wavelengths. In addition to purely electronic transitions, some prompt emission lines (see, e.g., Bodewits *et al.* 2022) from O, C, or OH are also detected at visible wavelengths, which can give information on their parent molecules like H₂O and CO₂. X-ray emissions have also been seen in comets, but this reveals the composition of the solar wind rather than the cometary coma (Bodewits *et al.* 2022).

1.3.1. Low-res spectroscopy and narrow-band imaging

Comets have been observed with low resolution spectroscopy at visible wavelengths for over a century, focusing on secondary products as illustrated in Fig. 4. Even though spectra often have a high density of lines due to the number of molecular emission bands in the visible spectral region, narrow-band imaging and low resolution spectroscopy were among the first tools available to constrain the composition of cometary atmospheres. Narrow-band filters isolate the light emitted by several gas species as well as the dust-reflected sunlight. When combined with a camera, narrow-band filters enable compositional and morphological studies of the coma. Narrow-band imaging and low-resolution spectroscopy of comets at visible wavelengths are among the most sensitive and routine observations available to study the composition of comets. Visible databases contain several hundred comets observed over decades, providing a means to study comet composition and its diversity statistically (A’Hearn *et al.* 1995; Schleicher 2008; Fink 2009; Langland-Shula and Smith 2011; Cochran *et al.* 2012). Those two techniques are covered in detail by Schle-

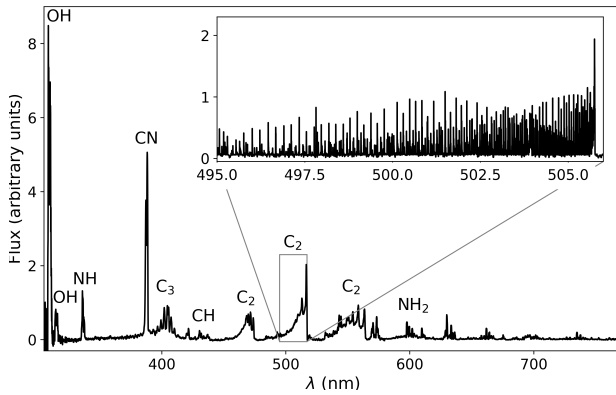


Fig. 4.— Optical spectrum of comet C/2015 ER61 (PANSTARRS) obtained with the ISIS spectrograph at the William Herschel Telescope (A. Fitzsimmons and M. Hyland, priv. comm.). The inset shows the region of the C₂ ($\Delta\nu = 0$) band observed with a much higher spectral resolution using the UVES spectrograph at the VLT (Yang *et al.* 2018).

icher and Farnham (2004) and Feldman *et al.* (2004) and we refer the reader to these publications for an extended discussion.

Because of terrestrial atmospheric extinction, observations blueward of 300 nm can only be performed from space. However, they are instrumental in constraining coma abundances of the main constituents of cometary ices. The main features observable in the UV spectra of comets from parent and fragment species are discussed by Bockelée-Morvan *et al.* (2004) and Feldman *et al.* (2004). An important example is Hydrogen, one of the main photodissociation products of water, which is detectable through its Lyman- α emission at 121.6 nm.

The last decade has seen a significant increase in the use of Integral Field Unit spectrographs (IFUs), particularly on large telescopes. This technique is especially advantageous for the observation of extended objects because it provides simultaneous spatial and spectral information. Observing comets with an IFU combines the advantages of spectroscopy and narrow-band imaging by enabling mapping of the spatial distributions of several gas species and the dust continuum at different wavelengths simultaneously. Given the rotational variability of comets on timescales as brief as a few hours, IFU observations have the advantage of simultaneous measurements of multiple species in contrast to narrow-band observations where different filters need to be cycled to sample each species. The first observations of comets with IFUs at visible wavelengths are relatively recent (Dorman *et al.* 2013; Vaughan *et al.* 2017; Opitom *et al.* 2019b) but they have demonstrated the potential of this type of observation to study the spatial distributions of secondary products and their production mechanisms in the coma.

1.3.2. High-resolution spectroscopy

The last 30 years have seen the advent of high resolution spectroscopic observations of comets. Fabry-Perot interferometers, providing high spectral resolutions but covering very limited wavelength ranges were among the first instruments used to perform high spectral resolution observations of comets (Roesler *et al.* 1985). Crossed-dispersed spectrographs with spectral resolutions from a few tens of thousands to as high as 200,000 and covering larger wavelength ranges are now available on large telescopes (UVES at the Very Large Telescope, HET at McDonald Observatory, HIRES at Keck, or HDS at the Subaru Telescope). This new generation of optical instrumentation allows emission lines composing molecular bands to be resolved and has opened a new era of visible observations of comets, as illustrated in Fig. 4.

A resolving power of $\sim 40,000$ is sufficient to separate emission lines from isotopologues of the same species. UV and visible high resolution spectroscopic observations provide the opportunity to measure the isotopic abundance ratios of several key elements (H, C, N, and O). High resolution spectroscopic observations of comets at optical wavelengths can also resolve ortho and para spin isomers, enabling estimates of the ortho-to-para abundance ratios (OPR) of water and NH₂ (Kawakita *et al.* 2001; Shinnaka *et al.* 2012; Aikawa *et al.* 2022, and section 7.6).

High resolution spectroscopic observations are also necessary to resolve telluric and cometary emission lines. For example, forbidden oxygen lines [OI] around 557, 630, and 636 nm and the sodium D doublet at 589.0 and 589.6 nm are blended with telluric lines at lower spectral resolution. High resolution spectroscopy is currently only feasible for relatively active comets (with high gas production rates) that are close to the Sun (typically within 3 au); however, high resolution spectrographs mounted on the next generation of extremely large telescopes, such as HIRES on the E-ELT, will more routinely allow these studies in a larger subset of comets.

1.4. In-situ mass spectrometry

Another way to investigate the neutral gas environment around comets is in-situ mass spectrometry. This method provides neutral gas abundances along the trajectory of the spacecraft and is therefore limited to dedicated missions. Neutral gas mass spectrometry has been carried out at two comets, the profiles of the *Giotto* and *Rosetta* comet missions are discussed below.

1.4.1. Comet mission profiles

In 1986 the *Giotto* spacecraft flew by comet 1P/Halley (Reinhard 1986). During the inbound portion of the fast, 68.4 km s⁻¹ flyby the Neutral Mass Spectrometer (NMS; Krankowsky *et al.* 1986) carried out continuous measurements of the neutral gas abundances (Eberhardt 1999) until, near closest approach, impacting dust grains led to the failure of the sensor.

The second comet visited by neutral gas mass spectrometers was 67P (*Glassmeier et al. 2007*). *Rosetta* carried the Rosetta Orbiter Spectrometer for Ion and Neutral Analysis (ROSINA; *Balsiger et al. 2007*) Double Focusing Mass Spectrometer DFMS and Reflectron-type Time-Of-Flight (TOF) on the orbiter. Furthermore, the two lander mass spectrometers Ptolemy (*Wright et al. 2007*) and the COMetary SAMpling and Composition experiment (COSAC; *Goesmann et al. 2007*) were carried by Philae. *Rosetta* carried out an extended 2-years investigation following 67P from beyond 3 au, through perihelion at 1.24 au, and out again past 3 au. It was at times gravitationally bound to the comet and hence typical relative velocities between *Rosetta* and 67P were on the order of 1 m/s, much smaller compared to typical neutral gas velocities on the order of 1 km s⁻¹. Fig. 5 shows an example mass spectrum containing parent and fragment species as well as minor isotopologues.

1.4.2. Instrument capabilities, mass resolution

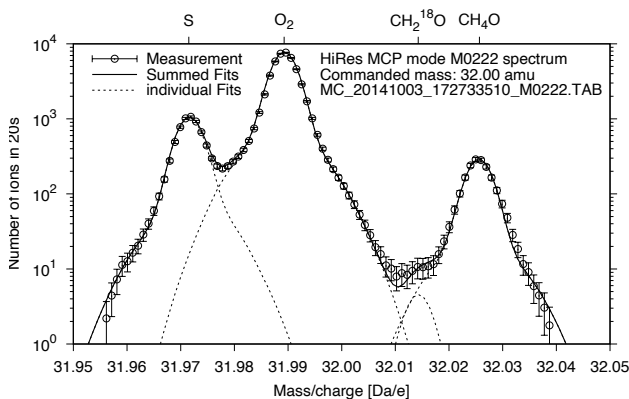


Fig. 5.— ROSINA DFMS mass spectra (*Balsiger et al. 2007*) of mass/charge 32 u/e with sulfur S (in parts a fragment of S-bearing species), molecular oxygen O₂, and methanol CH₃OH. Also, H₂C¹⁸O due to formaldehyde and fragmentation of methanol, both with the heavy oxygen isotope, can be found (cf. *Altwegg et al. 2020a*).

Neutral gas mass spectrometry has some advantages and disadvantages. For instance, the observed atoms and molecules do not require a strong electric dipole moment and hence volatile species such as O₂ and N₂ can be investigated. Furthermore, being in-situ, Earth’s atmosphere will not interfere and there are no optical depth issues requiring reversion to a minor isotopologue with only limited information on the specific isotope ratio (cf. section 7.3). On the down side, the ability to distinguish isomers is limited and is only possible when the differences associated to the fragmentation occurring during ionization (e.g., H₂O→OH⁺, H₂O→O⁺, etc.) are larger than the measurement uncertainties.

Table 1 lists the mass spectrometers that have carried out neutral gas measurements at comets. The instruments ei-

ther employed electric and magnetic fields or time-of-flight to separate ions by their mass-to-charge. In order to resolve ionized atoms and molecules on the same integer mass line, e.g., O⁺ and CH₄⁺ at 15.9944 and 16.0308 u/e, respectively, a mass resolution on the order of $m/\Delta m > 1000$ (FWHM) is required. If the resolution does not allow separation of the different contributors to a given mass line, e.g., O⁺, NH₂⁺, and CH₄⁺ on mass/charge 16 u/e, it may still be possible to disentangle their relative proportions: based on the calibrated fragmentation patterns, the contributions to a given mass line, e.g. H₂O→O⁺ and NH₃→NH₂⁺ can be subtracted from the total signal on mass/charge 16 u/e leaving only CH₄⁺. The signal of CH₄⁺ can then be related to the abundance of the cometary parent species methane, CH₄, in the local coma. This approach quickly becomes very complex in gas mixtures due to the large number of involved fragments and isomers.

1.4.3. Ion mass spectrometry

The composition of the neutral gas coma can also be constrained from in-situ plasma measurements (see chapter *Beth et al. 2022*). However, this approach requires additional modeling of the involved ionization, dissociation, and chemical reactions between neutrals, ions, and electrons. A suite of processes, such as photoionization, photodissociation, ion-neutral reactions and charge exchange, as well as ion-electron recombination, have to be included.

For instance, *Allen et al. (1987)* found evidence for the presence of ammonia and methane in comet 1P/Halley based on Giotto ion mass spectrometer (IMS; *Balsiger et al. 1987*) measurements. Furthermore, the D/H ratio in the water of the same comet was derived from IMS (*Balsiger et al. 1995*) and ion mode measurements of NMS (*Eberhardt et al. 1987*). At 67P, the total outgassing activity was estimated from the increasing He⁺/He²⁺ ratio of solar wind helium crossing the gas coma and charge-exchanging with neutrals (*Wedlund et al. 2016; Hansen et al. 2016*). The same process, when high charge state solar wind minor ions undergo charge exchange excitation with neutrals, led to the X-ray emission observed at comet C/1996 B2 (Hyakutake) (*Hüberli et al. 1997*, cf. section 1.3).

2. FROM OBSERVATIONS TO ABUNDANCES

For estimating relative abundances in ices that sublimate near the surface of the nucleus, either for the parent molecules directly observed or the assumed parent of a secondary product species, we convert the measured quantities, a line intensity converted into a column density or a local density (in-situ measurements) into production rate Q . The first step for spectroscopic observations requires modelling the excitation of considered energy levels of the molecule and radiative transfer. In all cases a knowledge of the spatial distribution of the molecule is needed. Most studies use the Haser model (*Haser 1957*) to describe the density of a sublimating parent molecule. Remote spectroscopic observations are nowadays often 2-D or 3-D data-cubes that com-

Table 1: Neutral gas mass spectrometers operated at comets.

Instrument	Craft	Mass separation technique	Mass range [u/e]	Resolution $m/\Delta m$	Reference
NMS	Giotto	EM-fields	1-56 ^a	unit ^b	<i>Krankowsky et al. (1986)</i>
ROSINA DFMS	Rosetta	EM-fields	12 to 180	3000 @ 1%	<i>Balsiger et al. (2007)</i>
ROSINA RTOF	Rosetta	Time of Flight	1 to >300	>500 @ 50%	<i>Balsiger et al. (2007)</i>
COSAC	Philae	Time of Flight	1 to 1500	300 @ 50%	<i>Goesmann et al. (2007)</i>
Ptolemy	Philae	Time of Flight	12 to 150	unit	<i>Wright et al. (2007)</i>

^a1-38 u/e in nominal double focusing mode, ^b unit mass resolution in the range 12-56 u/e.

bine spectral information at high resolution and 1-D (long slit spectroscopy) to 2-D (data-cubes, interferometric maps) spatial information. This is used to characterize the local density of the molecules and reveal evidence for departure from the basic Haser model: outgassing asymmetry and radial distribution for non-nucleus sources.

2.1. Deriving production rates

The processes that lead to excitation of molecular energy levels are multiple: collisions with neutral gas that tend to establish a local thermal equilibrium (LTE) at the local gas temperature, collisions with electrons created in the coma and from the solar wind, and radiative processes. The radiative environment for the inner coma is dominated by the solar radiation in the UV to IR range, the cosmic black body background at 2.73 K in the radio range and dust and nucleus thermal emission in the IR. Self absorption by optically thick lines in the IR to submillimeter range can also play an important role. Generally UV to IR emission will result from fluorescence excitation (absorption followed by rapid emission of photons due to the short lifetime of the electronic and vibrational states excited in this process) while rotational transitions in the radio domain result from spontaneous emission due to slow decay of the rotational levels (lifetimes of 10^2 to 10^6 s) populated by collisions or radiative processes, including pumping via vibrational bands. Dissociation products of molecules can also radiate via prompt emission when they are created in an excited electronic state, such as CO Cameron bands in the UV or OH in the IR. All processes have been reviewed in detail in *Bockelée-Morvan et al. (2004)* or *Bodewits et al. (2022)*. State-of-the-art models adapted to comets need to take into account non-steady-state calculation specific for cometary comae in which the gas is flowing away from the nucleus and the density seen by a given molecule decreases with time (*Marschall et al. 2022*).

Several parameters, such as the gas temperature and the expansion velocity can be inferred directly from observations: rotational temperatures measured in the IR or the radio from series of ro-vibrational or rotational lines and analysis of the line profiles resolved in the radio where width is directly related to the gas expansion velocity.

2.2. Spatial distribution of molecules in the coma

While imaging cometary dust is often the easiest way to study coma morphology it provides an incomplete picture as gas and dust spatial distributions are generally distinct. Determining and comparing the spatial distributions of volatile gases in the coma of comets can provide information both about their sources (direct sublimation from ice and/or extended coma sources) and about how ices are associated or separated in the nucleus. Both spacecraft and ground-based studies have provided abundant evidence that some molecules are principally released directly from their sublimating ices while others are released from the dissociation of other molecules in the coma; however, the contribution from these sources for a given molecule often differs from comet to comet and the progenitor species of secondary products are often difficult to identify. When no spatial information is available, it is difficult to assess whether some molecules are primarily parents or products. This can affect the accuracy of derived production rates if the parentage is wrongly assumed. Spatial studies of comets span a large range in scale and resolution, from the highest resolution studies of the inner coma by in-situ spacecraft to ground-based studies with various aperture sizes and different comet geocentric distances. The addition of spacecraft data and increasing ground-based capabilities has allowed more detailed studies of molecular spatial distributions in the coma.

2.2.1. Narrowband imaging and interferometric maps

Studies of cometary coma features have been conducted for many years at optical wavelengths and extending from the near-UV to the near-IR. Modern telescopes and imagers allow extensive spatial coverage in the coma while also providing sub-arcsecond spatial resolution over large format CCD arrays. Broadband continuum filters have provided detailed information on the dust structure in the comae of comets. Using targeted narrowband filters and continuum removal techniques or IFUs has allowed the isolation of coma gas structure, which is needed to provide complete information on coma morphology because coma gas and dust distributions are generally distinct. Gas phase species sampled at these wavelengths are product species or ions

(e.g., OH, NH, CN, C₂, C₃, CO⁺, H₂O⁺) (e.g., *Schleicher and Farnham 2004*). For certain bright comets the consistency of assumed parent scalelengths for these species can be tested, which is important as many of these values are poorly constrained. With increasing capabilities at radio and IR wavelengths, coordinated observations of the spatial distributions of parents and secondary products can be performed providing a more direct comparison of parent-product associations in individual comets.

Interferometric maps at radio wavelengths provide information on the spatial and velocity distributions of gas molecules and dust. Modern heterodyne receivers allow the determination of high-resolution line-of-sight velocities which enable three dimensional spatial structures of measured molecules to be obtained (e.g., *Qi et al. 2015*). The importance of radio interferometry in obtaining spatial maps for molecules released from different sources has been demonstrated (e.g., *Boissier et al. 2007; Cordiner et al. 2014; Cordiner et al. 2017; Roth et al. 2021*). Maps for molecular species show dramatic differences in their spatial distributions suggesting heterogeneity in the way ices are stored and associated within the nucleus. Under favorable circumstances radio interferometry with facilities such as NOEMA, ALMA or the SMA have determined the spatial distribution of parent and product species such as H₂CO, HCN, HNC (e.g. Fig 6), CH₃OH, CO, or CS. Future capabilities with facilities such as the ngVLA will allow higher sensitivities and cover longer wavelengths allowing NH₃ and OH to be mapped in the comae of comets at high spatial resolution (e.g., *Cordiner and Qi 2018*).

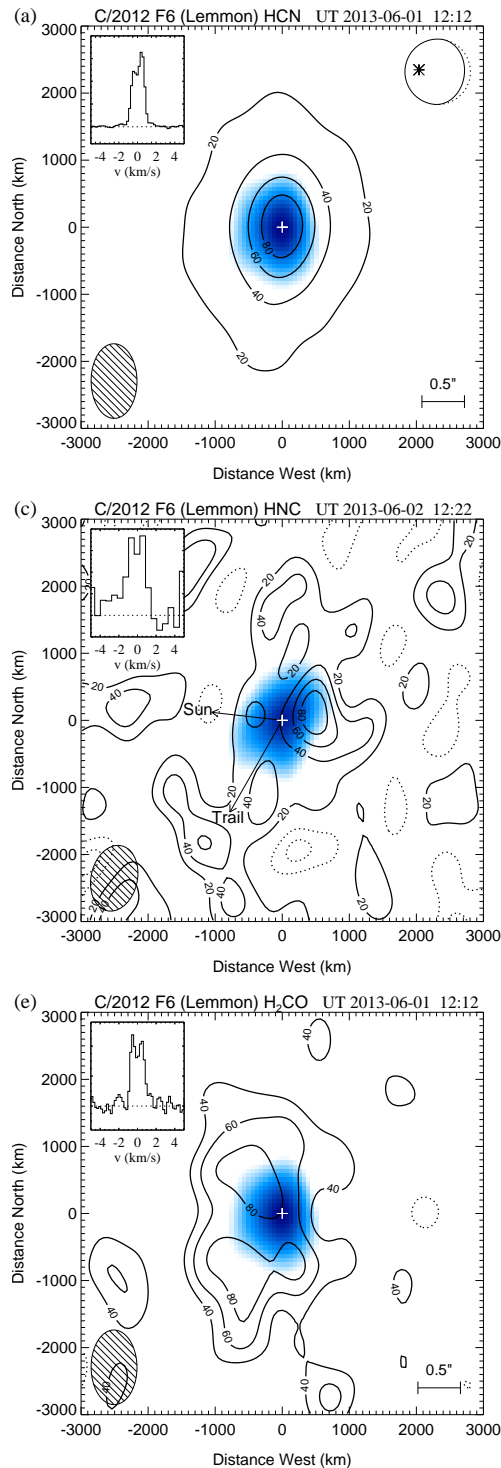


Fig. 6.— ALMA interferometric contour maps of (a) HCN, (c) HNC, and (e) H₂CO in C/2012 F6 (Lemmon). The signal distributions of HNC and H₂CO are much less peaked due to their production in the coma in contrast to HCN coming mostly from the nucleus (*Cordiner et al. 2014*). In the lower left corners the hatched ellipse shows the shape and size of the synthetic beam. The spectrum at the central point is shown in the upper left and the continuum flux is displayed in blue.

2.2.2. Infrared spatial profiles

The long-slit capabilities of IR ground-based observing enables the determination and comparison of spatial distributions of molecules in the inner coma. These comparisons address whether species observed simultaneously relate to a common or different outgassing sources and suggest potential nucleus associations. IR spatial analysis of comets have routinely determined the spatial distributions of H₂O, C₂H₆, CH₃OH, and HCN in many comets observed to date. Spatial distributions for CO and CH₄ are also readily obtained when the comet's geocentric velocity is sufficient to Doppler-shift cometary emissions from their atmospheric counterparts. For some of the brightest comets, spatial distributions have also been obtained for H₂CO, C₂H₂, NH₃, and OCS. Previous ground-based IR studies have suggested separate polar and apolar ice phases in the nucleus of some comets (e.g., *Mumma and Charnley 2011*); however, this association by ice polarity is not seen in some cases (e.g., *Dello Russo et al. 2022*). IR spatial analysis has revealed surprising evidence for extended sources for some species (Fig. 7A), as well as showing possible volatile associations of ices in the nucleus (Fig. 7B) (e.g., *Dello Russo et al. 2022*). Technological advances in ground-based IR instrumentation has allowed spatial analysis to be done in more detail and on a rapidly increasing number of comets. This work is beginning to address which spatial properties are specific to individual comets and which are more general properties of all comets.

2.2.3. In-situ radial profiles

Spacecraft missions have performed the highest resolution studies of how volatiles are released into the inner comae of comets. In contrast to remote sensing observations which derive spatial properties over the global coma, in-situ studies can reveal volatile and dust release from specific areas on the nucleus. The *EPOXI* flyby revealed a two-lobed nucleus for 103P/Hartley 2 with the bulk of the activity emanating from the smaller lobe (*A'Hearn et al. 2011*). Release from the small lobe was dominated by the spectral signature of CO₂ gas with entrained H₂O ice chunks, whereas H₂O vapor primarily sublimated from a different region along the waist between the lobes (*A'Hearn et al. 2011*). *EPOXI* spatial studies of volatiles were based on low-resolution IR spectroscopic measurements during a flyby so were a brief snapshot of the volatile coma structure of 103P and mainly sensitive to H₂O and CO₂, the strongest IR molecular bands. *Rosetta* studies of 67P enabled tracking of long-term molecular associations in the coma of many species with multiple instruments. In contrast to 103P, *Rosetta* observed dominant H₂O outgassing directly from ices in the nucleus of 67P and not from coma icy grains (e.g., *Luspay-Kuti et al. 2015*), suggesting a more direct association between coma gas and nucleus ice distributions.

Processes like sublimating icy grains and photochemistry are imprinted in the gas densities along radial pro-

files from the nucleus. Marked deviations from $1/r^2$ (assuming constant expansion velocity) indicate contribution from a distributed source, either through sublimation from grains in the coma or dissociation of larger molecules. At 67P, *Altwegg et al. (2016)* reported that the total gas density dropped with cometocentric distance as expected but glycine was most likely released from water ice on dust particles (*Hadraoui et al. 2019*). Based on *Giotto* NMS results at 1P/Halley, substantial distributed sources were reported for H₂CO, CO (*Meier et al. 1993; Eberhardt 1999*), and possibly H₂S, while CH₃OH behaved differently (*Eberhardt et al. 1994*). During the flyby, the *Giotto* spacecraft covered a wide range in phase angle and cometocentric distances (*Reinhard 1986*) and hence NMS measured gas released during different times from distinct regions on the nucleus with varying illumination. Therefore, temporally and spatially inhomogeneous outgassing could result in similar spatial profiles (cf. Fig. 3 of *Rubin et al. 2009*).

3. DRIVERS OF COMET ACTIVITY

Water is the most abundant species in cometary ices and the main driver of activity for comets within 2-3 au from the Sun. At larger heliocentric distances, the water sublimation rate decreases and water alone is not sufficient to sustain cometary activity. More volatile ices, like CO and CO₂, are believed to drive the distant activity of comets.

3.1. CO and distant activity

CO was first detected in comets close to the Sun in the UV via resonant fluorescence in the Fourth Positive Group ($A^1\Pi - X^1\Sigma^+$) with sounding rockets and satellites (*Bockelée-Morvan et al. 2004*, and reference therein). Since its first direct cometary detection in 29P/Schwassmann-Wachmann 1 in 1993 by *Senay and Jewitt (1994)* and *Crovisier et al. (1995)*, CO has been detected in the radio and in the IR in several comets at large heliocentric distances, and up to 14 au in comet C/1995 O1 (Hale-Bopp) (*Biver et al. 2002*). CO is one of the most volatile molecules, along with N₂, detected in comets. Due to its volatility, it can sublimate as far out as the Kuiper Belt ($T_{sub} \sim 25$ K, *Fray and Schmitt 2009*). Hence its signature has been searched for in many icy objects including Trans-Neptunian Objects (TNOs) and Centaurs (*Bockelée-Morvan et al. 2001; Jewitt et al. 2008; Womack et al. 2017*). CO sublimation might have been responsible for transient or outburst activity in Centaurs like 95P/Chiron (*Womack et al. 2017*) or 174P/Echeclus (*Wierzbachos et al. 2017*), but this has not been confirmed due to the difficulty to detect CO in these distant objects. Nevertheless, in several comets observed beyond 2–3 au (Table 2), a substantial outgassing of CO has been detected and often dominates the activity of the comet ($Q_{CO}/Q_{H_2O} > 1$). In those comets, CO sublimation can lift dust into the coma even at distances more than 20 au from the Sun. Radio lines also often show a strong blueshift (e.g., the bottom spectrum of Fig. 1), suggesting that CO sublimation is enhanced at the warmer subsolar point. This does not necessarily mean

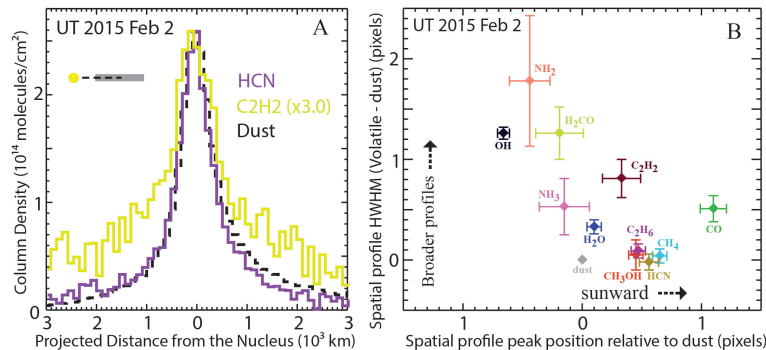


Fig. 7.— (A) Spatial profiles of C₂H₂, HCN, and dust in C/2014 Q2 (Lovejoy) showing evidence for a C₂H₂ extended source due to excess flux on the profile wings compared to HCN. (B) Spatial profile properties for volatiles and dust in C/2014 Q2 (Lovejoy) showing the distinct characteristics of spatial profiles based on profile peak position and width (*Dello Russo et al. 2022*).

that the ices of these comets are dominated by CO: comets like C/1995 O1 (Hale-Bopp) or C/2009 P1 (Garradd), when they were closer to the Sun (1.5 au or less) had comae dominated by water vapour with CO abundances around 5-25%. In fact the abundance of CO relative to water in comets varies by at least two orders of magnitude (0.3 to 35%, Table 3, Figs 9 and 10) in comets observed within 1.5 au from the Sun. JFCs (e.g., 67P, *Läuter et al. 2020*) tend to be depleted in CO with abundances generally not exceeding 3% relative to water. Comets with low CO abundances may have most of their CO trapped in water ice, so even beyond the sublimation of water, CO generally doesn't control activity in JFCs. Finally, some comets like C/2016 R2 (*Biver et al. 2018; McKay et al. 2019*, and Sect. 6.1.2) seem to be dominated by CO outgassing even at a distance where H₂O outgassing becomes significant in most comets.

3.2. CO₂ as driver of activity

The CO₂ abundance is very difficult to estimate from ground-based observations and most measurements of the CO₂ abundance in comets come from infrared space observatories (ISO, Spitzer, AKARI) or spacecraft (Deep Impact, EPOXI, Rosetta). Indirect measurements can be made from observation of the CO Cameron band in the UV and forbidden oxygen lines in the optical. The AKARI survey (*Ootsubo et al. 2012*) has revealed that in most cases CO₂ is a major constituent of cometary atmospheres, with abundances typically ranging from 5 to 30% with no clear differences based on dynamical origin. Beyond 2.5 au from the Sun the CO₂ abundance relative to water increases and CO₂ can become the major constituent of the coma, driving the activity of the comet. Even closer to the Sun, the outgassing of CO₂ can dominate the activity of the nucleus such as in the case of (3552) Don Quixote (Spitzer, *Mommert et al. 2020*) or 103P/Hartley (EPOXI, *A'Hearn et al. 2011*).

CO₂ behavior in 67P: The intricate pattern of activity in 67P is a result of the peculiar shape of its nucleus and associated illumination together with the obliquity of its rotation

axis of 52° (*Sierks et al. 2015*) and the different volatility of the involved gases (*Fray and Schmitt 2009*). The gas activity induced a decrease in the rotation period (from 12.4 to 12.0 hr) as the comet passed perihelion (*Kramer et al. 2019; Keller et al. 2015b*). Furthermore, the transport and re-deposition of (icy) grains around the nucleus (*Keller et al. 2017*) leads to very different surface morphologies (*El-Maarry et al. 2015*) leaving their imprint on the structures of the gas coma.

Fig. 8 shows a time series of H₂O and CO₂ measurements late in the *Rosetta* mission at a heliocentric distance of ~3 au, just after the outbound equinox. While the spacecraft orbited the comet at close distances in the terminator plane, it passed over regions in the south where CO₂ was the main driver of activity while H₂O dominated above the northern hemisphere. At that time the sub-solar latitude climbed from southern to northern latitudes, however, the south did remain the more active hemisphere for the remaining part of the mission out to almost 4 au despite the sub-solar latitude increasing again above 20 degrees northern. CO₂ remained the dominant molecule and a similar picture was obtained on a global scale from studies of the H₂O and CO₂ gas production rates of 67P at this distance (*Combi et al. 2020; Läuter et al. 2020*). The same behavior was also observed very early on in the mission, beyond 3 au on the inbound path of the comet. *Hässig et al. (2015)* reported an elevated CO₂/H₂O ratio above the the southern hemisphere from which pristine ices are sublimating due to the substantial erosion rates (*Keller et al. 2015a*) observed during the intense but short summer months (*Capria et al. 2017*). Local enhancements in CO₂/H₂O ratio have also been identified by remote sensing observations of the [O I] emission (*Bodewits et al. 2016*).

3.3. Monitoring of H₂O production

H₂O is the dominant volatile ice in comets and as such determining its production rate provides a measure of the overall comet volatile productivity when the comet is within

Table 2: Comets dominated by CO outgassing

Comet	Date	r_h (au)	Q_{CO} (molec.s $^{-1}$)	$Q_{\text{CO}}/Q_{\text{H}_2\text{O}}$	Ref.
C/1995 O1 (Hale-Bopp) ^a	May 1996	4.6	6×10^{28}	4.5	(Biver et al. 2002)
	Sep. 1996	3.3	15×10^{28}	~ 1	(Biver et al. 2002)
	Aug. 1997	2.3	24×10^{28}	~ 1	(Biver et al. 2002)
	Dec. 1997	3.9	10×10^{28}	3.8	(Biver et al. 2002)
C/1997 J2 (Meunier-Dupouy)	Mar. 1998	3.1	0.39×10^{28}	(^b)	(Biver et al. 2018)
29P/Schwassman-Wachmann 1	May 2010	6.2	4×10^{28}	~ 10	(Bockelee-Morvan et al. 2010)
C/2006 W3 (Christensen)	Nov. 2009	3.3	3×10^{28}	> 2.2	(Bockelee-Morvan et al. 2010)
	Aug. 2010	4.9	1.2×10^{28}	~ 5	(Boney et al. 2017) +(de Val-Borro et al. 2014)
C/2009 P1 (Garradd)	Apr. 2012	2.1	3×10^{28}	0.6	(Feaga et al. 2014)
C/2016 R2 (PanSTARRS)	Feb. 2018	2.8	8×10^{28}	~ 300	(McKay et al. 2019)
C/2017 K2 (PanSTARRS)	Feb. 2021	6.7	0.16×10^{28}	(^b)	(Yang et al. 2021)
174P/Echeclus	Jun. 2016	6.1	0.08×10^{28}	(^b)	(Wierzos et al. 2017)

^a: for comet Hale-Bopp, which activity was monitored from 7 au pre-perihelion to 14 au post-perihelion we provide the CO/H₂O ratio for the most distant detections of H₂O and the time when it crossed the $Q_{\text{CO}} = Q_{\text{H}_2\text{O}}$. Water outgassing dominated between September 1996 and August 1997. ^b: $Q_{\text{H}_2\text{O}}$ not measured, likely low.

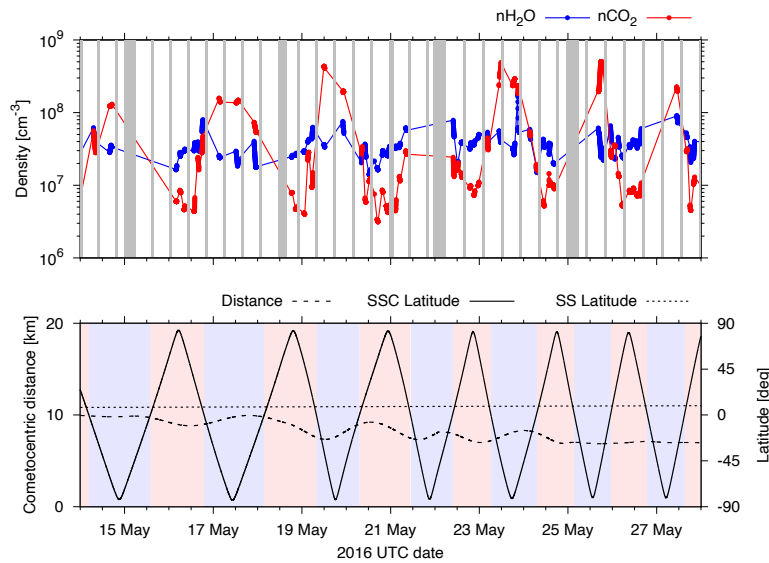


Fig. 8.— Top panel: H₂O and CO₂ densities at 67P measured in May 2016 (post outbound equinox) at ~ 3 au by ROSINA DFMS (cf. Gasc et al. 2017) during close terminator orbits. Grey areas mark times of thruster operations when the instrument was off, other gaps due to different measurement mode. Bottom panel: cometocentric distance (< 10 km), sub-spacecraft latitude (red: north, summer; blue: south, winter) and sub-solar latitude.

about 2 - 3 au from the Sun. H₂O is also the molecule to which the abundances of all other volatile species are generally compared. Thus, determining H₂O production rates and coma spatial distribution is an important goal in overall investigations of comet composition. H₂O production in comets can be directly measured or inferred through its secondary product species by several techniques over a range of wavelengths from both ground-based and space-based observatories.

3.3.1. Direct observations of H₂O

H₂O has strong IR vibrational bands near 2.7 and 6.3- μm associated with the O-H stretching and bending modes respectively that can be easily detected from remote or in-situ space-based observations (e.g., Weaver et al. 1987; Crovisier 1997; A'Hearn et al. 2011; Bockelee-Morvan et al. 2015). H₂O can also be detected from space through rotational line transitions at radio wavelengths (e.g., Neufeld et al. 2000; Lecacheux et al. 2003; Hartogh et al. 2011). Because of extinction from atmospheric H₂O, IR fundamental bands and rotational lines are gen-

erally inaccessible in comets from ground-based observing platforms. However, ground-based IR observations have routinely detected H₂O in comets through the years via non-resonance fluorescence emissions that are not opaque in the Earth’s atmosphere (e.g., *Mumma et al.* 1996; *Dello Russo et al.* 2000; *Villanueva et al.* 2012; *Faggi et al.* 2016). The spectral coverage of modern ground-based IR instruments allows the simultaneous sampling of H₂O with many other volatile species providing a direct measure of relative volatile abundances and comparison of coma spatial distributions that eliminate uncertainties due to temporal variability in volatile release and coma dynamics.

3.3.2. Tracers of H₂O: OH, H, OI

Because H₂O is by far the dominant source of OH, H and O in the coma of comets close to the Sun, H₂O production rates can be inferred from measurements of these species, as branching ratios of H₂O to these secondary products are generally well known. Observations of OH at radio wavelengths allows a determination of H₂O production rates, gas outflow velocity and asymmetries (e.g., *Crovisier et al.* 2013). OH can also be detected through prompt emission at IR wavelengths and has been used as a tracer for H₂O production in comets (e.g., *Bonev et al.* 2006). Optical and near-UV wavelengths enable the detection of H, O, and OH from both ground- and space-based observatories (e.g., *Combi et al.* 2019; *McKay et al.* 2013; *Opitom et al.* 2015). Because of the sensitivity of radio, optical, and near-UV techniques for observing H₂O product species, these have been the main methods over the years for long-term monitoring of volatile production in comets within an apparition. IR observatories and instrumentation now also have the sensitivity for long-term monitoring of H₂O production in comets, but are generally limited by telescope availability for such studies.

3.3.3. Water from icy grains

H₂O is characterized by its low volatility compared to other measured coma species, which has implications for its outgassing behavior. First, H₂O sublimation is generally not fully activated in a comet until it is between about 2 and 3 au from the Sun. Second, while H₂O sublimates into the coma directly from nucleus ices, H₂O icy grains can also be dragged into the coma by more volatile gases and survive as ice in the coma longer than other measured volatiles. The prevalence of H₂O icy grains in the coma may depend on the abundances of more volatile species such as CO₂ or CO that can also drive activity. For example, the correlation of CO₂ gas and H₂O ice in the inner coma of 103P/Hartley 2 suggests that areas of gas sublimation rich in CO₂ may have dragged H₂O ice into the coma from below the nucleus surface (*A’Hearn et al.* 2011). From ground-based observatories, the presence of icy grains in the coma can often be inferred by the spatial distribution of H₂O molecules in the global coma compared to other volatiles. Because H₂O icy grains can survive longer in the coma than other volatiles,

care must be taken when (1) determining abundances of volatiles relative to H₂O especially when the aperture size is small when projected on the comet, and (2) comparing H₂O production rates determined by techniques with significantly different aperture sizes.

3.3.4. Discrepancies in derived water production rates

Measurements of water abundances from different tracers are not always consistent, even for measurements close in time. Water production rates measured at 2 au pre-perihelion in comet C/2009 P1 (Garradd) ranged from about 8×10^{28} molecules/s from high-resolution IR observation of H₂O with VLT/CRIRES (*Paganini et al.* 2012) to $2 - 2.9 \times 10^{29}$ molecules/s from H₂O observations with the Herschel HIFI instrument, OH observations with UVOT/Swift in the near-UV (*Bockelée-Morvan et al.* 2012; *Bodewits et al.* 2014), and from H observation with SOHO/SWAN (*Combi et al.* 2013) on the largest spatial scale. Several factors could play a role in the discrepancies between production rates measured with different techniques. First, instruments used for measurements at different wavelengths and from ground- and space-based observatories have different fields of view (FoV). For example, the SWAN instrument onboard SOHO, used to derive water production rates from HI emission, has a FoV of $1^\circ \times 1^\circ$. On the other end, near-IR spectrographs (such as VLT/CRIRES or Keck/NIRSPEC) tend to have small slits of the order of a few arcseconds. Second, the use of different coma density models (e.g. Haser model, *Haser* 1957) versus the vectorial model (*Festou and Feldman* 1981a) can also lead to differences in the derived production rates (*Cochran and Schleicher* 1993). Finally, model parameter assumptions, such as scalelengths or gas velocities can also impact derived production rates (*Cochran and Schleicher* 1993; *Fink* 2009).

4. VOLATILE COMPOSITION OF THE COMA

Around 30 molecules have been identified remotely in cometary atmospheres with an abundance relative to water often varying by one order of magnitude. Fig. 9 shows the range of abundances measured and the number of comets in which they have been detected. The *Rosetta* mission has nearly doubled this number of molecules. The present status of abundances measured in comets and in 67P is summarized in Table 3 and detailed hereafter.

4.1. Hydrocarbons

Symmetric hydrocarbons such as CH₄, C₂H₆, C₂H₂, and C₂H₄ are investigated remotely in the IR. Based on the growing database of comet observations there is evidence that CH₄, C₂H₆, and C₂H₂ are depleted in Jupiter family comets compared to long-period comets from the Oort cloud. These and more complex hydrocarbons were detected in the coma of 67P using the ROSINA mass spectrometer during the *Rosetta* mission.

Table 3: Molecular abundances in cometary atmospheres

Molecule	Name	Abundance relative to water in %		
		from radio	from IR	in-situ in 67P ^a
CO	carbon monoxide	< 1.23–35	0.3–26	0.3–3 ^b
CO ₂	carbon dioxide	-	4–30	7.0 ^b
CH ₄	methane	-	0.15–2.7	0.4 ^b
C ₂ H ₆	ethane	-	0.1–2.7	0.8 ^b
C ₂ H ₂	acetylene	-	0.03–0.37	-
C ₂ H ₄	ethylene	-	0.2	-
C ₃ H ₈	propane	-	-	0.018 ± 0.004
C ₆ H ₆	benzene	-	-	0.00069 ± 0.00014
C ₇ H ₈	toluene	-	-	0.0062 ± 0.0012
CH ₃ OH	methanol	0.7–6.1	< 0.13–4.3	0.5–1.5 ^b
H ₂ CO	formaldehyde	0.13–1.4 ^d	< 0.02–1.1	0.5
HCOOH	formic acid	0.03–0.18	-	0.013
CH ₃ CHO	acetaldehyde	0.05–0.08	-	0.047
c-C ₂ H ₄ O	ethylene oxide	< 0.006	-	-
(CH ₂ OH) ₂	ethylene glycol	0.07–0.35	-	0.011
CH ₃ OCH ₂ OH	methoxymethanol	< 9	-	-
HCOOCH ₃	methyl formate	0.06–0.08	-	0.0034
CH ₂ OHCHO	glycolaldehyde	0.016–0.039	-	-
CH ₃ COOH	acetic acid	< 0.026	-	-
C ₂ H ₅ OH	ethanol	0.11–0.19	-	0.10 ^b
CH ₃ OCH ₃	dimethyl ether	< 0.025	-	-
CH ₃ COCH ₃	acetone	≤ 0.011	-	0.0047
C ₂ H ₅ CHO	propanal	-	-	-
CH ₂ CO	ketene	≤ 0.0078	-	-
N ₂	molecular nitrogen	(< 0.002 – 1000 from N ₂ ⁺) ^c	-	0.089 ± 0.024
NH ₃	ammonia	0.18–0.60	0.1–3.6	0.4 ^b
HCN	hydrogen cyanide	0.05–0.25	0.03–0.5	0.20 ^b
HNC	hydrogen isocyanide	0.0015–0.035	-	-
CH ₃ CN	methyl cyanide	0.008–0.054	-	0.0059
HC ₃ N	cianoacetylene	0.002–0.068	-	0.0004
HNCO	isocyanic acid	0.009–0.080	-	0.027
NH ₂ CHO	formamide	0.015–0.022	-	0.004
C ₂ H ₃ CN	vinyl cyanide	< 0.0027	-	-
C ₂ H ₅ CN	ethyl cyanide	< 0.0036	-	-
C ₂ N ₂	cyanogen	-	-	0.0004 ± 0.0002
H ₂ S	hydrogen sulphide	0.09–1.5	-	2.0 ^b
SO	sulphur monoxide	0.04–0.30	-	0.071
SO ₂	sulphur dioxide	0.03–0.23	-	0.127
CS	carbon monosulphide	0.03–0.20	-	-
CS ₂	carbon disulphide	-	-	0.02 ^b
OCS	carbonyl sulphide	0.05–0.40	0.04–0.40	0.07 ^b
H ₂ CS	thioformaldehyde	0.009–0.090	-	0.0027
S ₂	sulphur dimer	(0.001–0.25) ^c	-	0.002
NS	nitrogen sulphide	0.006–0.012	-	-
CH ₃ SH	methyl mercaptan	< 0.023	-	0.038
HF	hydrogen fluoride	0.018	-	0.003–0.048
HCl	hydrogen chloride	< 0.011	-	0.002–0.059
HBr	hydrogen bromide	-	-	0.00012–0.00083
PH ₃	phosphine	< 0.07	-	< 0.003
PN	phosphorus nitride	< 0.003	-	< 0.001
PO	phosphorus oxide	< 0.013	-	0.011
CH ₃ NH ₂	methylamine	< 0.055	-	-
NH ₂ CH ₂ COOH	glycine I	< 0.18	-	0.000017
Ar	argon	-	-	0.00058 ± 0.00022
Kr	krypton	-	-	0.000049 ± 0.000022
Xe	xenon	-	-	0.000024 ± 0.000011
O ₂	molecular oxygen	-	-	2.0 ^b

Table updated from information in *Bockelée-Morvan and Biver (2017); Biver et al. (2021a); Rubin et al. (2019); Dello Russo et al. (2016a); Lippi et al. (2021)*. ^a: Based on *Biver et al. (2019); Rubin et al. (2019); Läuter et al. (2020); Hänni et al. (2021)*. ^b: value based on the integrated gas loss over the whole Rosetta mission (2 years). ^c: From observations in the visible-UV. ^d: Assuming a daughter distribution.

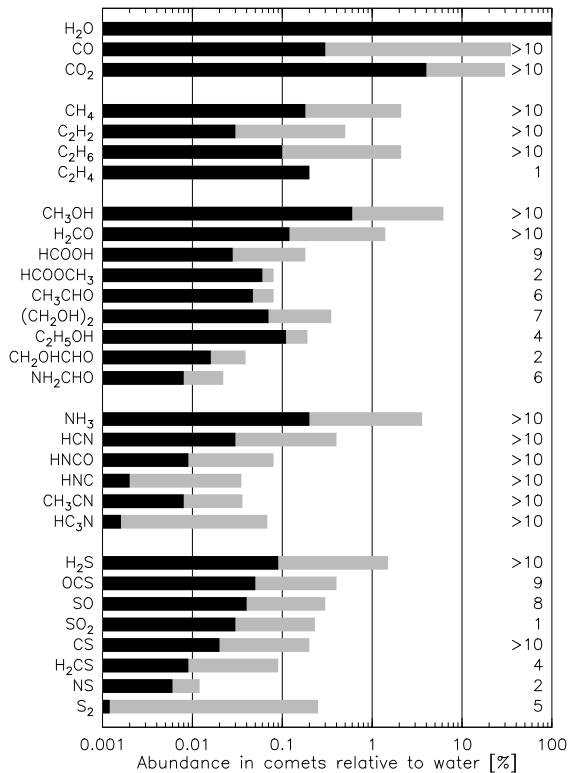


Fig. 9.— The range of abundances relative to water for the molecules observed remotely in cometary comae. The number of comets in which the molecule has been detected is indicated to the right (updated from *Bockelée-Morvan and Biver 2017*).

4.1.1. CH₄ (methane)

CH₄ is the simplest and most volatile saturated hydrocarbon (C_nH_{2n+2}), so its relative abundance in comets may provide clues about the region of formation and processing history of cometary ices (*Gibb et al. 2003*). CH₄ has a strong IR fundamental band (ν_3) near 3.3 μm ; however, its detection in comets from Earth-based observatories requires a sufficient cometary geocentric velocity ($|\text{d}\delta/\text{d}t| > \sim 15 \text{ km s}^{-1}$) to shift comet lines away from corresponding terrestrial counterparts. CH₄ is typically one of the most abundant hydrocarbons in comets with mixing ratios CH₄/H₂O ranging from $\sim 0.15 - 3\%$, with typical abundances $\sim 0.8\%$ (*Dello Russo et al. 2016a*, and references therein).

4.1.2. C₂H₆ (ethane)

C₂H₆ ν_7 band near 3.35 μm is favorable for detection in comets owing to the large intrinsic strength and a pile-up of ro-vibrational lines within Q-branches. Lines from the ν_5 band of C₂H₆ near 3.45 μm are also generally detected although the strongest lines are several times weaker than the ν_7 Q-branches. The terrestrial C₂H₆ component

is very weak so no specific geocentric Doppler-shift is required for its detection in comets from the ground. Mixing ratios C₂H₆/H₂O range from $\sim 0.1 - 2\%$, with typical abundances $\sim 0.6\%$ (*Dello Russo et al. 2016a*, and references therein), so mixing ratios of C₂H₆/CH₄ ~ 1 in comets are typical.

4.1.3. C₂H₂ (acetylene)

Ro-vibrational lines from the ν_3 and $\nu_2 + \nu_4 + \nu_5$ vibrational bands of C₂H₂ near 3 μm have been detected in many comets. However, detection of C₂H₂ is not routine owing to its low abundances, presence of lines in regions of low atmospheric transmittance, and blending with stronger lines of other species. Mixing ratios C₂H₂/H₂O range from $< 0.03 - 0.5\%$, with typical abundances $\sim 0.1\%$ (*Dello Russo et al. 2016a*, and references therein). The typically low abundances of C₂H₂ relative to C₂H₆ in comets may indicate the importance of H-atom addition reactions on pre-cometary ices in the nebula.

4.1.4. Other hydrocarbons

Although C₂H₄ (ethylene) emissions are numerous in $\sim 3.2 - 3.35 \mu\text{m}$ region, they are relatively weak, located in many areas of generally low atmospheric transmittance, and are subject to blends from stronger and more abundant species. For these reasons C₂H₄ has been detected in only two comets: 67P from *Rosetta* ROSINA measurements (*Luspay-Kuti et al. 2015; Rubin et al. 2015a; Altwegg et al. 2017b*) and C/2014 Q2 (Lovejoy) from ground-based IR measurements with C₂H₄/H₂O $\sim 0.2\%$ (*Dello Russo et al. 2022*). Other more complex hydrocarbons also have strong IR bands but they have not been detected from the ground because of various factors including low abundances, spectral confusion with more abundant species (mostly CH₃OH), and lack of adequate fluorescence models. Many long carbon chain molecules were detected for the first time in 67P with ROSINA (e.g., *Altwegg et al. 2017b*), showing the complexity of hydrocarbons stored in comets.

4.1.5. Aromatic hydrocarbons

The aromatic hydrocarbons benzene, C₆H₆, and toluene, C₇H₈ were detected by ROSINA in 67P (*Schuhmann et al. 2019*) and the latter also tentatively by the Ptolemy mass spectrometer on the Philae lander (*Altwegg et al. 2017b*). Furthermore, tentative detections of xylene, C₈H₁₀, and naphthalene, C₁₀H₈, were reported by *Altwegg et al. (2019)*. The latter most likely associated with dust grains and released at elevated temperatures (*Lamy and Perrin 1988*).

4.2. CHO-species and complex organics

Organic molecules containing C, H and O are significant constituents of cometary comae comprising about 3–5% relative to water. Since the first detections of methanol and formaldehyde in 1986-1990 via in-situ mass spectrometry and radio and infrared remote observations, the num-

ber and complexity of organic molecules discovered in cometary comae has steadily increased (Bockelée-Morvan *et al.* 2004). They generally follow their detection in the Interstellar Medium, from which they may have inherited their diversity. Complex organic molecules (COMs) are often defined by astrophysicists as CHO-bearing molecules with six atoms or more, but there is no strict definition.

4.2.1. CH_3OH (methanol)

Methanol is the most abundant COM in cometary comae. It was first suggested and subsequently shown to be mainly responsible for the $3.52\ \mu\text{m}$ feature in the low resolution IR spectrum of comet 1P/Halley in 1986 and in spectra of subsequently observed comets such as C/1989 X1 (Austin) and C/1990 V1 (Levy), in which its detection in the mm range via rotational lines was unambiguous (Bockelée-Morvan *et al.* 2004, and references therein). Since then methanol has been routinely detected in comets, both in the radio via its rotational lines and with high-resolution IR spectrometers via its ro-vibrational P, Q, R branches of the ν_2, ν_3, ν_9 bands in the $3.3\text{--}3.5\ \mu\text{m}$ range. At radio wavelengths, multiple lines (up to 70 in bright comets) are often observed and used to probe the gas temperature (Biver *et al.* 2015, 2021a). As of 2021, methanol has been detected in about 60 comets (55 in the radio and 37 in the IR, including two with in-situ mass spectrometry) with an abundance relative to water ranging from 0.5 to 6%, within 2 au from the Sun. IR and radio observation often yield similar production rates, with methanol rich comets exhibiting 3–4% methanol relative to water, and methanol poor comets around 1%, but the distribution is not clearly bimodal (Fig. 10).

4.2.2. Formaldehyde (H_2CO)

Formaldehyde was first unambiguously identified in a comet on 1P/Halley with the NMS instrument on the *Giotto* spacecraft. Subsequently H_2CO was detected in the radio in C/1989 X1 (Austin) and C/1990 K1 (Levy) (Colom *et al.* 1992) and in the IR via its ν_1 band at $3.59\ \mu\text{m}$ in 153P/Ikeya-Zhang (DiSanti *et al.* 2002). Measured abundances range from 0.12 to 1.4% relative to water for the total production of H_2CO including distributed sources.

4.2.3. Complex organics

Including $HCOOH$, complex CHO-species have been observed in several comets in the radio, for example in C/1996 B2 (Hyakutake), C/1995 O1 (Hale-Bopp), and in C/2014 Q2 (Lovejoy). In-situ mass spectrometry in comet 67P has identified COMs, some not yet detected in the interstellar medium.

- *Formic acid* ($HCOOH$) has been detected in 10 comets with an estimated abundance between 0.01 and 0.2% relative to water. But abundances can be uncertain by a factor of two or more owing to poor constraints on its photodissociation rate. (Biver *et al.* 2021a);

- *Acetaldehyde* (CH_3CHO) exhibits multiple lines of similar intensities which helps its detection in wide band spectroscopic surveys. It has been detected in 7 comets with a very similar abundances of 0.05–0.08% relative to water.
- *Ethylene-glycol* in its lowest energy conformer gG' -(CH_2OH)₂ has been identified in the radio spectra of 7 comets with an abundance of 0.07 to 0.35% relative to water, which is a substantial percentage for such a large molecule. It is notably higher than measurements by *Rosetta* (Rubin *et al.* 2019, but it was not measured at the time of peak activity) and measured values in star forming regions (Biver and Bockelée-Morvan 2019).
- *Methyl formate* ($HCOOCH_3$) has only been detected in two comets in the radio ($\sim 0.07\%$ relative to water). It is the most abundant isomer of mass 60, with *glycolaldehyde* (CH_2OHCHO), four times less abundant, and *acetic acid* (CH_3COOH) at least two times less abundant in comet C/2014 Q2 (Lovejoy) (Biver *et al.* 2015). These molecules appear depleted in 67P compared to previous ground-based measurements (Table 3).
- *Alcohols: Ethanol* (C_2H_5OH) has been identified in four comets with an abundance around 0.1%, one order of magnitude lower than methanol. More complex alcohols have been identified in 67P by *Rosetta*/ROSINA (Altwegg *et al.* 2019).

The more complex CHO-molecules, especially those with 3 carbons have not been detected with remote observation, due to their complex spectra and decreasing abundance with molecular complexity. Only *Rosetta*/ROSINA had the sensitivity to detect species such as C_3H_6O , C_3H_8O , C_4H_8O , $C_4H_{10}O$, and $C_5H_{12}O$ (Altwegg *et al.* 2019) but other techniques are required to distinguish isomers.

4.3. Nitrogen bearing species

N-bearing volatiles are generally detectable both at IR and radio wavelengths. Evidence from both remote sensing and in-situ missions have established that comets contain many of the necessary ingredients for life from simple HCN and NH_3 to the amino acid glycine. Some N-bearing species show spatial distributions consistent with extended sources in the coma, providing further evidence for complex nitrogen molecules in comets.

4.3.1. N_2 (molecular nitrogen)

The presence of N_2 in comets has until recently been a matter of debate as its direct detection from radio or IR techniques is not possible. However, N_2^+ can be observed at near-UV wavelengths to trace N_2 abundances in comets. Detections of the $B^2\Sigma_u^+ - X^2\Sigma_g^+$ First Negative (0,0) band of N_2^+ at 391.4 nm have been claimed in the

tails of comets from low-resolution spectroscopic observations, first in photographic spectra (*Swings and Haser* 1956; *Cochran et al.* 2000) and subsequently in the coma of 1P/Halley (*Wyckoff and Theobald* 1989) and C/1987 P1 (Bradfield). However, these early detections have been questioned because at low spectral resolution N_2^+ emissions from the comet and the terrestrial atmosphere can be difficult to differentiate. More reliable detections of N_2^+ have only been reported in the last decade: in the coma of C/2002 VQ94 (LINEAR) and C/2016 R2 (PANSTARRS) using high spectral resolution (*Korsun et al.* 2014; *Cochran and McKay* 2018; *Opitom et al.* 2019a) and in the coma of the centaur 29P/Schwassmann-Wachmann 1 from low-resolution spectroscopic observations (*Ivanova et al.* 2016). In addition to the (0,0) band, the (1,1) and (0,1) bands were also detected in comet C/2016 R2 (*Opitom et al.* 2019a). The presence of N_2 in comets was confirmed by its detection in 67P by *Rosetta*/ROSINA (*Rubin et al.* 2015a), showing this highly volatile molecule is retained in the nucleus of an evolved Jupiter-family comet.

While N_2 is surely the dominant N-bearing volatile in some comets, its extremely high volatility makes it susceptible to depletion by evolutionary effects so its abundance is probably highly variable in comets, e.g., in 67P NH_3 contributed more to the nitrogen reservoir than N_2 (*Rubin et al.* 2019).

The N_2/CO ratio in cometary ices can be estimated from ground-based detection of CO^+ and N_2^+ emission band at optical wavelengths, as was done for three comets (*Korsun et al.* 2014; *Cochran and McKay* 2018; *Ivanova et al.* 2016). Inferring the relative abundance of neutrals from ion emission intensity ratio is not always straightforward but *Raghuram et al.* (2021) showed that this can be done when the ion production is controlled by photon and photoelectron impact ionization of the neutrals (rather than ion-neutral chemistry). *Rosetta* provided a direct measure of the relative abundance ($N_2/CO = 0.029 \pm 0.012$, *Rubin et al.* 2019, and Table 3), about five times higher than the value measured earlier in the mission at 3.1 au (*Rubin et al.* 2015a). The evolutionary difference between the northern and southern hemispheres (*Keller et al.* 2015a) coupled with the different illumination conditions during the two observation phases led to differences in the measured N_2/CO ratio, similar to the observations of the ratios of other species (*Läuter et al.* 2020; *Combi et al.* 2020). The presence of both species puts constraints on the maximum temperature of the material inside 67P since its formation. When comparing the measured N_2/CO ratio to the estimated primordial solar system ratio (*Lodders* 2010) a formation temperature well below 30 K for amorphous ices (cf. *Rubin et al.* 2015b, 2020) and <50 K for crystalline ices was derived (*Mousis et al.* 2016a). These results may be further modified when taking into account how these species may not be present in their pure ice forms but trapped in either CO_2 or H_2O ices (*Kouchi and Yamamoto* 1995).

4.3.2. NH_3 (ammonia)

Ammonia is an important biogenic molecule as it was likely an intermediary for synthesis of amino acids on the early Earth (*Bernstein et al.* 2002; *Muñoz Caro et al.* 2002). NH_3 can be targeted at both radio and IR wavelengths in comets but it has been measured in fewer comets than HCN owing to the relative difficulty of its detection. Mixing ratios NH_3/H_2O range from < 0.1 – 5%, with typical abundances ~ 0.5 - 1% (*Dello Russo et al.* 2016a, and references therein).

4.3.3. HCN (hydrogen cyanide)

HCN is the simplest nitrile parent volatile as well as an important intermediary for synthesis of biochemical compounds, and can be routinely detected in comets at both millimeter and IR wavelengths. HCN/H_2O mixing ratios in comets are typically ~ 0.1 – 0.2%, with no obvious differences between Jupiter-family and long-period comets. Notably, production rates of HCN in comets derived at millimeter wavelengths are typically about a factor of two smaller than those derived at IR wavelengths (*Magee-Sauer et al.* 2002; *Biver et al.* 2002). The reason for this difference has not been discovered. Modern capabilities at IR and radio wavelengths can provide sensitive spatial maps of HCN in the coma of comets. Results generally suggest that HCN in the coma comes predominately from direct sublimation from nucleus ices.

4.3.4. HNC (hydrogen isocyanide)

Hydrogen isocyanide has been detected in several comets at millimeter wavelengths. HNC also has strong vibrational bands near 5 μm , but these transitions have not been detected in comets to date. The HNC/HCN mixing ratio has been shown to increase with decreasing heliocentric distance, with a mean value around 7% at 1 au (*Lis et al.* 2008).

4.3.5. other N-bearing molecules

Additional N-bearing molecules (e.g., NH_2CHO , $HNCO$, CH_3CN , and HC_3N) have been detected in a few comets at radio wavelengths with mixing ratios on the order of 10% with respect to HCN (Table 3, *Bockelée-Morvan and Biver* 2017). More complex N-bearing molecules have also been searched for in the radio and some detected by ROSINA, but in all cases they are minor contributors to the nitrogen budget in cometary atmospheres.

- CH_3CN and HC_3N were first identified in comets Hyakutake and Hale-Bopp and have been detected in over 10 comets during the last 20 years. CH_3CN is routinely detected in cometary comae, typically representing 10 to 30% of the HCN abundance. On the other hand, the abundance of HC_3N can be more variable: generally between only 2 and 13% relative to HCN, its abundance in comet C/2002 X5 at 0.2 au from the Sun was found to be up to 40% relative to

HCN (Biver *et al.* 2011). A variation with heliocentric distance of the HC_3N abundance is not excluded.

- *isocyanic acid*, HNCO has also been detected in over 10 comets since 1996. Its abundance (Table 3) can vary between about 10 and 60% relative to HCN. This acid could also be associated with ammonium salts and its spatial distribution and the heliocentric variation of its abundance needs to be investigated.
- *formamide*, NH_2CHO has only been detected in a handful of comets (Fig. 9), with some uncertainties on its abundance due to an unknown lifetime (Biver *et al.* 2021a). Nevertheless it does not exceed 2×10^{-4} relative to water in comets and formamide could also be produced in the coma (Cordiner and Charnley 2021).

More complex N-bearing molecules have also been identified in comets (Sect.4.5.3).

4.3.6. The apparent nitrogen depletion in comets

Geiss (1988) reported an apparent lack of nitrogen in the coma of comet 1P/Halley when compared to the Sun, meteorites and terrestrial samples. These results were based on the abundances of the major N-bearing molecules NH_3 and HCN (including HNC) obtained during the *Giotto* fly-by. Similarly, abundances of NH_3 , HCN, and other minor N-bearing species in most comets measured with remote sensing techniques are consistent with this observed nitrogen deficiency (Table 3). Gases in the coma of 67P were analyzed (Rubin *et al.* 2019), this time also including molecular nitrogen, N_2 (Rubin *et al.* 2015a), which revealed a similar under-abundance of nitrogen.

The heliocentric distance dependence of $\text{NH}_3/\text{H}_2\text{O}$ in comets shows evidence for increasing ratios for smaller heliocentric distances, up to >3% for comet D/2012 S1 (ISON) (Altwegg *et al.* 2020b; Dello Russo *et al.* 2016a). This is consistent with the additional release of NH_3 from grains when a thermal threshold is reached. It has been suggested that ammonium salts may be present on the surface of comet 67P, similar to the surface of some observed asteroids, based on a broad spectral reflectance feature (Quirico *et al.* 2016; Poch *et al.* 2020). Ammonium salts are made up of the NH_3 base and an acid providing an H^+ to the base. Mass spectrometric measurements in the coma, most likely due to dust grains entering the ion source of ROSINA, revealed all possible sublimation products of the five different ammonium salts NH_4^+Cl^- , NH_4^+CN^- , $\text{NH}_4^+\text{OCN}^-$, $\text{NH}_4^+\text{HCOO}^-$, and $\text{NH}_4^+\text{CH}_3\text{COO}^-$ (Altwegg *et al.* 2020b). Direct identification of ammonium salts is difficult as they mostly dissociate into the base and corresponding acid upon sublimation of the salt. Ammonium salts may hence be released from distributed grain sources that subsequently release simpler volatiles into the coma. Assuming that the $\text{NH}_3/\text{H}_2\text{O}$ ratio of comets close to the Sun is more representative of the actual content of nitrogen, the apparent lack of cometary nitrogen could be an observational bias related

to the difficulty in directly measuring nitrogen contained in less volatile sources.

4.4. Sulfur bearing species

Eight sulfureted molecular species (or radicals) have been identified in multiple comets from remote observations primarily at radio wavelengths: H_2S , CS, SO, SO_2 , OCS, H_2CS , NS and S_2 , (Table 3, Fig. 9). The OCS ν_3 vibrational band has also been detected in the infrared at $4.85\mu\text{m}$ (e.g., Dello Russo *et al.* 1998; Saki *et al.* 2020). S_2 has only been detected in the UV via electronic transitions around 295 nm (e.g. Reylé and Boice 2003). Atomic S has also been observed in the UV (e.g., Meier and A’Hearn 1997) but is interpreted as mostly a secondary photo-dissociation product of the other sulfureted species. The total S/O ratio observed in the volatile phase ranges from 0.5 to 2%, in agreement with in-situ measurements in the coma of comet 67P by *Rosetta*/ROSINA (Rubin *et al.* 2019; Calmonte *et al.* 2016).

4.4.1. Hydrogen sulfide (H_2S)

H_2S , the dominant sulfur-bearing molecule in comets, has been detected in 34 comets since 1990 (Bockelee-Morvan *et al.* 1991), almost exclusively by its rotational lines at 168.8 and 216.7 GHz, or by in-situ mass spectrometry in comet 67P. Its abundance relative to water can vary by a factor 16 from 0.09% in the carbon-chain depleted JFC comet 21P to 1.5% in comet Hale-Bopp. However, no systematic differences in H_2S abundances are seen between JFCs and OCCs. *Rosetta* measured an average abundance of 1.1% relative to water (Calmonte *et al.* 2016) typical of a relatively H_2S -rich comet. In H_2S depleted comets, the total abundance of other sulfur-bearing species can be larger than H_2S itself.

4.4.2. Sulfur monoxide and dioxide (SO and SO_2)

The abundance of SO_2 has been measured at radio-wavelengths in two comets and abundances relative to water are in the range < 0.009 to 0.23%. SO_2 was also detected by *Rosetta* in comet 67P (0.13%). The linear molecule SO has stronger millimeter lines and has been detected in 8 comets. Although it is often assumed that SO is produced by the photolysis of SO_2 ($\beta_{0,\text{SO}_2} = 2.5 \times 10^{-4}\text{s}^{-1}$ at 1 au), there is evidence of a secondary source of SO, as suggested from interferometric maps (Boissier *et al.* 2007). *Rosetta*/ROSINA find 0.07% of SO relative to water in 67P, with evidence of direct release from the sublimation of SO ice and not as a secondary product of SO_2 (Calmonte *et al.* 2016).

4.4.3. CS and CS_2

CS has been detected in comets remotely via UV and radio spectroscopy for decades (Meier and A’Hearn 1997; Biver *et al.* 1999) with abundances between 0.03 and 0.2%. CS is a radical for which there is little information on its photolysis properties. A photo-dissociation rate around

$2.5 \times 10^{-5} \text{s}^{-1}$ at 1 au from the Sun was estimated from radio observations (Boissier *et al.* 2007; Biver *et al.* 2011). It is usually assumed that CS is a product species coming from the photo-dissociation of CS₂ (photo-dissociation rate $\beta_{0, \text{CS}_2} = 1.7 \times 10^{-3} \text{s}^{-1}$ at 1 au, Jackson *et al.* 1986). However some observations suggest a longer lifetime for the parent of CS (section 5.3.1). Rosetta/ROSINA detected CS₂ at very low abundances in 67P (Calmonte *et al.* 2016; Rubin *et al.* 2019), but unfortunately CS could not be detected.

4.4.4. OCS, Thioformaldehyde (H₂CS)

Including IR and radio techniques OCS, has been detected in 10 comets with an abundance relative to water ranging from 0.04 to 0.4%. An average value of 0.07% (Läuter *et al.* 2020) was measured in comet 67P by Rosetta.

Thioformaldehyde (H₂CS), because of its likely short lifetime and low abundance (0.009-0.09% relative to water) has been detected remotely in only two comets. ROSINA measurements in the coma of 67P yield an even lower abundance of 0.003% (Rubin *et al.* 2019).

4.4.5. S₂, S₃, S₄

Sulfur has also been detected in the form of disulfur (S₂) in cometary comae via UV spectroscopy (Reylé and Boice 2003, and references therein), and even in the form of S₃ and S₄ (Calmonte *et al.* 2016) in the coma of 67P by Rosetta. UV observations yield abundances of S₂ ranging from 0.001 to 0.02%, comparable to ROSINA findings (0.002%). But some S₂ and most of the S₃ and S₄ detected by ROSINA are estimated to be secondary products not coming from nucleus ices but from a likely warmer dust component due to their low volatility (Calmonte *et al.* 2016).

4.4.6. NS, CH₃SH, and other sulfur-bearing molecules

Several other sulfur-bearing species have been identified in the coma of 67P such as methyl mercaptan or methanethiol (CH₃SH) and C₂H₆S (Calmonte *et al.* 2016) and more complex species such as CH₄S₂, CH₄OS, C₂H₆OS, and C₃H₈OS according to Altwegg *et al.* (2019). CH₃SH has not yet been detected in a comet in the radio domain, but the abundance found in 67P (0.04% relative to water) is comparable to upper limits found in other comets (0.02-0.06%). NS was not detected in the coma of 67P but its abundance was estimated to be 0.006-0.012% in comets C/2014 Q2 and C/1995 O1. The origin of this radical is still unknown (Irvine *et al.* 2000).

4.5. Other minor species

4.5.1. Halogens

Dhooghe *et al.* (2017) reported the detection of three main halogen-bearing molecules HF, HCl, and HBr in the coma of 67P; the measured fragmentation pattern (cf. section 1.4.1) indicates at least one additional Cl-bearing compound aside from the already identified HCl, CH₃Cl, and NH₄Cl (cf. section 5.3.2, and Fayolle *et al.* 2017; Altwegg

et al. 2020b), and an increasing relative proportion of chlorine with distance indicates the likely presence of a distributed source (De Keyser *et al.* 2017).

4.5.2. Phosphorus-bearing molecules

Phosphorous has been identified in the gas phase around 67P (Altwegg *et al.* 2016) with PO being the main carrier while minor contributions of PN and PH₃ cannot be ruled out (Rivilla *et al.* 2020). Phosphorous is an important element for life and its presence supports the theory that comets may have contributed key molecules related to the emergence of life on the early Earth (Oró 1961; Schwartz 2006).

4.5.3. Glycine, amines,...

The presence of the most simple amino acid glycine has been established in the dust samples returned by the Stardust mission to comet 81P/Wild 2 (Elsila *et al.* 2009). Glycine (C₂H₅NO₂) and two of its precursor molecules, methylamine (CH₃NH₂) and ethylamine (C₂H₅NH₂), have also been detected in the coma of 67P (Altwegg *et al.* 2016). Together with the suite of C, H, O, N and S-bearing organic compounds (cf. Tab. 3 and Altwegg *et al.* 2017b) as well as phosphorous (cf section 4.5.2), comets contain elements key in prebiotic chemistry and molecules identified as possible biomarkers in the search for life elsewhere (Seager *et al.* 2016). More complex amino acids may form through aqueous alteration (Burton *et al.* 2012) but were not identified in either 81P or 67P, which limits how their material is reprocessed in larger parent bodies.

4.5.4. Noble gases Ar, Kr, Xe

The noble gases argon, krypton, and xenon have been identified in the coma of 67P (Balsiger *et al.* 2015; Marty *et al.* 2017; Rubin *et al.* 2018) with Ar abundances much lower than reported in C/1995 O1 (Hale-Bopp) by Stern *et al.* (2000). Neon, on the other hand, was below the detection limit (Rubin *et al.* 2018).

The measured relative abundances of noble gases (Tab. 3) may indicate trapping at elevated temperatures if the original abundances were solar or subsequent loss of the more volatile Ar and Ne during the comet's transition from the scattered disk, through the Centaur stage, and to its current orbit (Maquet 2015; Guilbert-Lepoutre *et al.* 2016). Another possibility, suggested by Marty *et al.* (2017), is the addition of an exotic component of xenon required to explain its isotopic composition.

4.6. O₂ (molecular oxygen)

The measured O₂ abundance in the coma of comet 67P (3.1±1.1)% relative to H₂O measured at ~1.5 au pre-perihelion (Bieler *et al.* 2015; Rubin *et al.* 2019), made it the dominant coma species after H₂O, CO₂, and CO. Furthermore, Bieler *et al.* (2015) reported a strong correlation with water despite the very different sublimation temperatures of the corresponding pure ices (Fray and Schmitt 2009). Based

on these results the presence of O₂ has also been inferred in the coma of 1P/Halley from measurements by *Giotto* NMS (Rubin *et al.* 2015b). At 67P, during suitable periods when CO₂ was at times even the dominant molecule in the coma (Läuter *et al.* 2020), O₂ was found to be correlated to CO₂ (Luspay-Kuti *et al.* 2022).

There are several possible mechanisms for the formation of O₂ in comets (cf. review by Luspay-Kuti *et al.* 2018). Dulieu *et al.* (2017) proposed the dismutation of H₂O₂ during the sublimation process, where H₂O₂ would be co-produced with the water ice explaining the correlation of H₂O and O₂. On the other hand, a high conversion of 2 H₂O₂ → 2 H₂O + O₂ would be required. Mousis *et al.* (2016b) is consistent with radiolysis of water ice as the origin of molecular oxygen with subsequent trapping in the ice, which is also consistent with the correlation between the two species. However, it is not clear these different scenarios can reproduce the observed amounts of O₂. Yet another mechanism was proposed by Yao and Giapis (2017) based on Eley-Rideal reactions forming O₂ involving energetic water ions. However, this mechanism is inconsistent with the low fluxes of energetic H₂O⁺ ions and their poor correlation with neutral water in the coma (Heritier *et al.* 2018). Additionally, all these production scenarios are at odds with the different oxygen isotope ratios between the two species (cf. section 7.3).

To date, the most promising scenario remains a primordial origin of O₂ as proposed by Taquet *et al.* (2016) where the O₂ is formed through ice grain surface chemistry and/or in the gas phase (Rawlings *et al.* 2019). A primordial origin is also favored by Luspay-Kuti *et al.* (2022).

5. FRAGMENT SPECIES

The first molecule identified in the coma of comets, C₂, is a secondary product. Secondary products are not present in cometary ices but are produced in the coma by the photo-dissociation of more complex molecules. For example, the photodissociation of water can lead to the production of OH, H, H₂, O, OH⁺, O⁺, or H⁺ in the coma. Most secondary products can be observed at optical wavelengths and are among the easiest species to detect in the coma of comets. They are commonly used to infer the composition of cometary ices when observations of parent species are lacking. However, inferring the composition of cometary ices from the abundance of secondary products in the coma is not straightforward as the parents of some radicals have not been identified. Some secondary products may also have multiple parents or be released from organic-rich grains. Species parentage in the coma of comets is a complex problem requiring further investigation and coordination of observations with modern techniques in multiple spectral regions.

5.1. Radicals

The main radicals observed in the coma of comets are OH, CN, C₂, C₃, CH, CS, NH, and NH₂. The NS radical

was also detected in the coma of a handful of comets. CO is a special case as it can be both a parent or secondary product. Feldman *et al.* (2004) explore in detail the main emissions of these radicals. They are typically observed through electronic transitions at optical wavelengths but some like OH also have transitions in the UV, radio, and IR. Most of these radicals are easy to observe at optical wavelengths and their abundances have been measured in the coma of hundreds of comets. The first taxonomic classifications of comets based on their composition relied on the systematic observations of these radicals.

The most abundant of these radicals is OH, which is produced by the photo-dissociation of water. Because the OH (0-0) band around 308 nm is one of the brightest emissions in the optical spectrum of comets, OH is often used as a water tracer and abundances of other radicals observed at optical wavelengths are often measured relative to OH. Just like for parent species, the relative abundances of radicals with respect to water (or OH) varies among comets, by more than one order of magnitude (A'Hearn *et al.* 1995; Schleicher 2008; Cochran *et al.* 2012; Langland-Shula and Smith 2011; Fink 2009). CN abundances relative to OH vary between less than 0.1% to almost 1% while C₂ exhibits a wider range of abundances: in carbon-chain depleted comets (see section 6.1.1), C₂ abundance can be lower than 0.01%, but it can reach maximum values similar to CN for typical comets. C₃ is generally less abundant than C₂ and CN, (C₃/OH = 0.005 – 0.2%). NH and NH₂ have relatively similar abundances as they are both thought to originate from the photo-dissociation of NH₃ ranging between less than 0.1% to a few %. Abundances of CH are the least well constrained of the radicals observed at optical wavelengths, partly because it isn't isolated by any of the narrow-band filters commonly used and it is usually faint in most comets. Estimates of its abundance range from about 0.3 to typically a few %.

High resolution spectroscopy has allowed the detailed characterization of the molecular band structure of several of these radicals. It has also paved the way for new modelling and laboratory measurements. For example, new models or laboratory measurements of the OH and NH₂ emission bands at optical wavelengths have been used to derive isotopic ratios of H, C, N, and O (Rousselot *et al.* 2014; Hutsemékers *et al.* 2008). Significant progress has also been made in the observations and modelling of CN, and especially the (A-X) red system, whose (0-0) band has a bandhead around 1100 nm (Paganini and Mumma 2016; Shinnaka *et al.* 2017).

5.2. Atoms

In addition to radicals, emissions from atoms are also detected at UV and visible wavelengths. HI, OI, CI, NI, SI and the ions CII, OII, have all been observed in the coma of comets, in the 80-200 nm range via solar fluorescence (Feldman *et al.* 2004) and electron impact dissociative excitation of their parent in the inner coma of 67P (Bodewits

et al. 2022; *Feldman et al.* 2015). HI Lyman- α emission at 121.6 nm, which totals almost 98% of far-UV emission in comets, has been used to estimate the water abundance in the coma of several dozen comets, in particular using the SWAN instrument onboard SOHO (*Combi et al.* 2019). At optical wavelengths, the most prominent atomic features are the three forbidden OI emission lines at 557.73 nm, 630.03 nm, and 636.38 nm. These lines have been used for a number of years to estimate the water production rate and more recently as an indirect way to estimate the ratio between H₂O and CO₂ abundances in the coma of comets (*Festou and Feldman* 1981b; *Schultz et al.* 1992; *Morghenthaler et al.* 2001; *McKay et al.* 2013; *Decock et al.* 2013). Forbidden [CI] lines at 872.7, 982.4, and 985.0 nm, coming from the photo-dissociation of neutral C-bearing species, have also been detected in the coma of C/1995 O1 (Hale-Bopp) and C/2016 R2 (PANSTARRS) (*Oliveresen et al.* 2002; *Opitom et al.* 2019a). Recently, lines at 519.79 and 520.03 nm in the coma of C/2016 R2 (PANSTARRS) were identified as forbidden nitrogen lines (*Opitom et al.* 2019a). To this day, [NI] lines have only been detected in the coma of a single comet.

The sodium D-line doublet was identified in comets over a century ago (*Newall* 1910). This emission is difficult to observe from ground-based observatories due to telluric sodium lines. It has been mostly observed in the coma of comets well within 1 au from the Sun, manifesting as a neutral tail. Sodium detection in several comets is discussed by (*Feldman et al.* 2004). There is no present consensus on the origin of neutral sodium in comets as both nucleus ice and dust grain sources have been proposed (*Cremonese et al.* 2002). However, the detection of sodium in dust grains and in gas phase in the coma of 67P was reported from *Rosetta* data (*Schulz et al.* 2015; *Wurz et al.* 2015; *Rubin et al.* 2022).

In exceptional cases when a comet passes very close to the Sun, other heavier elements are detected in the coma. Emission lines from Ca, K, V, Cr, Mn, Fe, Co, Ni, and Cu were detected in the coma of sungrazing comet C/1965 S1 Ikeya-Seki (*Preston* 1967; *Slaughter* 1969). These elements are typically only detected in the coma of sungrazing comets because of the extremely high temperatures needed to release them through the sublimation of dust grains. Si was detected in the coma of comet C/2011 W3 (Lovejoy) with the UVS onboard SOHO (*Raymond et al.* 2018). *Fulle et al.* (2007) also reported the discovery of an atomic iron tail for comet C/2006 P1 (McNaught) at a heliocentric distance of 0.3 au from observations with the STEREO spacecraft. More recently *Manfroid et al.* (2021) showed that FeI and NiI emission lines are present in the coma of comets at a variety of heliocentric distances, from 0.7 to > 3 au. This discovery was surprising as neither iron or nickel were detected by *Rosetta*. Their detection at large distances from the Sun rules out a production from the sublimation of dust grains as is the case for sungrazing comets. *Manfroid et al.* (2021) suggest that iron and nickel could be contained in cometary ices within organometallic com-

plexes (e.g. [Fe(PAH)]⁺) or carbonyls such as Fe(CO)₅ and Ni(CO)₄.

5.3. Species parentage and release mechanisms

While some species like OH have well identified production mechanisms, it is not the case of all radicals. Some radicals have several potential parents, while for others no parent has been identified to date. Understanding the parentage of secondary products in the coma of comets provides a window into the composition of the nucleus.

5.3.1. Identifying parent molecules

NH and NH₂. It is generally believed that both NH and NH₂ result from the photo-dissociation of ammonia. NH would be a third-generation product, with NH₃ being first dissociated into NH₂, and subsequently into NH. Comparison of the abundances of NH, NH₂, and NH₃ to confirm this parentage is limited by a lack of simultaneous measurements of these species, the difficulty in detecting NH₃, and the uncertainty of NH scalelengths (*Fink et al.* 1991; *Feldman et al.* 2004).

CN. It has long been postulated that photo-dissociation of HCN is the dominant source of CN in the comae of comets. If this is true, then CN and HCN production rates measured simultaneously should be consistent with each other. However, for some comets, derived HCN abundances are significantly lower than those reported for CN (*Fray et al.* 2005; *Dello Russo et al.* 2009, 2016b). Inconsistencies between HCN and CN production rates were also observed in coma of 67P, from measurements with the ROSINA mass spectrometer (*Hänni et al.* 2020). *Bockelee-Morvan and Crovisier* (1985) argued that the spatial profile of CN in the coma did not match a Haser model assuming release by the photodissociation of HCN. This is strong evidence that another source other than HCN plays a role in the production of CN in the coma of at least some comets. Other parent molecules have been investigated by *Fray et al.* (2005) who find that C₂N₂, HC₃N, and CH₃CN, have lifetimes consistent with the parent of CN, even though their abundances in comets are likely insufficient to explain CN abundances. Sublimation of carbon-rich dust grains, CHON particles, or other macro-molecules in the coma have also been suggested as potential extended sources of CN.

C₂ and C₃. The formation pathways of C₂ and C₃ are even less clear. Molecules like C₂H₂ and C₂H₆ were suspected to be potential parents of C₂ (e.g., *Jackson* 1976) even before they were first detected at IR wavelengths in the 1990's (*Brooke et al.* 1996; *Mumma et al.* 1996). The photodissociation of C₃ itself is also thought to contribute to the formation of C₂. C₃ parents are less obvious but C₄H₂ and C₃H₄ were proposed in the 60s-70s by *Swings* (1965) and *Stief* (1972). Other potential parents for the two radicals include HC₃N and C₂H₄. Because the spatial distribution of C₂ in the inner coma of comets is often flatter than what would be expected from the simple photo-dissociation of a parent molecule, *Combi and Fink* (1997) suggested that

C₂ might be released from a distributed source like CHON grains or by a two-step process. To this day, attempts to link C₂ and C₃ to potential parents through photochemical modelling have had mixed results: *Helbert et al.* (2005) concluded that C₃ could have C₃H₄ as main parent in C/1995 O1 (Hale-Bopp) while *Weiler* (2012) found that the breakdown of C₂H₆ does not produce C₂ efficiently enough to be a major parent in most comets. As pointed out by *Hölscher* (2015), some of the reactions in the chemical models used to estimate the origin of C₂ and C₃ have poorly known rate coefficients. Additionally, only some of the parents considered in the chemical networks mentioned above have been detected from ground-based observations of comets: HC₃N, C₂H₆, C₂H₂ (see, e.g., *Bockelée-Morvan and Biver* 2017). *Rosetta* detected many saturated molecules and even more unsaturated ones containing at least 2 carbon atoms that could be potential C₂ and C₃ parents (*Schuhmann et al.* 2019). Among all potential parents, C₃H₄ is not the most abundant, so it is likely not the only (or even primary) C₃ source in the coma of 67P. *Altwegg et al.* (2019) conclude that there are probably many parents leading to the production of these two radicals, with their exact contributions likely variable from comet to comet.

CS. Another radical with uncertain parent is CS. It has been assumed to generally come from the photodissociation of CS₂. Most observations show evidence of production in the coma at least compatible with its production from CS₂, but a few constraints on the parent scale-length yield 2 – 4× longer lifetimes ($\tau_0 = 1/\beta_0 = 1000 - 2500$ s, *Biver et al.* 1999; *Roth et al.* 2021, respectively) for the parent of CS than expected if the parent is CS₂. The low CS₂ abundances measured at 67P by *Rosetta*/ROSINA compared to CS abundances measured in other comets (Table 3) suggests that it is not the main parent of CS.

5.3.2. Distributed sources and production versus r_h

Few comets are observed spectroscopically at small heliocentric distances (r_h) and information on long term variability of composition from small heliocentric distances to greater than 1 au is lacking. However, there is emerging evidence from global molecular associations within the comet population that production rates of some molecules increase at smaller heliocentric distances relative to others (e.g., *Dello Russo et al.* 2016a). These species, including C₂H₂, H₂CO, and NH₃, have been traditionally considered as parents released from nucleus ices. From infrared observations of D/2012 S1 (ISON), *DiSanti et al.* (2016) report an increase of the NH₃, NH₂, HCN, H₂CO, and C₂H₂ to H₂O ratio within 0.5 au while from optical observations (*McKay et al.* 2014) report increase of CN, C₂, CH, and C₃ abundances relative to H₂O. From *Rosetta* measurements, *De Keyser et al.* (2017) found changes of the relative abundance of the hydrogen halides HF and HCl with decreasing heliocentric distance in the coma of 67P. Observations also show evidence of a strong dependency of

the CS abundance with heliocentric distance in the coma of comets (*Biver et al.* 2006, 2011, and references therein), roughly as $Q_{CS}/Q_{H_2O} \propto r_h^{-1}$, down-to heliocentric distances as low as 0.1 au. A possible explanation for this behavior is significant release of these species from a distributed source of less volatile grains once a thermal threshold is reached. Because of the relative difficulty of detecting species like C₂H₂ and NH₃ in comets, confirming extended release through spatial distributions is challenging; however, there is evidence of extended release of these from spatial studies in bright comets (e.g., *Dello Russo et al.* 2016b, 2022; *DiSanti et al.* 2016). The presence of ammonium salts (NH₄⁺X⁻) in cometary ices was inferred based on observations with *Rosetta*/ROSINA (*Altwegg et al.* 2020b) and laboratory experiments (*Poch et al.* 2020). Sublimation of ammonium salts, which happens at higher temperature than for species like HCN or even water, could account for the additional source of HCN and NH₃ at small heliocentric distances.

Other evidence also seem to indicate that some volatiles usually considered as parent volatiles could be released from extended sources even at typical heliocentric distances beyond 1 au. OCS showed a broad spatial distribution that is evidence of a possible extended source in C/1995 O1 Hale-Bopp (*Dello Russo et al.* 1998), but high signal-to-noise measurements of OCS are rare so it is unclear if this behavior is typical. Chemical models also suggest that much of the HC₃N and NH₂CHO seen in comets at radio wavelengths could be produced from reactions in the coma (e.g., *Cordiner and Charnley* 2021). Some comets have an inferred upper limit for the SO₂ abundance that is lower than the measured abundance for SO (e.g., C/2014 Q2, *Biver et al.* 2015), which also suggests that there is another source of SO, or that SO is a parent molecule. Further interferometric observations are needed to test the sources of SO in a larger subset of comets.

Radio observations have also shown that the abundance of H₂CO relative to water (e.g., *Biver et al.* 2002) and the HNC/HCN ratio (*Lis et al.* 2008) increase with decreasing heliocentric distance. While infrared observations indicate significant nucleus sources of formaldehyde (H₂CO) (*Dello Russo et al.* 2016a), measurements from the *Giotto* flyby (*Meier et al.* 1993) and radio and interferometric data point to an extended emission of formaldehyde for several comets (*Colom et al.* 1992; *Biver et al.* 1999; *Roth et al.* 2021). Millimeter studies and ALMA observations suggest that the unknown formaldehyde parent would have a scale-length between 1000 and 6800 km (*Bockelée-Morvan et al.* 2000; *Cordiner et al.* 2014; *Cordiner et al.* 2017), which is shorter than the dissociation scalelength of CH₃OH, which mostly dissociates into H₂CO according to (*Huebner and Mukherjee* 2015). Thermal degradation of polyoxymethylene (POM, *Fray et al.* 2006) has been proposed as parent source of formaldehyde. Similarly, radio interferometric data indicate that HNC is mostly produced in the coma within a few thousands of km (*Cordiner et al.* 2014; *Roth et al.* 2021) and could be released from the degrada-

tion of nitrogen-rich grains (Cordiner *et al.* 2017) or come from the photodissociation of a more complex nitrile parent (Rodgers and Charnley 2001). More studies are necessary to better quantify the importance of extended sources for the production of species like OCS, H₂CO, HNC, or NH₃ and their variation among comets.

6. VARIATIONS OF COMA COMPOSITION

Cometary composition is often deduced by measurements obtained at few (or one) points in time. These snapshots are frequently the only information that is available on the chemistry of a particular comet. Recently, longer timescale measurements of comets have had been increasingly obtained. It is clear in many cases from ground-based observations obtained over long time periods and *Rosetta* measurements of 67P over much of its orbit that measured relative abundances of volatile species often vary with time. This variability within a comet must be accounted for when comparing measured compositions between comets. A key question is whether these temporal effects seen in individual comets due to heterogeneous active areas are signatures preserved from comet formation (natal) or have evolved through various processes over time.

6.1. Differences in composition between comets

6.1.1. Taxonomic classes

Following the work done by A’Hearn *et al.* (1995) based on narrowband visible photometry of product species in 85 comets and a subsequent update on over 153 comets (Schleicher 2008), IR and radio spectroscopy based datasets also enable classification of comets according to the composition of parent volatiles. Dello Russo *et al.* (2016a) and Lippi *et al.* (2021) have established a taxonomy based on the composition of 20 to 30 comets observed at IR wavelengths, using the abundances of HCN, CH₄, C₂H₆, C₂H₂, CH₃OH, H₂CO, CO and NH₃. Earlier attempts based on radio spectroscopy haven’t established significant sub-grouping based on, e.g., principal component analysis of the abundances of four to eight molecules. Difficulties are often linked to the consistency of the dataset, dealing with the largest number of comets versus dealing with a more limited number of objects with more precise abundance determinations for a larger number of molecules. Histograms showing the distribution of abundances relative to water (or OH) based on visible, IR and radio data show that for most molecules the distribution of abundances is typically Gaussian with a total width smaller than a factor ~ 10 (Figs. 10–11). Evidence from the optical taxonomy from A’Hearn *et al.* (1995) shows that a group of comets is depleted in carbon-chain (C₂ and C₃) molecules, by typically one order of magnitude (Fig. 11). Dello Russo *et al.* (2016a) has established that arbitrary groupings of comets can be made based on their hydrocarbon, CH₃OH, HCN, NH₃, CO and H₂CO content and, as established by A’Hearn *et al.* (1995) for product species, also showed that the heliocentric dependence of parent abundances are also vari-

able. Comets depleted in C₂H₂ in the IR are not necessarily correlated with the carbon-chain depleted group of comets from optical measurements. There is however some evidence that carbon-chain depleted comets have a rather low abundance of methanol in radio investigations (Biver *et al.* 2021b). However, for some molecules the distribution shown in Figs. 10–11 might be better fitted by two Gaussians which suggests that additional data are needed to characterize molecular trends in comets.

6.1.2. Outliers

Even considering the dispersion in molecular abundances seen within the comets observed over the last decades, a few comets show more extreme differences of one or two orders of magnitude in some molecular abundances. Comet C/2016 R2 (PanSTARRS) seems to be a member of a class of “blue” comets comprising also C/2002 VQ₉₄ (LINEAR), C/1961 R1 (Humason), C/1908 R1 (Morehouse) and possibly 29P/Schwassmann-Wachmann 1. A few other cases based on visible spectroscopy are given in Cochran *et al.* (2000). As observed at 2.7 au from the Sun, the coma of comet C/2016 R2 shows a very unusual composition, strongly enriched in CO, N₂ and CO₂, compared to other comets even at the same heliocentric distance (Table 2 and Biver *et al.* 2018; McKay *et al.* 2019; Korsun *et al.* 2014). The CO:N₂:CH₃OH:HCN ratio are typically orders of magnitude different from other comets. Explanations for such differences could be that either these comets are fragments of a differentiated TNO that were formed mostly from the volatile part of its surface, or that they formed further away than most of the comets, beyond the CO/N₂ ice lines (Mousis *et al.* 2021). The interstellar comet 2I/Borisov is also relatively enriched in CO compared to HCN (Cordiner *et al.* 2020), but still much closer to the tail of the distribution observed in solar system comets.

Optical observations have also revealed potential compositional outliers such as comets 96P/Machholz and C/1988 Y1 (Yanaka): Schleicher (2008) found them very depleted in CN and C₂ with abundances relative to OH typically two orders of magnitude lower than the average value measured in comets while (Fink 2009) found them typical regarding their NH₂ content.

6.2. Heterogeneity, evolution of the coma

6.2.1. Temporal variability, outbursting and split comets

Secular evolution in composition with time can also be investigated either on a short or longer time scales for periodic comets. For example, 2P/Encke (Radeva *et al.* 2013; Roth *et al.* 2018) showed large compositional changes between two apparitions (2003 and 2017), showing a substantial decrease of C₂H₆ and CH₃OH by factors of 8 and 4 respectively, whereas H₂CO abundances relative to water increased by a factor of 3. However, these observations were not obtained during the same orbital phase and might be related to seasonal changes on the nucleus of 2P. On the other hand, comet 21P/Giacobini-Zinner was observed at three

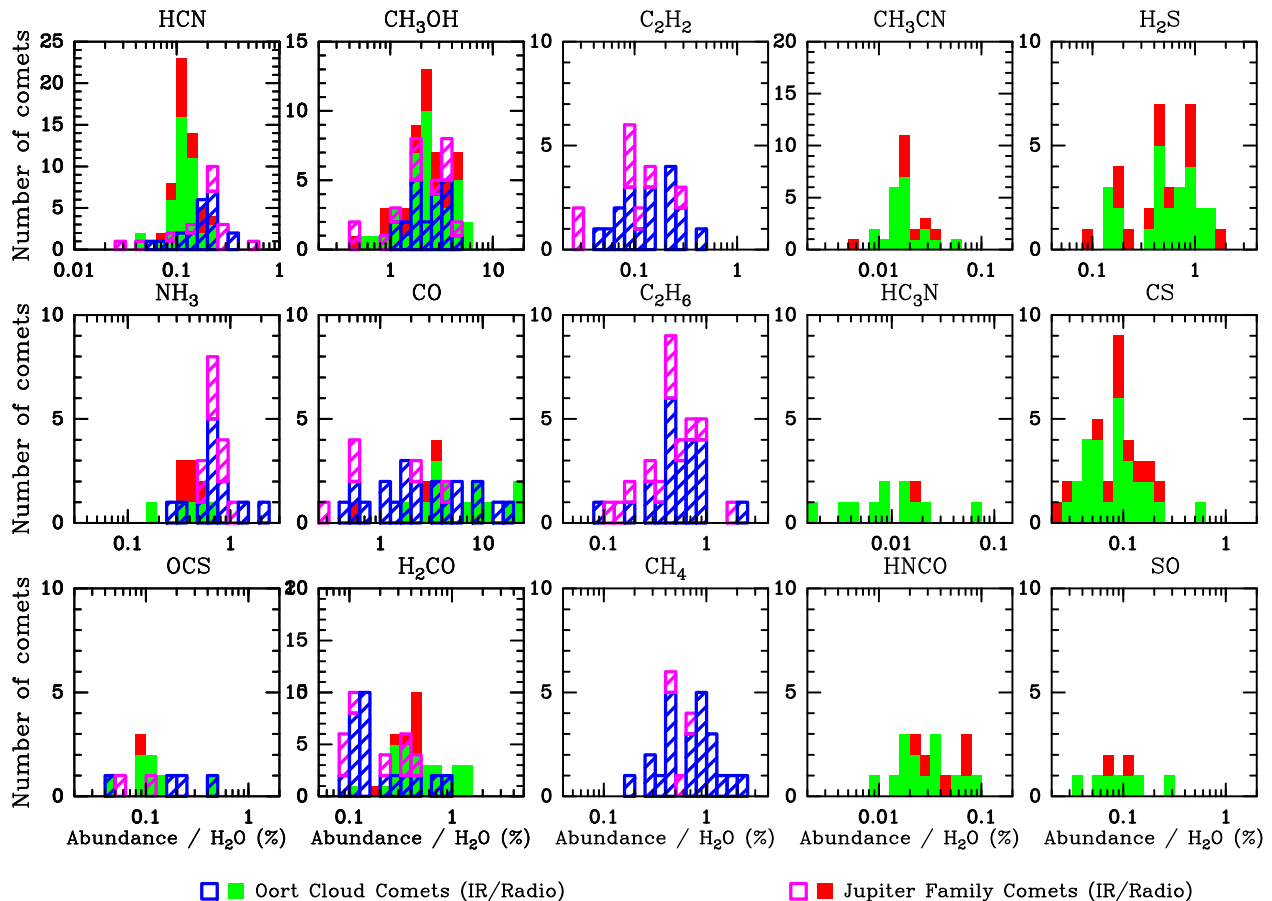


Fig. 10.— Histograms (number of comets in each bin of abundance relative to water) of molecules observed in several comets both in the radio and in the infrared. Radio data correspond to filled bars and infrared are hatched. Blue-green colors are for comets originating from the Oort cloud (OCC), on periodic to parabolic orbits of any inclination. Red-pink colors are for JFCs in low inclination orbit with short period. HCN shows more systematic scatter from infrared data while in the other cases similar behavior is observed from the two techniques, infrared being able to sample comets with lower CO abundance. Excepted for CO which is less abundant on average in JFC (by a factor 4 *Dello Russo et al.* 2016a), there is no significant difference between JFCs and OCCs, with a scatter in abundance that can reach one order of magnitude.

apparitions close to its perihelion time, in 1998, 2005, and 2018, and showed only minor short-term daily variations in abundances, with about the same average coma composition during each apparition (*Weaver et al.* 1999; *Mumma et al.* 2000; *DiSanti et al.* 2013; *Roth et al.* 2020; *Biver et al.* 2021b; *Moulane et al.* 2020). Generally the carbon-chain depleted comets within the visible taxonomy (previous Section) show this characteristic behavior at each perihelion which is indicative that a specific coma composition is generally characterizing each comet.

Comet compositional heterogeneity can often be rigorously tested when a comet breaks up or fragments. First, fragmenting comets release volatiles from the previously protected interior of the nucleus that is likely more indicative of primitive material. Second, when a comet completely disintegrates or loses a significant amount of its mass, subsequent measurements of coma material should

be representative of the bulk nucleus. Third, when comets fragment into pieces that are large enough to separately investigate, the chemistry of different parts of the original nucleus can be sampled and compared. 73P/Schwassmann-Wachmann 3 split in several pieces in 1995, and subsequently came within 0.08 au of the Earth in 2006 allowing observations with high sensitivity. Fragments C, B, and G showed a very similar composition from radio (*Biver et al.* 2008), IR (*Dello Russo et al.* 2007), and visible investigations (*Schleicher and Bair* 2011). Measurements so far suggest that the degree of heterogeneity within comet nuclei is variable, and the likely cause of time variation (selective sublimation due to temperature threshold, seasonal variation due heat wave propagation or modification of near surface composition after multi-perihelion passages) might not exclude a more homogeneous composition seen in many comets.

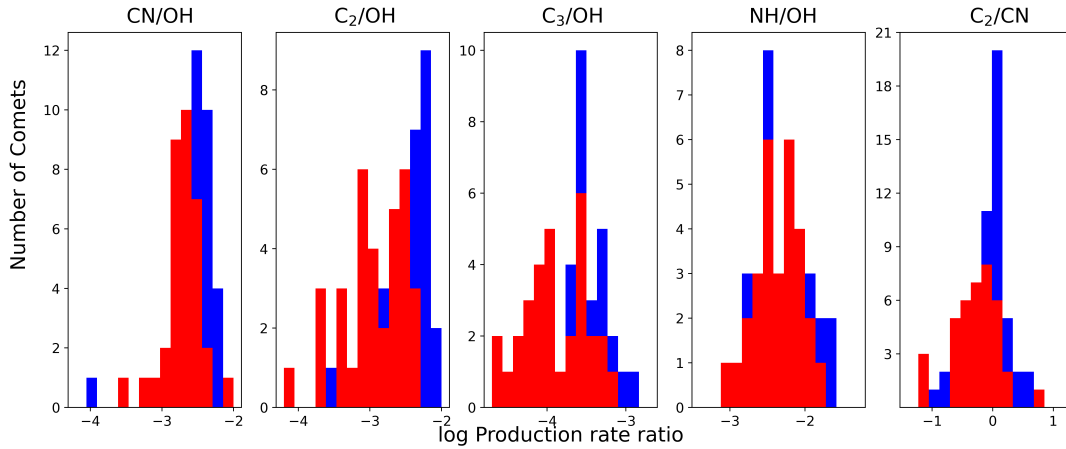


Fig. 11.— Histograms of abundances relative to OH or CN based on observations of radicals in the visible range from *Osip et al. (2010)*, based on the data set of *A’Hearn et al. (1995)*. Blue color is for comet originating from the Oort cloud (OCC), on periodic to parabolic orbits of any inclination. Red color is for JFC in low inclination orbit with short period.

6.2.2. Local differences in the coma

Seasonal and diurnal variations in the (relative) abundances of volatile parent species have been observed in H_2O and CO_2 (cf. section 3.2) but also in many other species (*Feaga et al. 2007; Hässig et al. 2015*). Non-homogeneity has also been reported for the radical species OH, [O I], CN, NH, and NH_2 , albeit more diffuse given their origin from dissociation of cometary parent molecules (*Bodewits et al. 2016*). *Le Roy et al. (2015)* reported relative abundances for a suite of species measured at comet 67P at 3.1 au inbound. In this comparative study strong differences in the coma composition above the northern summer versus the southern winter hemisphere were obtained. CO varied from 2.7% to 20% and CO_2 from 2.5 to 80% with respect to H_2O north to south. *Bockelée-Morvan et al. (2015)* reported a range of 2 to 30% for CO_2 using VIRTIS-H but this may be explained by the difference in the measurement technique, taking into account that local measurements can lead to much higher variations compared to remote sensing observations representing global integrated densities along a column (cf. section 1). When the southern winter hemisphere was poorly illuminated, increased ratios of CO, CO_2 , CH_4 , C_2H_2 , C_2H_6 , HCOOH , HCOOCH_3 , HCN, OCS and CS_2 with respect to H_2O were measured, whereas for some other organics the differences were less striking (*Le Roy et al. 2015*). A difference was also noted from ground-based measurements of the global CN abundance (*Opitom et al. 2017*). This was expected due to the low volatility of water relative to these species. However, CO, CO_2 , CH_4 , C_2H_2 , C_2H_6 , HCN, OCS, and CS_2 were also more abundant in absolute numbers above the southern winter hemisphere at 3.1 au inbound. This hints at a heterogeneous nucleus, most likely caused by evolutionary processes as the southern hemisphere is subject to significantly higher

rates of erosion per orbit (*Keller et al. 2015a*). A plausible explanation is that erosion exposes fresh material from the comet’s interior to sublimation. However, once the southern hemisphere became more active during the short and intense summer months, the measured ratios with respect to water above the south at ~ 1.5 au (*Rubin et al. 2019*) were similar to within a factor of a few to the ones measured above the northern hemisphere at ~ 3.1 au (*Le Roy et al. 2015*). This indicates that the measured heterogeneity is also illumination dependent and hence temperature driven and occurs on seasonal as well as diurnal time-scales (*Hässig et al. 2015*), further modified by recondensation of H_2O (*De Sanctis et al. 2015*). It may also provide clues as to how different species are embedded inside the ices of the nucleus.

6.2.3. Groups of Molecules sharing similar behaviors

Cometary volatile species exhibit different outgassing patterns when it comes to seasonal (see, e.g., *Biver et al. 2002*) and diurnal patterns (cf. *Hässig et al. 2015*). It is no surprise that the volatility of the different ices can play a crucial role in the outgassing behavior of the nucleus. Hence, the relative abundances of the major volatiles CO and CO_2 with respect to H_2O tend to be lower near the comet’s perihelion compared to larger heliocentric distances (cf. *Ootsubo et al. 2012*).

Rosetta allowed an investigation of the relative abundances of species on diurnal and seasonal time-scales. Very early in the mission, substantial amounts of O_2 were detected (cf. section 4.6 and *Bieler et al. 2015*). Interestingly, there was also high correlation between the production of O_2 and H_2O , despite the vastly different sublimation temperatures of the corresponding pure ices (*Fray and Schmitt 2009*). On the other hand O_2 showed much lower correlation to CO and N_2 . A similar picture was also obtained for

other volatiles, e.g. NH_3 and H_2O (Läuter et al. 2020; Biver and Bockelée-Morvan 2019) and among the noble gases Ar, Kr, Xe together with N_2 (Balsiger et al. 2015; Rubin et al. 2018).

Gasc et al. (2017) investigated the change in outgassing of H_2O , CO_2 , CO , H_2S , CH_4 , HCN , O_2 , and NH_3 as a function of heliocentric distance during the outbound path past the second equinox. As mentioned above, H_2O , O_2 , and NH_3 dropped rapidly as the comet moved away from the Sun. CO_2 , CO , H_2S , CH_4 , and HCN , on the other hand, dropped much more gradually and furthermore exhibited strong heterogeneity where the region of peak outgassing did not follow the sub-solar latitude. Little correlation to the pure-ice sublimation temperatures were observed, i.e., O_2 (~ 30 K) behaved very similar to H_2O (~ 144 K) but very different from CH_4 (~ 36 K). The strongest decrease in outgassing was observed for water while the CO_2 activity dropped by the smallest amount of the species listed above.

Volatile production rates measured over large timescales suggested two distinct ice phases in 67P, associated with either H_2O or CO_2 release (Hässig et al. 2015; Fink et al. 2016; Gasc et al. 2017). Two types of ices, a polar phase dominated by H_2O and an apolar phase dominated by CO and CO_2 , have also been observed in the interstellar medium and young stellar objects (Boogert et al. 2015; Mumma and Charnley 2011). At 67P, CO_2 appeared correlated with C_2H_6 , CO , H_2S , and CH_4 (Luspay-Kuti et al. 2015; Hässig et al. 2015; Gasc et al. 2017), whereas H_2O appeared correlated with CH_3OH , NH_3 , and O_2 (Luspay-Kuti et al. 2015; Gasc et al. 2017). Some relationships varied with time; for example, HCN was sometimes correlated with CO_2 (Gasc et al. 2017) and at other times with H_2O (Luspay-Kuti et al. 2015). The correlation of O_2 with H_2O furthermore suggests that polarity was not the sole reason for this behavior. On the other hand, the different formation and processing mechanisms of some of these species, such as grain surface, gas phase chemistry, radiolysis, and thermal processing are likely key. Because the drop in outgassing of all these cometary parent molecules is bracketed by the two major species (Rubin et al. 2019; Läuter et al. 2020; Combi et al. 2020), H_2O and CO_2 , Gasc et al. (2017) suggested that all minor species are trapped in different proportions within H_2O and CO_2 and then released during phase transitions or co-desorbed during sublimation (Kouchi and Yamamoto 1995; Mousis et al. 2016b). It is possible that at one time minor species were present in their pure ices but that they are not anymore (or only to a very limited degree), with cometary activity governed by water and carbon dioxide. In this scenario, outgassing may be further modified by recondensation and resublimation processes (De Sanctis et al. 2015).

For both comets and the interstellar medium, laboratory measurements are key to understanding this behavior (Kouchi and Yamamoto 1995; Collings et al. 2004; Laufer et al. 2017). However, mixed ice experiments in the laboratory are quite challenging for species present in trace amounts, i.e. $\ll 1\%$ with respect to H_2O and/or CO_2 . But

this corresponds to exactly the situation encountered at 67P. Furthermore, as the volatile coma structure in comets is explored by spacecraft it becomes important to connect these high-resolution spatial results with the global coma results obtained for a large number of comets from remote sensing observations.

6.2.4. Present day composition: Natal or evolved?

Ices within comet nuclei have been protected since formation by an overburden of material; thus, cometary volatiles observed today likely retain signatures from their birth. Yet comets are not perfectly preserved early solar system relics, as each nucleus has experienced a unique processing history over its long life, especially (but not only) during close passages to the Sun. Determining the degree to which comets retain their natal character is a fundamental question, but one that is difficult to answer. First, comets from the Jupiter family and the Oort cloud have quite different dynamical histories; however, comet forming regions were vast which leads to significant expected and observed compositional diversity within each dynamical class. Second, while some systematic compositional differences have been seen between comets from different dynamical classes on average, this could plausibly reflect either different evolutionary histories or distinct formative regions.

As volatile abundances have been determined in an increasing number comets, there are several avenues of investigation that allow natal versus evolutionary effects in comets to be tested. (1) Determining abundances of the most volatile parents (e.g., N_2 , CO , CH_4) shows the proficiency of comets in preserving these low sublimation temperature (hypervolatile) species. (2) Observations of Jupiter-family comets over multiple apparitions with modern instrumentation that allow detailed compositional information to be obtained is now feasible. (3) Spatial distributions of parent molecules in the coma provide evidence for how ices are associated or sequestered in the nucleus. Determining spatial distributions in many comets can test which spatial properties and possible ice associations in the nucleus are comet-specific and which are global among the population of comets.

7. ISOTOPIC AND ORTHO-TO-PARA RATIOS

Isotopic ratios provide key information on the origin of cometary material. The abundances of the heavier elements in a molecule were determined by the reservoir of heavy isotopes such as HD, atomic D or H_2D^+ , present during formation of these ices and the chemical reactions that happened during this time (e.g., Taquet et al. 2013). Reactions in the gas phase or in grain-gas interactions lead to various fractionation mechanisms in the ISM. Then when the planets formed in a warmer environment in the protoplanetary disk, further fractionation occurred due to sublimation, photodissociation screening, mixing, and recondensation at various distances and temperatures. The results of these

temperature and processing conditions, including isotopologues abundances, may have been frozen in cometary ices. So, isotopic ratios measured in the sublimating gas phase today may reveal their original value 4.6 Gy ago. However, the impact of isotopic exchange in the ice phase and during sublimation is a subject of debate.

The ortho-to-para ratio (OPR) or spin temperature may be an estimate of the temperature of the molecules when they condensed into the icy grains that formed cometary nuclei. The change of spin state of a molecule is in principle strictly forbidden during collisions or radiative transitions and can only occur through chemical reactions, so present-day spin temperatures may be unchanged since cometary ices formed.

7.1. D/H ratios

D/H is the isotopic ratio of greatest interest as hydrogen is the most abundant element in the universe and the difference in the atomic mass (a factor of two) is the largest, causing significant differences in D/H ratios in various molecules. The main molecular reservoir of deuterium in the cold universe and Solar System is HD, but in comets it is HDO. Strong enrichment in deuterium in water ($D/H=10^{-4}$ to 10^{-3}) and other molecules is observed in star forming regions (e.g., *Drozdovskaya et al. 2021*; *Jensen et al. 2021*) and in the Solar System. The reference D/H on Earth, the Vienna Standard Mean Ocean Water (VSMOW) value, is 1.558×10^{-4} , while in the local interstellar medium (ISM) the D/H value in molecular hydrogen is 2×10^{-5} . The HDO abundance in cometary ices is of key interest, especially when considering that comets may have contributed a significant amount of water to the young Earth. The D/H in water is half the HDO/H₂O, since there are two H atoms that can be substituted by D: $D/H = 1/2 \times (HDO/H_2O \text{ or } DHO/H_2O)$.

D/H in cometary water has been measured in a dozen comets (Fig. 12) with sensitive upper limits obtained in a few others. Cometary D/H varies between one and four times the VSMOW value as measured by different techniques. Radio spectroscopy samples HDO in the coma generally over thousands of km around the nucleus via the $J_{K_a K_c} = 1_{01} - 0_{00}$ line at 464.9 GHz, the $1_{10} - 1_{01}$ line at 509.3 GHz, or the $2_{11} - 2_{12}$ line at 241.6 GHz. HDO production rates determined at radio wavelengths are subject to uncertainty in the excitation model. IR spectroscopy (as well as UV spectroscopy of OD) is in theory less sensitive to coma temperature since it integrates several rovibrational lines within a vibrational band (electronic band in the UV). In both cases precise determination of the HDO/H₂O, requires the detection of several HDO lines as well as the simultaneous detection of the water. However, H₂O and HDO are typically sampled through observations of lines in different spectral regions that require additional instrument settings. Values of the D/H in water measured in comets have no apparent correlation to the dynamical origin (Jupiter-Family vs Oort cloud long period). It has been

suggested recently by *Lis et al. (2019)* that the D/H could be anti-correlated with hyperactivity of the comet. For example, comets with an equivalent active surface larger than 100% would have terrestrial D/H while those with small active surface like comet 67P have higher D/H. More measurements of D/H in comets are needed to test if this effect is real and whether this could be dictated by differences in formation conditions between hyperactive and low activity comets.

D/H has also been measured in a handful of other molecules in the volatile phase: DCN was remotely detected in C/1995 O1 Hale-Bopp (*Meier et al. 1998*) with a D/H eight times the VSMOW value. Measurements with ROSINA on-board the *Rosetta* spacecraft have found even higher enrichment in deuterium in other molecules such as D₂O ($D_2O/HDO = 1.8 \pm 0.9\%$), HDS, CH₃OD/CH₂DOH. These are often expected as fractionation processes in the ISM and star forming regions yield similar enrichments (*Drozdovskaya et al. 2021*). D/H measurements in cometary comae are presented in Table 4.

Table 4: D/H in cometary molecules

Deuterated molecule	D/H value	comet
HDO	$1.4 - 6.5 \times 10^{-4}$	Several
HDCO	$< 70 \times 10^{-4}$	C/2014 Q2 ^b
HDS	$12 \pm 3 \times 10^{-4}$	67P ^{a*}
	$< 170 \times 10^{-4}$	C/2014 Q2 ^b
	$< 80 \times 10^{-4}$	17P/Holmes ^x
DCN	$23 \pm 4 \times 10^{-4}$	Hale-Bopp ^{c,d}
NH ₂ D	$11 \pm 2 \times 10^{-4}$	67P ^a
	$< 400 \times 10^{-4}$	Hale-Bopp ^f
CH ₃ D	$24 \pm 3 \times 10^{-4}$	67P ^a
	$< 64 \times 10^{-4}$	C/2004 Q2 ^e
	$< 50 \times 10^{-4}$	C/2004 Q2 ^f
C ₂ H ₅ D	$24 \pm 3 \times 10^{-4}$	67P ^a
CH ₃ OD	$140 \pm 30 \times 10^{-4}$	67P ^g
CH ₂ DOH	(for same deuteration on each H)	
CH ₃ OD	$< 300 \times 10^{-4}$	Hale-Bopp ^d
	$< 100 \times 10^{-4}$	C/2014 Q2 ^x
CH ₂ DOH	$< 80 \times 10^{-4}$	Hale-Bopp ^d
	$< 35 \times 10^{-4}$	C/2014 Q2 ^x
Doubly deuterated species (see text for D ₂ O)		
CHD ₂ OH	$110 \pm 10 \times 10^{-4}$	67P ^g
CH ₂ DOD	(for same deuteration on each H)	

Refs.: ^a*Müller et al. (2022)*, ^b*Biver et al. (2016)*, ^c*Meier et al. (1998)*, ^d*Crovisier et al. (2004)*, ^e*Kawakita and Kobayashi (2009)*, ^f*Bonev et al. (2009)*, ^g*Drozdovskaya et al. (2021)*, ^xunpublished, * Note that the value in *Altwegg et al. (2019)* and in the abstract of *Altwegg et al. (2017a)* is wrong by a factor 2.

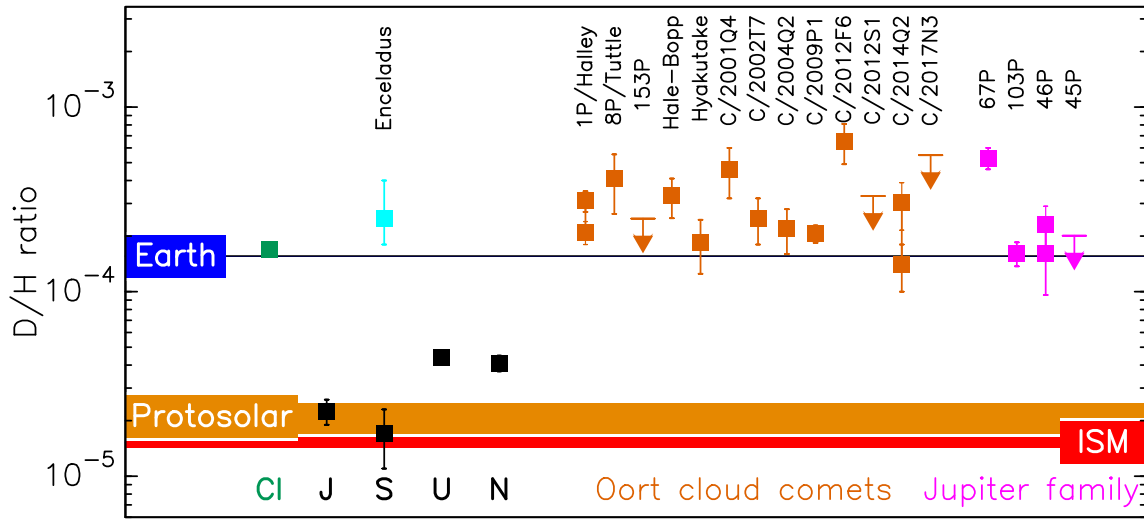


Fig. 12.— Values of the D/H in solar system objects, in H_2 for giant planets and the protosolar and ISM reservoirs or in water for Earth, CI meteorites, Enceladus and comets. Adapted from *Lis et al. (2019)*, with data from *Waite et al. (2009)*; *Hartogh et al. (2011)*; *Altwegg et al. (2019)*; *Biver et al. (2016)*; *Paganini et al. (2017)*; *Biver et al. (2022)*; *Lis et al. (2019)*, and references therein)

7.2. Abundance of ^{15}N in comets

The ratio of $^{14}\text{N}/^{15}\text{N}$ across the solar system shows significant diversity, ranging from the proto-solar value of 441 (*Marty et al. 2011*), to the terrestrial value of 272 (*Anders and Grevesse 1989*), to material very enriched in ^{15}N ($^{14}\text{N}/^{15}\text{N} \sim 50$) in insoluble organic matter in carbonaceous chondrites (*Bonal et al. 2010*). The origin of the diversity in ^{15}N across the solar system, and in comets, is still poorly understood.

The $^{14}\text{N}/^{15}\text{N}$ isotopic ratio has been measured in several comets from ground-based observations using HCN, CN, and NH_2 (*Bockelée-Morvan et al. 2015*). Initial measurements made for comet C/1995 O1 Hale-Bopp using sub-millimeter detection of HCN (*Jewitt et al. 1997*; *Ziurys et al. 1999*) derived a value of 323 ± 46 , consistent with the terrestrial value while the value measured for CN was over two times lower: 140 ± 35 (*Arpigny et al. 2003*). Subsequent measurements for a dozen comets made from high resolution spectroscopy of CN (*Jehin et al. 2009*), together with almost simultaneous measurements in comet 17P/Holmes from both HCN and CN, and a re-analysis of the Hale-Bopp data (*Bockelée-Morvan et al. 2008*), found an isotopic ratio consistent with the original CN measurement. For a sample of 20 comets of different origins and observed at different distances from the Sun *Manfroid et al. (2009)* measured an average $^{14}\text{N}/^{15}\text{N} = 147.8 \pm 5.7$. They also point out that the isotopic ratios are remarkably constant (within the uncertainties) for all comets, irrespective of their origin.

Ammonia is another major nitrogen reservoir in cometary ices but the lack of sensitivity of current instrumentation has prevented the measurement of $^{15}\text{NH}_3$ so far. The $^{14}\text{N}/^{15}\text{N}$

was only recently indirectly measured in NH_2 , assumed to be produced by the photodissociation of NH_3 . The measurement, performed both on co-added spectra of several comets and on individual comets is consistent within the uncertainties with that measured for $\text{C}^{14}\text{N}/\text{C}^{15}\text{N}$ (*Rousselot et al. 2014*; *Shinnaka et al. 2016*), as can be seen in Fig. 13. The first detection of molecular nitrogen in the coma of a comet by *Rosetta/ROSINA* and the subsequent measurement of a $^{14}\text{N}/^{15}\text{N}$ revealed a value consistent with the ratio measured for CN and NH_3 (*Altwegg et al. 2019*).

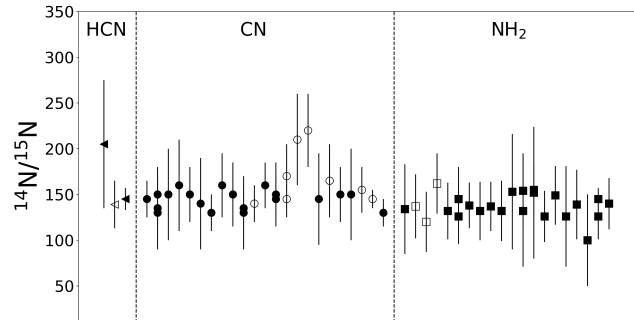


Fig. 13.— $^{14}\text{N}/^{15}\text{N}$ isotopic ratios in comets measured using HCN, CN, and NH_2 . Full symbols represent Oort Cloud comets while open symbols represent Jupiter Family comets from the Kuiper Belt. Data from *Bockelée-Morvan et al. (2008)*; *Manfroid et al. (2009)*; *Jehin et al. (2011)*; *Moulane et al. (2020)*; *Yang et al. (2018)*; *Shinnaka et al. (2016)*; *Biver et al. (2016)*; *Shinnaka et al. (2014)*; *Rousselot et al. (2015)*; *Shinnaka and Kawakita (2016)*.

The origin of the large variation of N fraction across the

solar system and the enrichment of ^{15}N in comets is still debated. The existence of two distinct nitrogen reservoirs, one atomic (likely leading to the formation of HCN and NH_3) and one molecular (N_2) has been suggested (*Hily-Blant et al.* 2017). We refer the reader to *Marty et al.* (2022) for a more in depth discussion of nitrogen fractionation in the early solar system.

7.3. Other isotopic ratios: S, O, C

Isotopic ratios of carbon, oxygen, and sulfur are available for a suite of comets (cf review by *Bockelée-Morvan et al.* 2015). Table 5 provides $^{12}\text{C}/^{13}\text{C}$ ratios measured in comets and corresponding references. Carbon isotope ratios are often consistent within uncertainties with the the terrestrial V-PDB (Vienna Pee Dee Belemnite) reference. As discussed in section 5.1, a subset of the ratios provided in Table 5 are measured in radicals (C_2 , CN) and may hence reflect a mixture of different parent species. This further complicates the identification of any species-dependent differences based on the chemical origin. Compared to the case of nitrogen (cf. section 7.2) only limited isotopic anomalies have been identified so far in comets. One notable exception is the case of H_2CO which shall be discussed later.

Table 6 shows measured $^{16}\text{O}/^{18}\text{O}$ isotopic ratios including $^{16}\text{O}/^{17}\text{O}$ in H_2O and O_2 and corresponding references. Most $^{16}\text{O}/^{18}\text{O}$ ratios have been measured in cometary water and are in most cases consistent within $1-\sigma$ with the terrestrial VSMOW reference. *Rosetta* revealed oxygen isotope ratios in a few additional species (*Altwegg et al.* 2020a). These initial results reveal a remarkable heterogeneity among the different chemical groups. Both the $^{16}\text{O}/^{17}\text{O}$ and $^{16}\text{O}/^{18}\text{O}$ ratios in H_2O and O_2 differ, on the other hand, the ratios $^{18}\text{O}/^{17}\text{O} = 4.5 \pm 1.0$ (O_2) and 4.9 ± 0.6 (H_2O) are both consistent with each other and within $1-\sigma$ of the VSMOW reference (5.3). CO_2 and CH_3OH have $^{16}\text{O}/^{18}\text{O}$ ratios comparable to H_2O , but the ratios obtained for H_2CO , SO , SO_2 , and OCS are about half while that for O_2 remains somewhere in between. Furthermore, *Schroeder et al.* (2019) analyzed oxygen isotopes over the course of the full *Rosetta* mission and revealed no variation in the $^{16}\text{O}/^{18}\text{O}$ ratio as a function of cometary activity.

Table 7 lists the measured $^{32}\text{S}/^{33}\text{S}$ and $^{32}\text{S}/^{34}\text{S}$ ratios and corresponding references. The number of observed comets is limited and the observed species are radicals such as CS or the S^+ ion originating from fragmentation of various S-bearing species inside the *Giotto* NMS (cf. section 1.4.1). Nevertheless, these results are consistent with the $^{32}\text{S}/^{34}\text{S}$ measurements of cometary parent species obtained at 67P: the $^{32}\text{S}/^{34}\text{S}$ ratios are consistent with the terrestrial reference samples within uncertainties and also the ratio $^{32}\text{S}/^{34}\text{S} = 21.6 \pm 2.7$ (*Paquette et al.* 2017) measured in cometary dust by *Rosetta*/COSIMA (COmetary Secondary Ion Mass Analyzer; *Kissel et al.* 2007). However, deviations from the terrestrial and solar system references have been observed in the $^{32}\text{S}/^{33}\text{S}$ ratios, namely the ^{33}S isotope was found to be depleted in H_2S , OCS , and CS_2 . Similar

Table 5: Carbon isotope ratios in comets

Species	Comet reference:	$^{12}\text{C}/^{13}\text{C}$ ($89^a/89^b$)
C_2	C/1975 V1 (West)	60 ± 15^c
	4 comets	93 ± 10^d
	C/2002 T7	85 ± 20^e
	C/2001 Q4	80 ± 20^e
	C/2012 S1	94 ± 33^f
CN	1P/Halley	65 ± 9^g
		89 ± 17^h
		95 ± 12^i
	C/1995 O1 (Hale-Bopp)	90 ± 15^j
		165 ± 40^k
	C/1990 K1 Levy	90 ± 10^d
	C/1989 X1 Austin	85 ± 20^d
	C/1989 Q1 O-L-R	93 ± 20^d
	122P/de Vico	90 ± 10^l
	88P/Howell	90 ± 10^m
	9P/Tempel 1	95 ± 15^n
	17P/Holmes	90 ± 20^o
	21 comets	91 ± 4^p
	103P/Hartley 2	95 ± 15^q
C/2012 F6	95 ± 25^r	
C/2015 ER ₆₁	100 ± 15^s	
21P/G.-Z.	100 ± 10^t	
HCN	C/1995 O1	111 ± 12^u
		94 ± 8^o
	17P/Holmes	114 ± 26^o
	C/2014 Q2	109 ± 14^v
	C/2012 F6	124 ± 64^v
C/2012 S1	88 ± 18^w	
CO	67P	86 ± 9^x
CO ₂	67P	84 ± 4^y
CH ₄	67P	88 ± 10^z
C ₂ H ₆	67P	93 ± 10^z
H ₂ CO	67P	40 ± 14^{aa}
CH ₃ OH	67P	91 ± 10^{aa}

^aV-PDB terrestrial (*Meija et al.* 2016) and ^bsolar (*Lodders* 2010), in comets: ^c*Lambert and Danks* (1983), ^d*Wyckoff et al.* (2000), ^e*Rousselot et al.* (2012), ^f*Shinnaka et al.* (2014), ^g*Wyckoff et al.* (1989), ^h*Jaworski and Tatum* (1991), ⁱ*Kleine et al.* (1995), ^j*Lis et al.* (1997), ^k*Arpigny et al.* (2003), ^l*Jehin et al.* (2004), ^m*Hutsemékers et al.* (2005), ⁿ*Jehin et al.* (2006), ^o*Bockelée-Morvan et al.* (2008), ^p*Manfroid et al.* (2009), ^q*Jehin et al.* (2011), ^r*Bockelée-Morvan and Biver* (2017), ^s*Yang et al.* (2018), ^t*Moulane et al.* (2020), ^u*Jewitt et al.* (1997), ^v*Biver et al.* (2016), ^w*Cordiner et al.* (2019), ^x*Rubin et al.* (2017), ^y*Hässig et al.* (2017), ^z*Müller et al.* (2022), and ^{aa}*Altwegg et al.* (2020a).

to the oxygen isotopes, the deviations are notable and in excess of what is typically found in the material in the inner solar system aside from the much less abundant presolar

Table 6: Oxygen isotope ratios in comets

Species	Comet reference:	$^{16}\text{O}/^{17}\text{O}$ (2632 ^a /2798 ^b)	$^{16}\text{O}/^{18}\text{O}$ (498.7 ^a /530 ^b)	
H ₂ O	1P/Halley		518±45 ^c 470±40 ^d	
	153P		530±60 ^{e,f}	
	C/2001 Q4		~530±60 ^f	
	C/2002 T7		~550±75 ^f 425±55 ^g	
	C/2004 Q2		508±33 ^f	
	C/2012 F6		300±150 ^h	
	C/2009 P1		523±32 ⁱ	
	67P	2347±191 ^m	445±45 ^j	
	O ₂	67P	1544±308	345±40 ^k
	CO ₂	67P		494±8 ^l
CH ₃ OH	67P		495±40 ^k	
H ₂ CO	67P		256±100 ^k	
SO	67P		239±52 ^k	
SO ₂	67P		248±88 ^k	
OCS	67P		277±70 ^k	

^aVSMOW terrestrial (Clayton 2003) and ^bsolar (McKeegan et al. 2011), in comets: ^cBalsiger et al. (1995), ^dEberhardt et al. (1995), ^eLecacheux et al. (2003), ^fBiver et al. (2007), ^gHutsemékers et al. (2008), ^hBockelée-Morvan and Biver (2017), ⁱBockelée-Morvan et al. (2012), ^jSchroeder et al. (2019), ^kAltwegg et al. (2020a), ^lHässig et al. (2017), ^mMüller et al. (2022).

grains (Hoppe et al. 2018).

Altwegg et al. (2020a) reported significant ¹⁸O and ¹³C enrichment in H₂CO compared to CH₃OH and terrestrial/solar system standards, while the ¹⁸O/¹³C ratios are in agreement. This is remarkable as both molecules were thought to originate from the same pathway, i.e., the hydrogenation of CO (Watanabe and Kouchi 2002). There are observations in the interstellar medium that reveal a similar picture, comparable carbon isotope ratios in CO and CH₃OH but significant deviations in H₂CO (Wirström et al. 2011a,b). Large isotopic fractionation has also been modeled and found in other O-bearing species in the gas phase of cold clouds (10 K) in the interstellar medium (Loison et al. 2019). Hence, despite the resemblance to the findings at 67P, the question remains to what extent these results can be related to each other.

Furthermore the difference in both the ¹⁶O/¹⁷O and ¹⁶O/¹⁸O ratios in H₂O and O₂ is important and suggests that O₂ does not directly originate from H₂O (cf. section 4.6). This favors a primordial origin of O₂ based chemistry occurring on grain surfaces (Taquet et al. 2016). The ¹⁶O/¹⁸O isotope ratio varies by up to a factor of 2 in the observed species. For the S-bearing subset, SO, SO₂, and OCS, the ³²S/³⁴S isotope ratio, however, is consistent with terrestrial and solar reference material.

Table 7: Sulfur isotope ratios in comets

Species	Comet reference:	$^{32}\text{S}/^{33}\text{S}$ (126.9 ^a /126.7 ^b)	$^{32}\text{S}/^{34}\text{S}$ (22.6 ^a /22.5 ^b)
S ⁺	1P/Halley		23±6 ^c
CS	C/1995 O1		27±3 ^d
	C/2014 Q2		24.7±3.5 ^e
	C/2012 F6		20±5 ^e
H ₂ S	C/1995 O1		16.5±3.5 ^f
	46P/Wirtanen		20.6±2.9 ^g
	67P	(10/2014)	187±9 ^h
OCS	67P	(05/2016)	132±3 ^h
	67P	(10/2014)	
	67P	(03/2016)	
CS ₂	67P	(05/2016)	165±12 ^h
	67P	(10/2014)	157±7 ^h
	67P	(05/2016)	151±8 ^h
SO	67P		23.5±2.5 ⁱ
SO ₂	67P		21.3±2.1 ⁱ

^aV-CDT terrestrial (Ding et al. 2001) and ^bsolar (Lodders 2010) and in comets: ^cAltwegg (1995), ^dJewitt et al. (1997), ^eBiver et al. (2016), ^fCrovisier et al. (2004), ^gBiver et al. (2021a), ^hCalmonte et al. (2017), ⁱAltwegg et al. (2020a). Note that the 1P/Halley value represents a mixture of species fragmenting into S (cf. section 1.4.1). Also note that Calmonte et al. (2017) analyzed 2 periods for H₂S, OCS, and CS₂, one early (10/2014) and the other late (05/2016) in the Rosetta mission.

7.4. Noble gas isotopes

The relative abundances of a suite of noble gas isotopes reported in section 4.5.4 were obtained by *Rosetta*. Argon and krypton isotope ratios seem to be in agreement with the solar and terrestrial reference material listed in table 8 within measurement uncertainties. For xenon, however, deviations from these standards were measured in 67P. In particular ¹²⁹Xe was enriched while both ¹³⁴Xe and ¹³⁶Xe were considerably depleted. Taking cometary Xe, mixing it with solar wind Xe, and taking mass-dependent isotopic fractionation into account, Marty et al. (2017) and Marty et al. (2022) estimated a contribution of 22.5±5% of cometary xenon to the terrestrial atmosphere.

7.5. Halogen isotopes

The measured isotopic ratios of ³⁵Cl/³⁷Cl and ⁷⁹Br/⁸¹Br in 67P were consistent with solar system values when taking the uncertainties into account which points to molecular cloud chemistry. The isotope ratio ³⁵Cl/³⁷Cl did not change throughout the mission (Dhooghe et al. 2021).

Table 8: Noble gas isotope ratios in comet 67P and reference material.

Species	Isotopes						Reference
Argon	$^{36}\text{Ar}/^{38}\text{Ar}$						
67P	5.4±1.4						<i>Balsiger et al. (2015)</i>
solar wind	5.470±0.003						<i>Heber et al. (2012)</i>
terr atm.	5.319±0.008						<i>Lee et al. (2006)</i>
Krypton	$^{84}\text{Kr}/^{80}\text{Kr}$	$^{84}\text{Kr}/^{82}\text{Kr}$	$^{84}\text{Kr}/^{83}\text{Kr}$	$^{84}\text{Kr}/^{86}\text{Kr}$			
67P	23±14	4.9±0.4	5.3±0.4	3.4±0.2		<i>Rubin et al. (2018)</i>	
solar	24.4	4.88	4.93	3.31		<i>Lodders (2010)</i>	
terr atm.	24.9	4.92	4.96	3.30		<i>Aregbe et al. (2001)</i>	
Xenon	$^{132}\text{Xe}/^{128}\text{Xe}$	$^{132}\text{Xe}/^{129}\text{Xe}$	$^{132}\text{Xe}/^{130}\text{Xe}$	$^{132}\text{Xe}/^{131}\text{Xe}$	$^{132}\text{Xe}/^{134}\text{Xe}$	$^{132}\text{Xe}/^{136}\text{Xe}$	
67P	13±4	0.7±0.1	5.4±0.9	1.2±0.1	4.2±0.9	8.6±3.0	<i>Marty et al. (2017)</i>
solar	11.8	0.96	6.02	1.21	2.73	3.35	<i>Lodders (2010)</i>
terr atm.	14.1	1.02	6.62	1.27	2.58	3.04	<i>Valkiers et al. (1998)</i>

7.6. Ortho-to-para and spin state ratios

Molecules that have identical nuclei having non-zero nuclear spin, especially hydrogen atoms having a spin of 1/2, can exist in different energy levels due to their total spin value I . Molecules such as water, formaldehyde or ammonia can be in two different spin states, ($I = 1$ *ortho*, or 3/2) or ($I = 0$ *para*, or 1/2), or A and E states and can be characterized by their *ortho-to-para* (OPR), or A/E abundance ratio. CH₄ can be in three different spin states ($I = 0, 1$ or 2). H₂O, the most common species where OPRs are measured, achieves a statistical equilibrium value of 3/1 for temperatures above ~ 50 K, whereas the para species is increasingly favored as the temperature decreases below 50 K. OPRs have shown variability in measured values in comets (e.g., *Faure et al. 2019*), with values for T_{spin} consistent with statistical equilibrium above 50 K in some cases, while others are sometimes clustered close to 30 K (*Bockelée-Morvan et al. 2004; Kawakita and Kobayashi 2009*, and references therein). To what extent differences in OPRs among comets relate to differences in the formation temperatures of ices in the solar nebula or sublimation and coma processes remains an open question (e.g., *Bonev et al. 2007, 2013; Faure et al. 2019; Aikawa et al. 2022; Bodewits et al. 2022*). There is some evidence that once OPRs are locked into H₂O ice upon its formation, conversion is difficult (e.g., *Miani and Tennyson 2004*), so it is possible that OPRs have remained stable since ices were incorporated into the nucleus and represent the chemical formation temperature of cometary ices (e.g., *Kawakita 2005*). However, other laboratory results suggest OPRs are not ancient but instead are reset to their high-temperature equilibrium value after sublimation, independent of formation processes (*Hama et al. 2018*).

8. PERSPECTIVES

Over the last fifteen years since Comets II was published, increasing remote sensing capabilities have greatly increased the number of comets where the volatile composition and spatial distributions in the coma have been determined. Additionally, in-situ analysis through comet

missions have allowed the study of volatile release and coma spatial distributions with unprecedented detail. The *EPOXI* flyby provided the highest spatial resolution measurements of how volatiles were released from the nucleus of 103P/Hartley 2 (*A'Hearn et al. 2011*) near perihelion, and supporting ground-based studies showed that spatial distributions in the global coma were consistent with spacecraft observations (e.g., *Dello Russo et al. 2011; Mumma et al. 2011; Bonev et al. 2013; Kawakita et al. 2013*). The two-year *Rosetta* rendezvous with 67P allowed the chemical composition of a comet to be determined with unprecedented detail and many new and more complex volatiles were detected through observations with the ROSINA mass spectrometer (e.g., *Rubin et al. 2019; Altwegg et al. 2017b*). *Rosetta* and *EPOXI* observations also revealed distinct outgassing behavior for 67P and 103P/Hartley 2.

8.1. The state of molecular line databases

Knowledge of the synthetic spectrum of a molecule or radical is essential to identify the species and compute its abundance in cometary comae. Knowing the fragmentation patterns in mass spectrometers is also necessary to evaluate the amount of the considered molecular species observed. There are still many unidentified lines in cometary spectra, especially in the high spectral resolution optical and IR spectra where the number of lines can be large. Laboratory measurements and ab-initio calculations are regularly providing new catalogs of lines, available in databases such as the JPL one (<https://spec.jpl.nasa.gov>, *Pickett et al. 1998*) or CDMS (<https://cdms.astro.uni-koeln.de/>, *Müller et al. 2005*) for rotational transitions, and HITRAN (<https://lweb.cfa.harvard.edu/HITRAN/>, *Gordon et al. 2017*) or GEISA (<https://cds-espri.ipsl.upmc.fr/etherTypo/index.php?id=950&L=1>, *Jacquinet-Husson et al. 2016*) for ro-vibrational lines. Other databases are available but there is always a need for new data to be able to search for, detect, and quantify new molecular species or radicals in cometary atmospheres. For exam-

ple, acetaldehyde was present in spectra of C/1995 O1 (Hale-Bopp) but could only be identified later when accurate frequencies were available (Crovisier *et al.* 2004). Several molecular species identified by ROSINA in the coma of 67P, such as CH₃OSH, CH₃S₂H, C₃H₇NH₂ (Altwegg *et al.* 2019, Table 4), do not yet have published spectra. Similarly, data on line frequencies and strengths are also needed to extract new species from already existing spectra such as in the case of ¹⁵NH₂ (Rousselot *et al.* 2014). There is also an on-going need for basic chemical information such as provided by the National Institute of Standards and Technology (NIST, chemistry WebBook: <https://webbook.nist.gov/chemistry>), for the fragmentation patterns of molecules in mass spectrometers.

In all cases the progress in the detection and determination of abundances of more and more complex species in cometary atmospheres, enabled by increased performance of observatories, cannot come without laboratory work and the release of new molecular data (see Poch *et al.* 2022).

8.2. Comparison to ISM and pathway for new searches

Comets are considered as possible samples of interstellar material from which the solar system formed. Molecular complexity found in comets has allowed comparison to the composition of nearby star forming regions, especially the low mass protostar IRAS 16293-2422(B) (Biver *et al.* 2015; Biver and Bockelée-Morvan 2019; Drozdovskaya *et al.* 2019) in which abundances of COMs relative to CH₃OH measured in several comets (C/2014 Q2, 46P, 67P) are of the same order of magnitude. Inner regions of solar-type protostars (e.g., Taquet *et al.* 2015) and those with strong polar jets like L1157-B1 (Lefloch *et al.* 2017) reveal a complex chemistry that likely results from a process similar to the sublimation of comet ices. The heritage of cometary ices from the ISM is also reviewed in previous chapters (Bergin *et al.* 2022; Aikawa *et al.* 2022). Such similarities in composition drives our search for new molecules in cometary comae, since many more complex species have been already detected in the ISM (McGuire 2018). This requires more and more sensitivity as abundances generally decrease with molecular complexity (e.g. number of C atoms in the molecule) (Crovisier *et al.* 2004). On the other hand, addressing the bulk abundances in cometary comae and ices is probably easier and less model dependent than in the ISM, due to the proximity of the source, optical thinness of the lines and access to in-situ observations via space missions.

8.3. Open questions and future prospects

Despite the substantial insights gained in comet composition over the years, many fundamental questions remain unanswered (Thomas *et al.* 2019). For instance, what are the processes governing outbursts and activity in general and their associated time and size scales. This includes how volatiles are distributed within the nucleus and the relation-

ship between the composition of the nucleus and measurements in the coma. Another question is how comets evolve as they are processed in the inner solar system. The stratigraphy of the outgassing layer, affected by erosion and fallback material, and the interaction of the gas with the dust cover and how this sets the dynamics of the neutral gas in the coma are also open questions. What is the interrelation between the neutral gas, dust, and plasma (e.g. the lifting and acceleration of dust by neutral gas and the formation of a diamagnetic cavity, the innermost region around an active comet devoid of solar wind particles and fields)?

Some of these questions will be addressed by future missions (Snodgrass *et al.* 2022) such as the Chinese ZengHe mission (Zhang *et al.* 2021), which will visit MBC 311P/PanSTARRS, or ESA's Comet Interceptor (CI) mission (Snodgrass and Jones 2019), which proposes to fly by a long-period comet (LPC), or, if possible, a dynamically new comet (DNC) or an interstellar object (ISO). Further mission concepts have been proposed (Thomas *et al.* 2019) and are discussed in an accompanying chapter. A high priority in the coming decades is the collection and return of a comet nucleus sample, and eventually a cryogenic sample that includes volatiles. This will allow analysis with the most advanced laboratory instrumentation on Earth, providing the next leap in our knowledge of the volatile content and structure of ices in a comet.

Despite these likely future advances, mission studies will remain rare and confined to a very few objects within a diverse population. Therefore, remote sensing techniques will remain important in studying the composition and diversity of comets as a population. Technological advances in ground and space-based facilities and instrumentation will continue to push towards improved sensitivity, efficiency, spectral coverage, and spatial resolution which increases the number and variety of comets available for both compositional and coma spatial studies. In addition to improvements to existing facilities, new telescopes including the James Webb Space Telescope (JWST; Kelley *et al.* 2016), the Vera C. Rubin Observatory (Jones *et al.* 2009; Schwamb *et al.* 2018), the Thirty Meter Telescope (Skidmore *et al.* 2015), and the European Extremely Large Telescope (ELT; Jehin *et al.* 2009; Brandl *et al.* 2008) are expected to become available in the coming years and further advance our understanding of the composition and activity of comets.

Finally, we are now starting to be able to compare the composition of solar system comets to that of comets formed around other stars. Two interstellar objects have been detected crossing through our solar system. One of them was active and its composition could be compared to that of solar system comets. The existence of comets around other stars, inferred for the first time in the late 1980s, also provides us with a way to assess the composition of comets in other planetary systems. Comparing the composition of exocomets to solar system comets remains difficult, as they are observed under different circumstances, either when they pass very close to their stars (like sungraz-

ing comets) or directly in the debris disk. Observations of interstellar comets and the study of exocomets with upcoming facilities will give us the opportunity to understand how different formation conditions influence the composition of comets and the nature of our solar system compared to its neighbors.

Acknowledgments.

MR was funded by the State of Bern and the Swiss National Science Foundation (200020_182418, 200020_207312).

REFERENCES

- A'Hearn M. F., Millis R. C., Schleicher D. O. et al. (1995) *The ensemble properties of comets: Results from narrowband photometry of 85 comets, 1976-1992.*, *Icarus*, 118, 223–270.
- Aikawa Y., Okuzumi S., and Pottippidan K. (2022) in *Comets III* (K. Meech and M. Combi, eds.), p. 2.
- Allen M., Delitsky M., Huntress W. et al. (1987) in *Exploration of Halley's Comet*, pp. 502–512, Springer.
- Altwegg K. (1995) *Sulfur in the coma of comet Halley from in situ measurements*, Habilitation thesis, University of Bern, Switzerland.
- Altwegg K., Balsiger H., Bar-Nun A. et al. (2016) *Prebiotic chemicals—amino acid and phosphorus—in the coma of comet 67P/Churyumov-Gerasimenko*, *Science advances*, 2, e1600285.
- Altwegg K., Balsiger H., Berthelier J.-J. et al. (2017a) *D₂O and HDS in the coma of 67P/Churyumov-Gerasimenko*, *Philosophical Transactions of the Royal Society A: Mathematical, Physical and Engineering Sciences*, 375, 20160253.
- Altwegg K., Balsiger H., Berthelier J.-J. et al. (2017b) *Organics in comet 67P—a first comparative analysis of mass spectra from ROSINA-DFMS, COSAC and Ptolemy*, *Monthly Notices of the Royal Astronomical Society*, 469, S130–S141.
- Altwegg K., Balsiger H., Combi M. et al. (2020a) *Molecule-dependent oxygen isotopic ratios in the coma of comet 67P/Churyumov-Gerasimenko*, *Monthly Notices of the Royal Astronomical Society*, 498, 5855–5862.
- Altwegg K., Balsiger H., and Fuselier S. A. (2019) *Cometary Chemistry and the Origin of Icy Solar System Bodies: The View After Rosetta*, *Annu. Rev. Astron. Astrophys.*, 57, 113–155.
- Altwegg K., Balsiger H., Hänni N. et al. (2020b) *Evidence of ammonium salts in comet 67P as explanation for the nitrogen depletion in cometary comae*, *Nature astronomy*, 4, 533–540.
- Anders E. and Grevesse N. (1989) *Abundances of the elements: Meteoritic and solar*, *Geochim. Cosmochim. Acta*, 53, 197–214.
- Aregbe Y., Valkiers S., Poths J. et al. (2001) *A primary isotopic gas standard for krypton with values for isotopic composition and molar mass traceable to the Système International d'Unités*, *International Journal of Mass Spectrometry*, 206, 129–136.
- Arpigny C., Jehin E., Manfroid J. et al. (2003) *Anomalous Nitrogen Isotope Ratio in Comets*, *Science*, 301, 1522–1525.
- A'Hearn M. F., Belton M. J., Delamere W. A. et al. (2011) *EPOXI at comet Hartley 2*, *Science*, 332, 1396–1400.
- Balsiger H., Altwegg K., Bar-Nun A. et al. (2015) *Detection of argon in the coma of comet 67P/Churyumov-Gerasimenko*, *Science advances*, 1, e1500377.
- Balsiger H., Altwegg K., Benson J. et al. (1987) *The ion mass spectrometer on Giotto*, *Journal of Physics E: Scientific Instruments*, 20, 759.
- Balsiger H., Altwegg K., Bochsler P. et al. (2007) *Rosina-Rosetta orbiter spectrometer for ion and neutral analysis*, *Space Science Reviews*, 128, 745–801.
- Balsiger H., Altwegg K., and Geiss J. (1995) *D/H and O-18/O-16 ratio in the hydronium ion and in neutral water from in situ ion measurements in comet Halley*, *J. Geophys. Res.*, 100, 5827–5834.
- Bergin T., Alexander C., Drozdovskaya M. et al. (2022) in *Comets III* (K. Meech and M. Combi, eds.), p. 1.
- Bernstein M. P., Dworkin J. P., Sandford S. A. et al. (2002) *Racemic amino acids from the ultraviolet photolysis of interstellar ice analogues*, *Nature*, 416, 401–403.
- Beth A., Wedlund C., Galand M. et al. (2022) in *Comets III* (K. Meech and M. Combi, eds.), p. 16.
- Bieler A., Altwegg K., Balsiger H. et al. (2015) *Abundant molecular oxygen in the coma of comet 67P/Churyumov-Gerasimenko*, *Nature*, 526, 678–681.
- Biver N. and Bockelée-Morvan D. (2019) *Complex Organic Molecules in Comets from Remote-Sensing Observations at Millimeter Wavelengths*, *ACS Earth and Space Chemistry*, 3, 1550–1555.
- Biver N., Bockelée-Morvan D., Boissier J. et al. (2021a) *Molecular composition of comet 46P/Wirtanen from millimetre-wave spectroscopy*, *Astron. Astrophys.*, 648, A49.
- Biver N., Bockelée-Morvan D., Colom P. et al. (2002) in *Cometary Science after Hale-Bopp*, pp. 5–14, Springer.
- Biver N., Bockelée-Morvan D., Colom P. et al. (2011) *Molecular investigations of comets C/2002 X5 (Kudo-Fujikawa), C/2002 VI (NEAT), and C/2006 P1 (McNaught) at small heliocentric distances*, *Astron. Astrophys.*, 528, A142.
- Biver N., Bockelée-Morvan D., Crovisier J. et al. (2002) *Chemical Composition Diversity Among 24 Comets Observed At Radio Wavelengths*, *Earth Moon and Planets*, 90, 323–333.
- Biver N., Bockelée-Morvan D., Crovisier J. et al. (1999) *Spectroscopic Monitoring of Comet C/1996 B2 (Hyakutake) with the JCMT and IRAM Radio Telescopes*, *Astron. J.*, 118, 1850–1872.
- Biver N., Bockelée-Morvan D., Crovisier J. et al. (2007) *Sub-millimetre observations of comets with Odin: 2001 2005*, *Planet. Space Sci.*, 55, 1058–1068.
- Biver N., Bockelée-Morvan D., Crovisier J. et al. (2008) in *Asteroids, Comets, Meteors 2008*, vol. 1405, p. 8149.
- Biver N., Bockelée-Morvan D., Crovisier J. et al. (2006) *Radio wavelength molecular observations of comets C/1999 T1 (McNaught-Hartley), C/2001 A2 (LINEAR), C/2000 WM₁ (LINEAR) and 153P/Ikeya-Zhang*, *Astron. Astrophys.*, 449, 1255–1270.
- Biver N., Bockelée-Morvan D., Hofstadter M. et al. (2019) *Long-term monitoring of the outgassing and composition of comet 67P/Churyumov-Gerasimenko with the Rosetta/MIRO instrument*, *Astronomy & Astrophysics*, 630, A19.
- Biver N., Bockelée-Morvan D., Lis D. C. et al. (2021b) *Molecular composition of short-period comets from millimetre-wave spectroscopy: 21P/Giacobini-Zinner, 38P/Stephan-Oterma, 41P/Tuttle-Giacobini-Kresák, and 64P/Swift-Gehrels*, *Astron. Astrophys.*, 651, A25.
- Biver N., Bockelée-Morvan D., Moreno R. et al. (2015) *Ethyl al-*

- cohol and sugar in comet C/2014 Q2 (Lovejoy), *Science Advances*, 1, 1500863.
- Biver N., Bockelée-Morvan D., Paubert G. et al. (2018) *The extraordinary composition of the blue comet C/2016 R2 (PanSTARRS)*, *Astron. Astrophys.*, 619, A127.
- Biver N., Moreno R., Bockelée-Morvan D. et al. (2022) *HDO in comet 46P/Wirtanen with ALMA: distribution profile and D/H ratio in water, in preparation.*
- Biver N., Moreno R., Bockelée-Morvan D. et al. (2016) *Isotopic ratios of H, C, N, O, and S in comets C/2012 F6 (Lemmon) and C/2014 Q2 (Lovejoy)*, *Astron. Astrophys.*, 589, A78.
- Bockelée-Morvan D. and Biver N. (2017) *The composition of cometary ices*, *Philosophical Transactions of the Royal Society of London Series A*, 375, 20160252.
- Bockelée-Morvan D., Biver N., Crovisier J. et al. (2010) in *AAS/Division for Planetary Sciences Meeting Abstracts #42*, vol. 42 of *AAS/Division for Planetary Sciences Meeting Abstracts*, p. 3.04.
- Bockelée-Morvan D., Biver N., Jehin E. et al. (2008) *Large Excess of Heavy Nitrogen in Both Hydrogen Cyanide and Cyanogen from Comet 17P/Holmes*, *Astrophys. J. Lett.*, 679, L49.
- Bockelée-Morvan D., Biver N., Moreno R. et al. (2001) *Outgassing Behavior and Composition of Comet C/1999 S4 (LINEAR) During Its Disruption*, *Science*, 292, 1339–1343.
- Bockelée-Morvan D., Biver N., Swinyard B. et al. (2012) *Herschel measurements of the D/H and $^{16}\text{O}/^{18}\text{O}$ ratios in water in the Oort-cloud comet C/2009 P1 (Garradd)*, *Astron. Astrophys.*, 544, L15.
- Bockelée-Morvan D., Calmonte U., Charnley S. et al. (2015) *Cometary isotopic measurements*, *Space science reviews*, 197, 47–83.
- Bockelée-Morvan D., Colom P., Crovisier J. et al. (1991) *Microwave detection of hydrogen sulphide and methanol in comet Austin (1989c1)*, *Nature*, 350, 318–320.
- Bockelée-Morvan D. and Crovisier J. (1985) *Possible parents for the cometary CN radical - Photochemistry and excitation conditions*, *Astron. Astrophys.*, 151, 90–100.
- Bockelée-Morvan D., Crovisier J., Mumma M. J. et al. (2004) in *Comets II* (M. C. Festou, H. U. Keller, and H. A. Weaver, eds.), p. 391, University of Arizona Press.
- Bockelée-Morvan D., Debout V., Erard S. et al. (2015) *First observations of H₂O and CO₂ vapor in comet 67P/Churyumov-Gerasimenko made by VIRTIS onboard Rosetta*, *Astron. Astrophys.*, 583, A6.
- Bockelée-Morvan D., Hartogh P., Crovisier J. et al. (2010) *A study of the distant activity of comet C/2006 W3 (Christensen) with Herschel and ground-based radio telescopes*, *Astron. Astrophys.*, 518, L149.
- Bockelée-Morvan D., Lis D. C., Wink J. E. et al. (2000) *New molecules found in comet C/1995 O1 (Hale-Bopp). Investigating the link between cometary and interstellar material*, *Astron. Astrophys.*, 353, 1101–1114.
- Bodewits D., Bonev B., Cordiner M. et al. (2022) in *Comets III* (K. Meech and M. Combi, eds.), p. 13.
- Bodewits D., Farnham T. L., A'Hearn M. F. et al. (2014) *The Evolving Activity of the Dynamically Young Comet C/2009 P1 (Garradd)*, *Astrophys. J.*, 786, 48.
- Bodewits D., Lara L. M., A'Hearn M. F. et al. (2016) *Changes in the physical environment of the inner coma of 67P/Churyumov-Gerasimenko with decreasing heliocentric distance*, *The astronomical journal*, 152, 130.
- Boissier J., Bockelée-Morvan D., Biver N. et al. (2007) *Interferometric imaging of the sulfur-bearing molecules H₂S, SO, and CS in comet C/1995 O1 (Hale-Bopp)*, *Astron. Astrophys.*, 475, 1131–1144.
- Bonal L., Huss G. R., Krot A. N. et al. (2010) *Highly ^{15}N -enriched chondritic clasts in the CB/CH-like meteorite Isheyevo*, *Geochim. Cosmochim. Acta*, 74, 6590–6609.
- Bonev B. P., Mumma M. J., DiSanti M. A. et al. (2006) *A comprehensive study of infrared OH prompt emission in two comets. i. observations and effective-g-factors*, *The Astrophysical Journal*, 653, 774–787.
- Bonev B. P., Mumma M. J., Gibb E. L. et al. (2009) *Comet C/2004 Q2 (Machholz): Parent Volatiles, a Search for Deuterated Methane, and Constraint on the CH₄ Spin Temperature*, *Astrophys. J.*, 699, 1563–1572.
- Bonev B. P., Mumma M. J., Villanueva G. L. et al. (2007) *A Search for Variation in the H₂O Ortho-Para Ratio and Rotational Temperature in the Inner Coma of Comet C/2004 Q2 (Machholz)*, *Astrophys. J. Lett.*, 661, L97–L100.
- Bonev B. P., Villanueva G. L., DiSanti M. A. et al. (2017) *Beyond 3 au from the Sun: The Hypervolatiles CH₄, C₂H₆, and CO in the Distant Comet C/2006 W3 (Christensen)*, *Astron. J.*, 153, 241.
- Bonev B. P., Villanueva G. L., Paganini L. et al. (2013) *Evidence for two modes of water release in Comet 103P/Hartley 2: Distributions of column density, rotational temperature, and ortho-para ratio*, *Icarus*, 222, 740–751.
- Boogert A. A., Gerakines P. A., and Whittet D. C. (2015) *Observations of the icy universe, Annual Review of Astronomy and Astrophysics*, 53, 541–581.
- Brandl B. R., Lenzen R., Pantin E. et al. (2008) in *Ground-based and Airborne Instrumentation for Astronomy II* (I. S. McLean and M. M. Casali, eds.), vol. 7014 of *Society of Photo-Optical Instrumentation Engineers (SPIE) Conference Series*, p. 70141N.
- Brooke T. Y., Tokunaga A. T., Weaver H. A. et al. (1996) *Detection of acetylene in the infrared spectrum of comet Hyakutake*, *Nature*, 383, 606–608.
- Burton A. S., Stern J. C., Elsila J. E. et al. (2012) *Understanding prebiotic chemistry through the analysis of extraterrestrial amino acids and nucleobases in meteorites*, *Chemical Society Reviews*, 41, 5459–5472.
- Calmonte U., Altwegg K., Balsiger H. et al. (2016) *Sulphur-bearing species in the coma of comet 67P/Churyumov-Gerasimenko*, *Mon. Not. R. Astron. Soc.*, 462, S253–S273.
- Calmonte U., Altwegg K., Balsiger H. et al. (2017) *Sulphur isotope mass-independent fractionation observed in comet 67P/Churyumov-Gerasimenko by Rosetta/ROSINA*, *Monthly Notices of the Royal Astronomical Society*, 469, S787–S803.
- Capria M. T., Capaccioni F., Filacchione G. et al. (2017) *How pristine is the interior of the comet 67P/Churyumov-Gerasimenko?*, *Monthly Notices of the Royal Astronomical Society*, 469, S685–S694.
- Carter M., Lazareff B., Maier D. et al. (2012) *The EMIR multi-band mm-wave receiver for the IRAM 30-m telescope*, *Astron. Astrophys.*, 538, A89.
- Clayton R. N. (2003) *Oxygen isotopes in the solar system*, *Solar System History from Isotopic Signatures of Volatile Elements*, pp. 19–32.
- Cochran A. L., Barker E. S., and Gray C. L. (2012) *Thirty years of cometary spectroscopy from McDonald Observatory*, *Icarus*, 218, 144–168.
- Cochran A. L., Cochran W. D., and Barker E. S. (2000) *N₂⁺ and*

- CO^+ in Comets 122P/1995 SI (deVico) and C/1995 O1 (Hale-Bopp), *Icarus*, 146, 583–593.
- Cochran A. L. and McKay A. J. (2018) Strong CO^+ and N_2^+ Emission in Comet C/2016 R2 (Pan-STARRS), *Astrophys. J. Lett.*, 854, L10.
- Cochran A. L. and Schleicher D. G. (1993) Observational Constraints on the Lifetime of Cometary H_2O , *Icarus*, 105, 235–253.
- Collings M. P., Anderson M. A., Chen R. et al. (2004) A laboratory survey of the thermal desorption of astrophysically relevant molecules, *Monthly Notices of the Royal Astronomical Society*, 354, 1133–1140.
- Colom P., Crovisier J., Bockelee-Morvan D. et al. (1992) Formaldehyde in comets. I - Microwave observations of P/Brorsen-Metcalf (1989 X), Austin (1990 V) and Levy (1990 XX), *Astron. Astrophys.*, 264, 270–281.
- Combi M., Shou Y., Fougere N. et al. (2020) The surface distributions of the production of the major volatile species, H_2O , CO_2 , CO and O_2 , from the nucleus of comet 67P/Churyumov-Gerasimenko throughout the Rosetta Mission as measured by the ROSINA double focusing mass spectrometer, *Icarus*, 335, 113421.
- Combi M. R. and Fink U. (1997) A Critical Study of Molecular Photodissociation and CHON Grain Sources for Cometary C_2 , *Astrophys. J.*, 484, 879–890.
- Combi M. R., Mäkinen J. T. T., Bertaux J. L. et al. (2013) Water production rate of Comet C/2009 P1 (Garradd) throughout the 2011-2012 apparition: Evidence for an icy grain halo, *Icarus*, 225, 740–748.
- Combi M. R., Mäkinen T. T., Bertaux J. L. et al. (2019) A survey of water production in 61 comets from SOHO/SWAN observations of hydrogen Lyman-alpha: Twenty-one years 1996-2016, *Icarus*, 317, 610–620.
- Cordiner M. A., Boissier J., Charnley S. B. et al. (2017) ALMA Mapping of Rapid Gas and Dust Variations in Comet C/2012 S1 (ISON): New Insights into the Origin of Cometary HNC, *Astrophys. J.*, 838, 147.
- Cordiner M. A. and Charnley S. B. (2021) Neutral-neutral synthesis of organic molecules in cometary comae, *Mon. Not. R. Astron. Soc.*, 504, 5401–5408.
- Cordiner M. A., Milam S. N., Biver N. et al. (2020) Unusually high CO abundance of the first active interstellar comet, *Nature Astronomy*, 4, 861–866.
- Cordiner M. A., Palmer M. Y., de Val-Borro M. et al. (2019) ALMA Autocorrelation Spectroscopy of Comets: The $\text{HCN}/\text{H}^{13}\text{CN}$ Ratio in C/2012 S1 (ISON), *Astrophys. J. Lett.*, 870, L26.
- Cordiner M. A. and Qi C. (2018) in *Science with a Next Generation Very Large Array* (E. Murphy, ed.), vol. 517 of *Astronomical Society of the Pacific Conference Series*, p. 73.
- Cordiner M. A., Remijan A. J., Boissier J. et al. (2014) Mapping the Release of Volatiles in the Inner Comae of Comets C/2012 F6 (Lemmon) and C/2012 S1 (ISON) Using the Atacama Large Millimeter/Submillimeter Array, *The Astrophysical Journal*, 792, L2.
- Cremonese G., Huebner W. F., Rauer H. et al. (2002) Neutral sodium tails in comets, *Advances in Space Research*, 29, 1187–1197.
- Crovisier J. (1997) Infrared Observations Of Volatile Molecules In Comet Hale-Bopp, *Earth Moon and Planets*, 79, 125–143.
- Crovisier J., Biver N., Bockelee-Morvan D. et al. (1995) Carbon monoxide outgassing from Comet P/Schwassmann-Wachmann 1, *Icarus*, 115, 213–216.
- Crovisier J., Bockelee-Morvan D., Colom P. et al. (2004) The composition of ices in comet C/1995 O1 (Hale-Bopp) from radio spectroscopy-further results and upper limits on undetected species, *Astronomy & Astrophysics*, 418, 1141–1157.
- Crovisier J., Colom P., Biver N. et al. (2013) Observations of the 18-cm oh lines of comet 103p/hartley 2 at nançay in support to the epoxi and herschel missions, *Icarus*, 222, 679–683, stardust/EPOXI.
- De Keyser J., Dhooghe F., Altwegg K. et al. (2017) Evidence for distributed gas sources of hydrogen halides in the coma of comet 67P/Churyumov-Gerasimenko, *Monthly Notices of the Royal Astronomical Society*, 469, S695–S711.
- De Sanctis M. C., Capaccioni F., Ciarniello M. et al. (2015) The diurnal cycle of water ice on comet 67P/Churyumov-Gerasimenko, *Nature*, 525, 500–503.
- de Val-Borro M., Bockelee-Morvan D., Jehin E. et al. (2014) Herschel observations of gas and dust in comet C/2006 W3 (Christensen) at 5 AU from the Sun, *Astron. Astrophys.*, 564, A124.
- Decock A., Jehin E., Hutsemékers D. et al. (2013) Forbidden oxygen lines in comets at various heliocentric distances, *Astron. Astrophys.*, 555, A34.
- Dello Russo N., DiSanti M. A., Mumma M. J. et al. (1998) Carbonyl Sulfide in Comets C/1996 B2 (Hyakutake) and C/1995 O1 (Hale-Bopp): Evidence for an Extended Source in Hale-Bopp, *Icarus*, 135, 377–388.
- Dello Russo N., Kawakita H., Vervack R. J. et al. (2016a) Emerging trends and a comet taxonomy based on the volatile chemistry measured in thirty comets with high-resolution infrared spectroscopy between 1997 and 2013, *Icarus*, 278, 301–332.
- Dello Russo N., Mumma M. J., DiSanti M. A. et al. (2000) Water Production and Release in Comet C/1995 O1 Hale-Bopp, *Icarus*, 143, 324–337.
- Dello Russo N., Vervack R. J. J., Lisse C. M. et al. (2011) The Volatile Composition and Activity of Comet 103P/Hartley 2 During the EPOXI Closest Approach, *Astrophys. J. Lett.*, 734, L8.
- Dello Russo N., Vervack R. J. J., Weaver H. A. et al. (2009) The Parent Volatile Composition of 6p/d'Arrest and a Chemical Comparison of Jupiter-Family Comets Measured at Infrared Wavelengths, *Astrophys. J.*, 703, 187–197.
- Dello Russo N., Vervack R. J., Kawakita H. et al. (2022) Volatile abundances, extended coma sources, and nucleus ice associations in bright comet C/2014 Q2 (Lovejoy), *Planetary Science Journal*, 3, 46.
- Dello Russo N., Vervack R. J., Kawakita H. et al. (2016b) The compositional evolution of C/2012 S1 (ISON) from ground-based high-resolution infrared spectroscopy as part of a worldwide observing campaign, *Icarus*, 266, 152–172.
- Dello Russo N., Vervack R. J., Weaver H. A. et al. (2007) Compositional homogeneity in the fragmented comet 73P/Schwassmann-Wachmann 3, *Nature*, 448, 172–175.
- Dhooghe F., De Keyser J., Altwegg K. et al. (2017) Halogens as tracers of protosolar nebula material in comet 67P/Churyumov-Gerasimenko, *Monthly Notices of the Royal Astronomical Society*, 472, 1336–1345.
- Dhooghe F., De Keyser J., Hänni N. et al. (2021) Chlorine-bearing species and the $^{37}\text{Cl}/^{35}\text{Cl}$ isotope ratio in the coma of comet 67P/Churyumov-Gerasimenko, *Mon. Not. R. Astron. Soc.*, 508, 1020–1032.
- Ding T., Valkiers S., Kipphardt H. et al. (2001) Calibrated sulfur isotope abundance ratios of three IAEA sulfur isotope refer-

- ence materials and V-CDT with a reassessment of the atomic weight of sulfur, *Geochimica et Cosmochimica Acta*, 65, 2433–2437.
- DiSanti M. A., Bonev B. P., Gibb E. L. et al. (2016) *En Route to Destruction: The Evolution in Composition of Ices in Comet D/2012 S1 (ISON) between 1.2 and 0.34 AU from the Sun as Revealed at Infrared Wavelengths*, *Astrophys. J.*, 820, 34.
- DiSanti M. A., Bonev B. P., Villanueva G. L. et al. (2013) *Highly Depleted Ethane and Mildly Depleted Methanol in Comet 21P/Giacobini-Zinner: Application of a New Empirical ν_2 -band Model for CH₃OH near 50 K*, *Astrophys. J.*, 763, 1.
- DiSanti M. A., Dello Russo N., Magee-Sauer K. et al. (2002) in *Asteroids, Comets, and Meteors: ACM 2002* (B. Warmbein, ed.), vol. 500 of *ESA Special Publication*, pp. 571–574.
- Dorman G., Pierce D. M., and Cochran A. L. (2013) *The Spatial Distribution of C₂, C₃, and NH in Comet 2P/Encke*, *Astrophys. J.*, 778, 140.
- Drozdovskaya M. N., Schroeder I. I. R. H. G., Rubin M. et al. (2021) *Prestellar grain-surface origins of deuterated methanol in comet 67P/Churyumov-Gerasimenko*, *Mon. Not. R. Astron. Soc.*, 500, 4901–4920.
- Drozdovskaya M. N., van Dishoeck E. F., Rubin M. et al. (2019) *Ingredients for solar-like systems: protostar IRAS 16293-2422 B versus comet 67P/Churyumov-Gerasimenko*, *Mon. Not. R. Astron. Soc.*, 490, 50–79.
- Dulieu F., Minissale M., and Bockelée-Morvan D. (2017) *Production of O₂ through dismutation of H₂O₂ during water ice desorption: a key to understanding comet O₂ abundances*, *Astronomy & Astrophysics*, 597, A56.
- Eberhardt P. (1999) *Comet Halley's gas composition and extended sources: Results from the neutral mass spectrometer on Giotto, Composition and Origin of Cometary Materials*, pp. 45–52.
- Eberhardt P., Dolder U., Schulte W. et al. (1987) in *Exploration of Halley's Comet*, pp. 435–437, Springer.
- Eberhardt P., Meier R., Krankowsky D. et al. (1994) *Methanol and hydrogen sulfide in comet P/Halley*, *Astronomy and Astrophysics*, 288, 315–329.
- Eberhardt P., Reber M., Krankowsky D. et al. (1995) *The D/H and $^{18}\text{O}/^{16}\text{O}$ ratios in water from comet P/Halley*, *Astron. Astrophys.*, 302, 301.
- El-Maarry M. R., Thomas N., Giacomini L. et al. (2015) *Regional surface morphology of comet 67P/Churyumov-Gerasimenko from Rosetta/OSIRIS images*, *Astronomy & Astrophysics*, 583, A26.
- Elsila J. E., Glavin D. P., and Dworkin J. P. (2009) *Cometary glycine detected in samples returned by Stardust*, *Meteoritics & planetary science*, 44, 1323–1330.
- Faggi S., Villanueva G. L., Mumma M. J. et al. (2016) *Detailed Analysis of Near-IR Water (H₂O) Emission in Comet C/2014 Q2 (Lovejoy) with the GIANO/TNG Spectrograph*, *The Astrophysical Journal*, 830, 157.
- Faure A., Hily-Blant P., Rist C. et al. (2019) *The ortho-to-para ratio of water in interstellar clouds*, *Mon. Not. R. Astron. Soc.*, 487, 3392–3403.
- Fayolle E. C., Öberg K. I., Jørgensen J. K. et al. (2017) *Protostellar and cometary detections of organohalogens*, *Nature Astronomy*, 1, 703–708.
- Feaga L., A'Hearn M., Sunshine J. et al. (2007) *Asymmetries in the distribution of H₂O and CO₂ in the inner coma of Comet 9P/Tempel 1 as observed by Deep Impact*, *Icarus*, 191, 134–145.
- Feaga L. M., A'Hearn M. F., Farnham T. L. et al. (2014) *Uncor-*
- related Volatile Behavior during the 2011 Apparition of Comet C/2009 P1 Garradd*, *Astron. J.*, 147, 24.
- Feldman P. D., A'Hearn M. F., Bertaux J.-L. et al. (2015) *Measurements of the near-nucleus coma of comet 67P/Churyumov-Gerasimenko with the Alice far-ultraviolet spectrograph on Rosetta*, *Astron. Astrophys.*, 583, A8.
- Feldman P. D., Cochran A. L., and Combi M. R. (2004) in *Comets II* (M. C. Festou, H. U. Keller, and H. A. Weaver, eds.), p. 425, University of Arizona Press.
- Festou M. and Feldman P. D. (1981a) *The forbidden oxygen lines in comets*, *Astron. Astrophys.*, 103, 154–159.
- Festou M. and Feldman P. D. (1981b) *The forbidden oxygen lines in comets*, *Astron. Astrophys.*, 103, 154–159.
- Fink U. (2009) *A taxonomic survey of comet composition 1985-2004 using CCD spectroscopy*, *Icarus*, 201, 311–334.
- Fink U., Combi M. R., and Disanti M. A. (1991) *Comet P/Halley: Spatial Distributions and Scale Lengths for C 2, CN, NH 2, and H 2O*, *Astrophys. J.*, 383, 356.
- Fink U., Doose L., Rinaldi G. et al. (2016) *Investigation into the disparate origin of co2 and h2o outgassing for comet 67/p*, *Icarus*, 277, 78–97.
- Fray N., Bénilan Y., Biver N. et al. (2006) *Heliocentric evolution of the degradation of polyoxymethylene: Application to the origin of the formaldehyde (H₂CO) extended source in Comet C/1995 O1 (Hale-Bopp)*, *Icarus*, 184, 239–254.
- Fray N., Bénilan Y., Cottin H. et al. (2005) *The origin of the CN radical in comets: A review from observations and models*, *Planet. Space Sci.*, 53, 1243–1262.
- Fray N. and Schmitt B. (2009) *Sublimation of ices of astrophysical interest: A bibliographic review*, *Planetary and Space Science*, 57, 2053–2080.
- Fulle M., Leblanc F., Harrison R. A. et al. (2007) *Discovery of the Atomic Iron Tail of Comet MCNaught Using the Heliospheric Imager on STEREO*, *Astrophys. J. Lett.*, 661, L93–L96.
- Gasc S., Altwegg K., Balsiger H. et al. (2017) *Change of outgassing pattern of 67P/Churyumov-Gerasimenko during the March 2016 equinox as seen by ROSINA*, *Monthly Notices of the Royal Astronomical Society*, 469, S108–S117.
- Geiss J. (1988) in *Exploration of Halley's Comet*, pp. 859–866, Springer.
- Gibb E. L., Mumma M. J., Dello Russo N. et al. (2003) *Methane in Oort cloud comets*, *Icarus*, 165, 391–406.
- Glassmeier K.-H., Boehnhardt H., Koschny D. et al. (2007) *The Rosetta mission: flying towards the origin of the solar system*, *Space Science Reviews*, 128, 1–21.
- Goesmann F., Rosenbauer H., Roll R. et al. (2007) *COSAC, the cometary sampling and composition experiment on Philae*, *Space Science Reviews*, 128, 257–280.
- Gordon I. E., Rothman L. S., Hill C. et al. (2017) *The HITRAN2016 molecular spectroscopic database*, *J. Quant. Spec. Radiat. Transf.*, 203, 3–69.
- Guilbert-Lepoutre A., Rosenberg E. D., Prialnik D. et al. (2016) *Modelling the evolution of a comet subsurface: Implications for 67P/Churyumov-Gerasimenko*, *Monthly Notices of the Royal Astronomical Society*, 462, S146–S155.
- Häberli R. M., Gombosi T. I., De Zeeuw D. L. et al. (1997) *Modeling of cometary x-rays caused by solar wind minor ions*, *Science*, 276, 939–942.
- Hadraoui K., Cottin H., Ivanovski S. et al. (2019) *Distributed glycine in comet 67P/Churyumov-Gerasimenko*, *Astronomy & Astrophysics*, 630, A32.
- Hama T., Kouchi A., and Watanabe N. (2018) *The Ortho-to-para*

- Ratio of Water Molecules Desorbed from Ice Made from Para-water Monomers at 11 K*, *Astrophys. J. Lett.*, 857, L13.
- Hänni N., Altwegg K., Balsiger H. et al. (2021) *Cyanogen, cyanoacetylene, and acetonitrile in comet 67P and their relation to the cyano radical*, *Astron. Astrophys.*, 647, A22.
- Hänni N., Altwegg K., Pestoni B. et al. (2020) *First in situ detection of the CN radical in comets and evidence for a distributed source*, *Mon. Not. R. Astron. Soc.*, 498, 2239–2248.
- Hansen K. C., Altwegg K., Berthelier J.-J. et al. (2016) *Evolution of water production of 67p/churyumov–gerasimenko: an empirical model and a multi-instrument study*, *Monthly Notices of the Royal Astronomical Society*, 462, S491–S506.
- Hartogh P., Lis D. C., Bockelée-Morvan D. et al. (2011) *Ocean-like water in the Jupiter-family comet 103P/Hartley 2*, *Nature*, 478, 218–220.
- Haser L. (1957) *Distribution d'intensité dans la tête d'une comète*, *Bulletin de la Societe Royale des Sciences de Liege*, 43, 740–750.
- Hässig M., Altwegg K., Balsiger H. et al. (2015) *Time variability and heterogeneity in the coma of 67P/Churyumov-Gerasimenko*, *Science*, 347.
- Hässig M., Altwegg K., Balsiger H. et al. (2017) *Isotopic composition of CO₂ in the coma of 67P/Churyumov-Gerasimenko measured with ROSINA/DFMS*, *Astronomy & Astrophysics*, 605, A50.
- Heber V. S., Baur H., Bochsler P. et al. (2012) *Isotopic mass fractionation of solar wind: Evidence from fast and slow solar wind collected by the Genesis mission*, *The Astrophysical Journal*, 759, 121.
- Helbert J., Rauer H., Boice D. C. et al. (2005) *The chemistry of C₂ and C₃ in the coma of Comet C/1995 O1 (Hale-Bopp) at heliocentric distances $r_h \geq 2.9$ AU*, *Astron. Astrophys.*, 442, 1107–1120.
- Heritier K., Altwegg K., Berthelier J.-J. et al. (2018) *On the origin of molecular oxygen in cometary comae*, *Nature communications*, 9, 1–4.
- Hily-Blant P., Magalhaes V., Kastner J. et al. (2017) *Direct evidence of multiple reservoirs of volatile nitrogen in a protosolar nebula analogue*, *Astron. Astrophys.*, 603, L6.
- Hölscher A. (2015) *Formation of C3 and C2 in Cometary Comae*, Ph.D. thesis, -.
- Hoppe P., Rubin M., and Altwegg K. (2018) *Presolar isotopic signatures in meteorites and comets: new insights from the Rosetta mission to comet 67P/Churyumov–Gerasimenko*, *Space science reviews*, 214, 1–28.
- Huebner W. F. and Mukherjee J. (2015) *Photoionization and photodissociation rates in solar and blackbody radiation fields*, *Planet. Space Sci.*, 106, 11–45.
- Hutsemékers D., Manfroid J., Jehin E. et al. (2005) *Isotopic abundances of carbon and nitrogen in Jupiter-family and Oort Cloud comets*, *Astronomy & Astrophysics*, 440, L21–L24.
- Hutsemékers D., Manfroid J., Jehin E. et al. (2008) *The ¹⁶OH/¹⁸OH and OD/OH isotope ratios in comet C/2002 T7 (LINEAR)*, *Astron. Astrophys.*, 490, L31–L34.
- Irvine W. M., Senay M., Lovell A. J. et al. (2000) *NOTE: Detection of Nitrogen Sulfide in Comet Hale-Bopp*, *Icarus*, 143, 412–414.
- Ivanova O. V., Luk'yanyk I. V., Kiselev N. N. et al. (2016) *Photometric and spectroscopic analysis of Comet 29P/Schwassmann-Wachmann 1 activity*, *Planet. Space Sci.*, 121, 10–17.
- Jackson W. M. (1976) *Laboratory observations of the photochemistry of parent molecules: a review.*, vol. 393, pp. 679–704, Cambridge University Press.
- Jackson W. M., Butterworth P. S., and Ballard D. (1986) *The Origin of CS in Comet IRAS-Araki-Alcock 1983d*, *Astrophys. J.*, 304, 515.
- Jacquinet-Husson N., Armante R., Scott N. A. et al. (2016) *The 2015 edition of the GEISA spectroscopic database*, *Journal of Molecular Spectroscopy*, 327, 31–72.
- Jaworski W. A. and Tatum J. B. (1991) *Analysis of the Swings Effect and Greenstein Effect in Comet P/Halley*, *Astrophys. J.*, 377, 306.
- Jehin E., Hutsemekers D., Manfroid J. et al. (2011) *A Multi-wavelength study with the ESO VLT of comet 103P/Hartley 2 at the time of the EPOXI encounter*, *EPSC Abstracts*, p. 1463.
- Jehin E., Manfroid J., Cochran A. L. et al. (2004) *The Anomalous ¹⁴N/¹⁵N Ratio in Comets 122P/1995 S1 (de Vico) and 153P/2002 CI (Ikeya-Zhang)*, *Astrophys. J. Lett.*, 613, L161–L164.
- Jehin E., Manfroid J., Hutsemékers D. et al. (2009) *Isotopic Ratios in Comets: Status and Perspectives*, *Earth Moon and Planets*, 105, 167–180.
- Jehin E., Manfroid J., Hutsemékers D. et al. (2006) *Deep Impact: High-Resolution Optical Spectroscopy with the ESO VLT and the Keck I Telescope*, *Astrophys. J. Lett.*, 641, L145–L148.
- Jensen S. S., Jørgensen J. K., Furuya K. et al. (2021) *Modeling chemistry during star formation: water deuteration in dynamic star-forming regions*, *Astron. Astrophys.*, 649, A66.
- Jewitt D., Garland C. A., and Aussen H. (2008) *Deep Search for Carbon Monoxide in Cometary Precursors Using Millimeter Wave Spectroscopy*, *Astron. J.*, 135, 400–407.
- Jewitt D., Matthews H. E., Owen T. et al. (1997) *The 12C/13C, 14N/15N and 32S/ 34S Isotope Ratios in Comet Hale-Bopp (C/1995 O1)*, *Science*, 278, 90–93.
- Jones R., Chesley S., Connolly A. et al. (2009) *Solar System science with LSST, Earth, Moon, and Planets*, 105, 101–105.
- Kawakita H. (2005) *Comets as fossils of our solar system*, *Astronomical Herald*, 98, 757–763.
- Kawakita H. and Kobayashi H. (2009) *Formation Conditions of Icy Materials in Comet C/2004 Q2 (Machholz). II. Diagnostics Using Nuclear Spin Temperatures and Deuterium-to-Hydrogen Ratios in Cometary Molecules*, *Astrophys. J.*, 693, 388–396.
- Kawakita H., Kobayashi H., Dello Russo N. et al. (2013) *Parent volatiles in Comet 103P/Hartley 2 observed by Keck II with NIRSPEC during the 2010 apparition*, *Icarus*, 222, 723–733.
- Kawakita H., Watanabe J.-i., Ando H. et al. (2001) *The Spin Temperature of NH₃ in Comet C/1999S4 (LINEAR)*, *Science*, 294, 1089–1091.
- Keller H. U., Mottola S., Davidsson B. et al. (2015a) *Inso-lation, erosion, and morphology of comet 67P/Churyumov-Gerasimenko*, *Astronomy & Astrophysics*, 583, A34.
- Keller H. U., Mottola S., Hviid S. F. et al. (2017) *Seasonal mass transfer on the nucleus of comet 67P/Churyumov–Gerasimenko*, *Monthly Notices of the Royal Astronomical Society*, 469, S357–S371.
- Keller H. U., Mottola S., Skorov Y. et al. (2015b) *The changing rotation period of comet 67P/Churyumov-Gerasimenko controlled by its activity*, *Astronomy & Astrophysics*, 579, L5.
- Kelley M. S., Woodward C. E., Bodewits D. et al. (2016) *Cometary science with the James Webb space telescope*, *Publications of the Astronomical Society of the Pacific*, 128, 018009.
- Kissel J., Altwegg K., Clark B. et al. (2007) *COSIMA–high resolution time-of-flight secondary ion mass spectrometer for the*

- analysis of cometary dust particles onboard Rosetta, *Space science reviews*, 128, 823–867.
- Klein B., Hochgürtel S., Krämer I. et al. (2012) *High-resolution wide-band fast Fourier transform spectrometers*, *Astron. Astrophys.*, 542, L3.
- Kleine M., Wyckoff S., Wehinger P. A. et al. (1995) *The Carbon Isotope Abundance Ratio in Comet Halley*, *Astrophys. J.*, 439, 1021.
- Korsun P. P., Rousselot P., Kulyk I. V. et al. (2014) *Distant activity of Comet C/2002 VQ94 (LINEAR): Optical spectrophotometric monitoring between 8.4 and 16.8 au from the Sun*, *Icarus*, 232, 88–96.
- Kouchi A. and Yamamoto T. (1995) *Cosmoglaciology: Evolution of ice in interstellar space and the early solar system, Progress in crystal growth and characterization of materials*, 30, 83–107.
- Kramer T., Läuter M., Hviid S. et al. (2019) *Comet 67P/Churyumov-Gerasimenko rotation changes derived from sublimation-induced torques*, *Astronomy & Astrophysics*, 630, A3.
- Krankowsky D., Lämmerzahl P., Herrwerth I. et al. (1986) *In situ gas and ion measurements at comet Halley*, *Nature*, 321, 326–329.
- Lambert D. L. and Danks A. C. (1983) *High-resolution spectra of C2 Swan bands from comet West 1976 VI*, *Astrophys. J.*, 268, 428–446.
- Lamy P. L. and Perrin J.-M. (1988) *Optical properties of organic grains: Implications for interplanetary and cometary dust*, *Icarus*, 76, 100–109.
- Langland-Shula L. E. and Smith G. H. (2011) *Comet classification with new methods for gas and dust spectroscopy*, *Icarus*, 213, 280–322.
- Laufer D., Bar-Nun A., and Ninio Greenberg A. (2017) *Trapping mechanism of O₂ in water ice as first measured by Rosetta spacecraft*, *Monthly Notices of the Royal Astronomical Society*, 469, S818–S823.
- Läuter M., Kramer T., Rubin M. et al. (2020) *The gas production of 14 species from comet 67P/Churyumov-Gerasimenko based on DFMS/COPS data from 2014 to 2016*, *Monthly Notices of the Royal Astronomical Society*, 498, 3995–4004.
- Le Roy L., Altwegg K., Balsiger H. et al. (2015) *Inventory of the volatiles on comet 67P/Churyumov-Gerasimenko from Rosetta/ROSINA*, *Astronomy & Astrophysics*, 583, A1.
- Lecacheux A., Biver N., Crovisier J. et al. (2003) *Observations of the 557 GHz water line in comets with the Odin satellite*, *Astron. Astrophys.*, 402, L55–L58.
- Lee J.-Y., Marti K., Severinghaus J. P. et al. (2006) *A redetermination of the isotopic abundances of atmospheric Ar*, *Geochimica et Cosmochimica Acta*, 70, 4507–4512.
- Lefloch B., Ceccarelli C., Codella C. et al. (2017) *L1157-B1, a factory of complex organic molecules in a solar-type star-forming region*, *Mon. Not. R. Astron. Soc.*, 469, L73–L77.
- Lippi M., Villanueva G. L., Mumma M. J. et al. (2021) *Investigation of the Origins of Comets as Revealed through Infrared High-resolution Spectroscopy I. Molecular Abundances*, *Astron. J.*, 162, 74.
- Lis D. C., Bockelée-Morvan D., Boissier J. et al. (2008) *Hydrogen Isocyanide in Comet 73P/Schwassmann-Wachmann (Fragment B)*, *Astrophys. J.*, 675, 931–936.
- Lis D. C., Bockelée-Morvan D., Güsten R. et al. (2019) *Terrestrial deuterium-to-hydrogen ratio in water in hyperactive comets*, *Astron. Astrophys.*, 625, L5.
- Lis D. C., Keene J., Young K. et al. (1997) *Spectroscopic Observations of Comet C/1996 B2 (Hyakutake) with the Caltech Submillimeter Observatory*, *Icarus*, 130, 355–372.
- Lisse C., Bauer J., Cruikshank D. et al. (2020) *Spitzer’s Solar System studies of comets, centaurs and Kuiper belt objects*, *Nature Astronomy*, 4, 930–939.
- Lodders K. (2010) in *Principles and perspectives in cosmochemistry*, pp. 379–417, Springer.
- Loison J.-C., Wakelam V., Gratier P. et al. (2019) *Oxygen fractionation in dense molecular clouds*, *Monthly Notices of the Royal Astronomical Society*, 485, 5777–5789.
- Luspay-Kuti A., Hässig M., Fuselier S. A. et al. (2015) *Composition-dependent outgassing of comet 67P/Churyumov-Gerasimenko from ROSINA/DFMS. Implications for nucleus heterogeneity?*, *Astron. Astrophys.*, 583, A4.
- Luspay-Kuti A., Mousis O., Lunine J. I. et al. (2018) *Origin of molecular oxygen in comets: current knowledge and perspectives*, *Space science reviews*, 214, 1–24.
- Luspay-Kuti A., Mousis O., Pauzat F. et al. (2022) *Dual storage and release of molecular oxygen in comet 67p/churyumov-gerasimenko*, *Nature Astronomy*, pp. 1–7.
- Magee-Sauer K., Mumma M. J., DiSanti M. A. et al. (2002) *Hydrogen cyanide in comet C/1996 B2 Hyakutake*, *Journal of Geophysical Research (Planets)*, 107, 5096.
- Manfroid J., Hutsemékers D., and Jehin E. (2021) *Iron and nickel atoms in cometary atmospheres even far from the Sun*, *Nature*, 593, 372–374.
- Manfroid J., Jehin E., Hutsemékers D. et al. (2009) *The CN isotopic ratios in comets*, *Astron. Astrophys.*, 503, 613–624.
- Maquet L. (2015) *The recent dynamical history of comet 67P/Churyumov-Gerasimenko*, *Astronomy & Astrophysics*, 579, A78.
- Marschall R., Davidsson B., Rubin M. et al. (2022) in *Comets III* (K. Meech and M. Combi, eds.), p. 14.
- Marty B., Altwegg K., Balsiger H. et al. (2017) *Xenon isotopes in 67P/Churyumov-Gerasimenko show that comets contributed to Earth’s atmosphere*, *Science*, 356, 1069–1072.
- Marty B., Bermingham K., Nittler L. et al. (2022) in *Comets III* (K. Meech and M. Combi, eds.), p. 21.
- Marty B., Chaussidon M., Wiens R. C. et al. (2011) *A ¹⁵N-Poor Isotopic Composition for the Solar System As Shown by Genesis Solar Wind Samples*, *Science*, 332, 1533.
- McGuire B. A. (2018) *2018 Census of Interstellar, Circumstellar, Extragalactic, Protoplanetary Disk, and Exoplanetary Molecules*, *Astrophys. J. Suppl.*, 239, 17.
- McKay A., Cochran A., Dello Russo N. et al. (2014) in *Asteroids, Comets, Meteors 2014* (K. Muinonen, A. Penttilä, M. Granvik, A. Virkki, G. Fedorets, O. Wilkman, and T. Kohout, eds.), p. 344.
- McKay A. J., Chanover N. J., Morgenthaler J. P. et al. (2013) *Observations of the forbidden oxygen lines in DIXI target Comet 103P/Hartley*, *Icarus*, 222, 684–690.
- McKay A. J., DiSanti M. A., Kelley M. S. P. et al. (2019) *The Peculiar Volatile Composition of CO-dominated Comet C/2016 R2 (PanSTARRS)*, *Astron. J.*, 158, 128.
- McKeegan K., Kallio A., Heber V. et al. (2011) *The oxygen isotopic composition of the Sun inferred from captured solar wind*, *Science*, 332, 1528–1532.
- Meier R. and A’Hearn M. F. (1997) *Atomic Sulfur in Cometary Comae Based on UV Spectra of the S I Triplet near 1814 Å*, *Icarus*, 125, 164–194.
- Meier R., Eberhardt P., Krankowsky D. et al. (1993) *The extended*

- formaldehyde source in comet P/Halley, *Astronomy and Astrophysics*, 277, 677.
- Meier R., Owen T. C., Jewitt D. C. et al. (1998) *Deuterium in Comet C/1995 O1 (Hale-Bopp): Detection of DCN*, *Science*, 279, 1707.
- Meija J., Coplen T. B., Berglund M. et al. (2016) *Atomic weights of the elements 2013 (IUPAC Technical Report)*, *Pure and Applied Chemistry*, 88, 265–291.
- Miani A. and Tennyson J. (2004) *Can ortho-para transitions for water be observed?*, *J. Chem. Phys.*, 120, 2732–2739.
- Mommert M., Hora J. L., Trilling D. E. et al. (2020) *Recurrent Cometary Activity in Near-Earth Object (3552) Don Quixote*, *Planetary Science Journal*, 1, 12.
- Morghenthaler J. P., Harris W. M., Scherb F. et al. (2001) *Large-Aperture [O I] 6300 Å Photometry of Comet Hale-Bopp: Implications for the Photochemistry of OH*, *Astrophys. J.*, 563, 451–461.
- Moulane Y., Jehin E., Rousselot P. et al. (2020) *Photometry and high-resolution spectroscopy of comet 21P/Giacobini-Zinner during its 2018 apparition*, *Astronomy & Astrophysics*, 640, A54.
- Mouis O., Aguichine A., Bouquet A. et al. (2021) *Cold Traps of Hypervolatiles in the Protosolar Nebula at the Origin of the Peculiar Composition of Comet C/2016 R2 (PanSTARRS)*, *Planetary Science Journal*, 2, 72.
- Mouis O., Lunine J., Luspay-Kuti A. et al. (2016a) *A protosolar nebula origin for the ices agglomerated by comet 67P/Churyumov-Gerasimenko*, *The Astrophysical Journal Letters*, 819, L33.
- Mouis O., Ronnet T., Brugger B. et al. (2016b) *Origin of molecular oxygen in comet 67P/Churyumov-Gerasimenko*, *The Astrophysical Journal Letters*, 823, L41.
- Muñoz Caro G. M., Meierhenrich U. J., Schutte W. A. et al. (2002) *Amino acids from ultraviolet irradiation of interstellar ice analogues*, *Nature*, 416, 403–406.
- Müller D. R., Altwegg K., Berthelier J. J. et al. (2022) *High D/H ratios in water and alkanes in comet 67P/Churyumov-Gerasimenko measured with Rosetta/ROSINA DFMS*, *Astron. Astrophys.*, 662, A69.
- Müller H. S. P., Schlöder F., Stutzki J. et al. (2005) *The Cologne Database for Molecular Spectroscopy, CDMS: a useful tool for astronomers and spectroscopists*, *Journal of Molecular Structure*, 742, 215–227.
- Mumma M. J., Bonev B. P., Villanueva G. L. et al. (2011) *Temporal and Spatial Aspects of Gas Release During the 2010 Apparition of Comet 103P/Hartley 2*, *Astrophys. J. Lett.*, 734, L7.
- Mumma M. J. and Charnley S. B. (2011) *The chemical composition of comets—emerging taxonomies and natal heritage*, *Annual Review of Astronomy and Astrophysics*, 49, 471–524.
- Mumma M. J., DiSanti M. A., Dello Russo N. et al. (2000) *Detection of CO and Ethane in Comet 21P/Giacobini-Zinner: Evidence for Variable Chemistry in the Outer Solar Nebula*, *Astrophys. J. Lett.*, 531, L155–L159.
- Mumma M. J., DiSanti M. A., Russo N. D. et al. (1996) *Detection of abundant ethane and methane, along with carbon monoxide and water, in comet c/1996 b2 hyakutake: Evidence for interstellar origin*, *Science*, 272, 1310–1314.
- Neufeld D. A., Stauffer J. R., Bergin E. A. et al. (2000) *Submillimeter Wave Astronomy Satellite Observations of Water Vapor toward Comet C/1999 H1 (Lee)*, *Astrophys. J. Lett.*, 539, L151–L154.
- Newall H. F. (1910) *On the spectrum of the daylight comet 1910a*, *Mon. Not. R. Astron. Soc.*, 70, 459.
- Oliversen R. J., Doane N., Scherb F. et al. (2002) *Measurements of [C I] Emission from Comet Hale-Bopp*, *Astrophys. J.*, 581, 770–775.
- Ootsubo T., Kawakita H., Hamada S. et al. (2012) *AKARI Near-infrared Spectroscopic Survey for CO₂ in 18 Comets*, *Astrophys. J.*, 752, 15.
- Opitom C., Hutsemékers D., Jehin E. et al. (2019a) *High resolution optical spectroscopy of the N₂-rich comet C/2016 R2 (PanSTARRS)*, *Astron. Astrophys.*, 624, A64.
- Opitom C., Jehin E., Manfroid J. et al. (2015) *TRAPPIST photometry and imaging monitoring of comet C/2013 R1 (Lovejoy): Implications for the origin of daughter species*, *Astron. Astrophys.*, 584, A121.
- Opitom C., Snodgrass C., Fitzsimmons A. et al. (2017) *Ground-based monitoring of comet 67P/Churyumov-Gerasimenko gas activity throughout the Rosetta mission*, *Mon. Not. R. Astron. Soc.*, 469, S222–S229.
- Opitom C., Yang B., Selman F. et al. (2019b) *First observations of an outbursting comet with the MUSE integral-field spectrograph*, *Astron. Astrophys.*, 628, A128.
- Oró J. (1961) *Comets and the formation of biochemical compounds on the primitive Earth*, *Nature*, 190, 389–390.
- Osip D. J., A’Hearn M., and Raugh A. C. (2010) *Lowell Observatory Cometary Database - Production Rates*, *NASA Planetary Data System*, EAR-C-PHOT-5-RDR-LOWELL-COMET-DB-PR-V1.0.
- Paganini L. and Mumma M. J. (2016) *A Solar-pumped Fluorescence Model for Line-by-line Emission Intensities in the B-X, A-X, and X-X Band Systems of ¹²C¹⁴N*, *Astrophys. J. Suppl.*, 226, 3.
- Paganini L., Mumma M. J., Gibb E. L. et al. (2017) *Ground-based Detection of Deuterated Water in Comet C/2014 Q2 (Lovejoy) at IR Wavelengths*, *Astrophys. J. Lett.*, 836, L25.
- Paganini L., Mumma M. J., Villanueva G. L. et al. (2012) *The Chemical Composition of CO-rich Comet C/2009 P1 (Garrard) at R_h = 2.4 and 2.0 AU before Perihelion*, *Astrophys. J. Lett.*, 748, L13.
- Paquette J., Hornung K., Stenzel O. J. et al. (2017) *The ³⁴S/³²S isotopic ratio measured in the dust of comet 67P/Churyumov-Gerasimenko by Rosetta/COSIMA*, *Monthly Notices of the Royal Astronomical Society*, 469, S230–S237.
- Pickett H. M., Poynter R. L., Cohen E. A. et al. (1998) *Submillimeter, millimeter and microwave spectral line catalog*, *J. Quant. Spec. Radiat. Transf.*, 60, 883–890.
- Poch O., Gundlach B., Pommerol A. et al. (2022) in *Comets III* (K. Meech and M. Combi, eds.), p. 8.
- Poch O., Istiqomah I., Quirico E. et al. (2020) *Ammonium salts are a reservoir of nitrogen on a cometary nucleus and possibly on some asteroids*, *Science*, 367.
- Preston G. W. (1967) *The spectrum of Ikeya-Seki (1965f)*, *Astrophys. J.*, 147, 718–742.
- Qi C., Hogerheijde M. R., Jewitt D. et al. (2015) *Peculiar Near-nucleus Outgassing of Comet 17P/Holmes during its 2007 Outburst*, *Astrophys. J.*, 799, 110.
- Quirico E., Moroz L., Schmitt B. et al. (2016) *Refractory and semi-volatile organics at the surface of comet 67P/Churyumov-Gerasimenko: Insights from the VIRTIS/Rosetta imaging spectrometer*, *Icarus*, 272, 32–47.
- Radeva Y. L., Mumma M. J., Villanueva G. L. et al. (2013) *High-resolution infrared spectroscopic measurements of Comet 2P/Encke: Unusual organic composition and low rotational*

- temperatures, *Icarus*, 223, 298–307.
- Raghuram S., Bhardwaj A., Hutsemékers D. et al. (2021) *A physico-chemical model to study the ion density distribution in the inner coma of comet C/2016 R2 (Pan-STARRS)*, *Mon. Not. R. Astron. Soc.*, 501, 4035–4052.
- Rawlings J., Wilson T. G., and Williams D. A. (2019) *A gas-phase primordial origin of O₂ in comet 67P/Churyumov-Gerasimenko*, *Monthly Notices of the Royal Astronomical Society*, 486, 10–20.
- Raymond J. C., Downs C., Knight M. M. et al. (2018) *Comet C/2011 W3 (Lovejoy) between 2 and 10 Solar Radii: Physical Parameters of the Comet and the Corona*, *Astrophys. J.*, 858, 19.
- Reinhard R. (1986) *The Giotto encounter with comet Halley*, *Nature*, 321, 313–318.
- Reylé C. and Boice D. C. (2003) *An S₂ Fluorescence Model for Interpreting High-Resolution Cometary Spectra. I. Model Description and Initial Results*, *Astrophys. J.*, 587, 464–471.
- Rivilla V., Drozdovskaya M. N., Altwegg K. et al. (2020) *ALMA and ROSINA detections of phosphorus-bearing molecules: the interstellar thread between star-forming regions and comets*, *Monthly Notices of the Royal Astronomical Society*, 492, 1180–1198.
- Rodgers S. D. and Charnley S. B. (2001) *On the origin of HNC in Comet Lee*, *Mon. Not. R. Astron. Soc.*, 323, 84–92.
- Roesler F. L., Scherb F., Magee K. et al. (1985) *High spectral resolution line profiles and images of comet Halley*, *Advances in Space Research*, 5, 279–282.
- Roth N. X., Gibb E. L., Bonev B. P. et al. (2020) *Probing the Evolutionary History of Comets: An Investigation of the Hypervolatiles CO, CH₄, and C₂H₆ in the Jupiter-family Comet 21P/Giacobini-Zinner*, *Astron. J.*, 159, 42.
- Roth N. X., Gibb E. L., Bonev B. P. et al. (2018) *A Tale of “Two” Comets: The Primary Volatile Composition of Comet 2P/Encke Across Apparitions and Implications for Cometary Science*, *Astron. J.*, 156, 251.
- Roth N. X., Milam S. N., Cordiner M. A. et al. (2021) *Leveraging the ALMA Atacama Compact Array for Cometary Science: An Interferometric Survey of Comet C/2015 ER61 (PanSTARRS) and Evidence for a Distributed Source of Carbon Monosulfide*, *arXiv e-prints*, arXiv:2104.03210.
- Rousselot P., Decock A., Korsun P. P. et al. (2015) *High-resolution spectra of comet C/2013 R1 (Lovejoy)*, *Astron. Astrophys.*, 580, A3.
- Rousselot P., Jehin E., Manfroid J. et al. (2012) *The ¹²C₂¹²C¹³C isotopic ratio in comets C/2001 Q4 (NEAT) and C/2002 T7 (LINEAR)*, *Astron. Astrophys.*, 545, A24.
- Rousselot P., Piralí O., Jehin E. et al. (2014) *Toward a Unique Nitrogen Isotopic Ratio in Cometary Ices*, *Astrophys. J. Lett.*, 780, L17.
- Rubin M., Altwegg K., Balsiger H. et al. (2015a) *Molecular nitrogen in comet 67P/Churyumov-Gerasimenko indicates a low formation temperature*, *Science*, 348, 232–235.
- Rubin M., Altwegg K., Balsiger H. et al. (2018) *Krypton isotopes and noble gas abundances in the coma of comet 67P/Churyumov-Gerasimenko*, *Science advances*, 4, eaar6297.
- Rubin M., Altwegg K., Balsiger H. et al. (2017) *Evidence for depletion of heavy silicon isotopes at comet 67P/Churyumov-Gerasimenko*, *Astron. Astrophys.*, 601, A123.
- Rubin M., Altwegg K., Balsiger H. et al. (2019) *Elemental and molecular abundances in comet 67P/Churyumov-Gerasimenko*, *Monthly Notices of the Royal Astronomical Society*, 489, 594–607.
- Rubin M., Altwegg K., Berthelier J.-J. et al. (2022) *Refractory elements in the gas phase for comet 67P/Churyumov-Gerasimenko. Possible release of atomic Na, Si, and Fe from nanograins*, *Astron. Astrophys.*, 658, A87.
- Rubin M., Altwegg K., van Dishoeck E. F. et al. (2015b) *Molecular oxygen in Oort cloud comet 1P/Halley*, *The Astrophysical Journal Letters*, 815, L11.
- Rubin M., Engrand C., Snodgrass C. et al. (2020) *On the origin and evolution of the material in 67P/Churyumov-Gerasimenko*, *Space science reviews*, 216, 1–43.
- Rubin M., Hansen K. C., Gombosi T. I. et al. (2009) *Ion composition and chemistry in the coma of Comet 1P/Halley—A comparison between Giotto’s Ion Mass Spectrometer and our ion-chemical network*, *Icarus*, 199, 505–519.
- Saki M., Gibb E. L., Bonev B. P. et al. (2020) *Carbonyl Sulfide (OCS): Detections in Comets C/2002 T7 (LINEAR), C/2015 ER61 (PanSTARRS), and 21P/Giacobini-Zinner and Stringent Upper Limits in 46P/Wirtanen*, *Astron. J.*, 160, 184.
- Schleicher D. G. (2008) *The Extremely Anomalous Molecular Abundances of Comet 96P/Machholz 1 from Narrowband Photometry*, *Astron. J.*, 136, 2204–2213.
- Schleicher D. G. and Bair A. N. (2011) *The Composition of the Interior of Comet 73P/Schwassmann-Wachmann 3: Results from Narrowband Photometry of Multiple Components*, *Astron. J.*, 141, 177.
- Schleicher D. G. and Farnham T. L. (2004) in *Comets II* (M. C. Festou, H. U. Keller, and H. A. Weaver, eds.), p. 449, University of Arizona Press.
- Schroeder I. R., Altwegg K., Balsiger H. et al. (2019) *¹⁶O/¹⁸O ratio in water in the coma of comet 67P/Churyumov-Gerasimenko measured with the Rosetta/ROSINA double-focusing mass spectrometer*, *Astronomy & Astrophysics*, 630, A29.
- Schuhmann M., Altwegg K., Balsiger H. et al. (2019) *Aliphatic and aromatic hydrocarbons in comet 67P/Churyumov-Gerasimenko seen by ROSINA*, *Astron. Astrophys.*, 630, A31.
- Schultz D., Li G. S. H., Scherb F. et al. (1992) *Comet Austin (1989c1) O(¹D) and H₂O production rates*, *Icarus*, 96, 190–197.
- Schulz R., Hilchenbach M., Langevin Y. et al. (2015) *Comet 67P/Churyumov-Gerasimenko sheds dust coat accumulated over the past four years*, *Nature*, 518, 216–218.
- Schwamb M. E., Jones R. L., Chesley S. R. et al. (2018) *Large Synoptic Survey Telescope Solar System Science Roadmap*, *arXiv e-prints*, arXiv:1802.01783.
- Schwartz A. W. (2006) *Phosphorus in prebiotic chemistry*, *Phil. Trans. R. Soc. B*, 361, 1743–1749.
- Seager S., Bains W., and Petkowski J. (2016) *Toward a list of molecules as potential biosignature gases for the search for life on exoplanets and applications to terrestrial biochemistry*, *Astrobiology*, 16, 465–485.
- Senay M. C. and Jewitt D. (1994) *Coma formation driven by carbon monoxide release from comet Schwassmann-Wachmann 1*, *Nature*, 371, 229–231.
- Shinnaka Y. and Kawakita H. (2016) *Nitrogen Isotopic Ratio of Cometary Ammonia from High-resolution Optical Spectroscopic Observations of C/2014 Q2 (Lovejoy)*, *Astron. J.*, 152, 145.
- Shinnaka Y., Kawakita H., Jehin E. et al. (2016) *Nitrogen isotopic ratios of NH₂ in comets: implication for ¹⁵N-fractionation in cometary ammonia*, *Monthly Notices of the Royal Astronomical Society*, 459, 423–431.

- cal Society*, 462, S195–S209.
- Shinnaka Y., Kawakita H., Kobayashi H. et al. (2012) *Ortho-to-para Abundance Ratio of Water Ion in Comet C/2001 Q4 (NEAT): Implication for Ortho-to-para Abundance Ratio of Water*, *Astrophys. J.*, 749, 101.
- Shinnaka Y., Kawakita H., Kondo S. et al. (2017) *Near-infrared Spectroscopic Observations of Comet C/2013 R1 (Lovejoy) by WINERED: CN Red-system Band Emission*, *Astron. J.*, 154, 45.
- Shinnaka Y., Kawakita H., Nagashima M. et al. (2014) in *AAS/Division for Planetary Sciences Meeting Abstracts #46*, vol. 46 of *AAS/Division for Planetary Sciences Meeting Abstracts*, p. 209.14.
- Sierks H., Barbieri C., Lamy P. L. et al. (2015) *On the nucleus structure and activity of comet 67P/Churyumov-Gerasimenko*, *Science*, 347.
- Skidmore W., TMT International Science Development Teams, and Science Advisory Committee T. (2015) *Thirty Meter Telescope Detailed Science Case: 2015*, *Research in Astronomy and Astrophysics*, 15, 1945.
- Slaughter C. D. (1969) *The Emission Spectrum of Comet Ikeya-Seki 1965-f at Perihelion Passage*, *Astron. J.*, 74, 929.
- Snodgrass C., Feaga L., Jones G. et al. (2022) in *Comets III* (K. Meech and M. Combi, eds.), p. 6.
- Snodgrass C. and Jones G. H. (2019) *The European Space Agency’s comet interceptor lies in wait*, *Nature communications*, 10, 1–4.
- Stern S., Slater D., Festou M. et al. (2000) *The discovery of argon in comet C/1995 O1 (Hale-Bopp)*, *The Astrophysical Journal Letters*, 544, L169.
- Stief L. J. (1972) *Origin of C₃ in Comets*, *Nature*, 237, 29.
- Swings P. (1965) *Cometary Spectra*, *QJRAS*, 6, 28.
- Swings P. and Haser L. (1956) *Atlas of representative cometary spectra*, Louvain, Impr. Ceuterick.
- Taquet V., Furuya K., Walsh C. et al. (2016) *A primordial origin for molecular oxygen in comets: a chemical kinetics study of the formation and survival of O₂ ice from clouds to discs*, *Monthly Notices of the Royal Astronomical Society*, 462, S99–S115.
- Taquet V., López-Sepulcre A., Ceccarelli C. et al. (2015) *Constraining the Abundances of Complex Organics in the Inner Regions of Solar-type Protostars*, *Astrophys. J.*, 804, 81.
- Taquet V., Peters P. S., Kahane C. et al. (2013) *Water ice deuteration: a tracer of the chemical history of protostars*, *Astron. Astrophys.*, 550, A127.
- Thomas N., Ulamec S., Kührt E. et al. (2019) *Towards new comet missions*, *Space science reviews*, 215, 1–35.
- Valkiers S., Aregbe Y., Taylor P. et al. (1998) *A primary xenon isotopic gas standard with SI traceable values for isotopic composition and molar mass*, *International journal of mass spectrometry and ion processes*, 173, 55–63.
- Vaughan C. M., Pierce D. M., and Cochran A. L. (2017) *Jet Morphology and Coma Analysis of Comet 103P/Hartley 2*, *Astron. J.*, 154, 219.
- Villanueva G., Mumma M., DiSanti M. et al. (2012) *A multi-instrument study of comet c/2009 p1 (garradd) at 2.1au (pre-perihelion) from the sun*, *Icarus*, 220, 291–295.
- Villanueva G. L., Smith M. D., Protopapa S. et al. (2018) *Planetary Spectrum Generator: An accurate online radiative transfer suite for atmospheres, comets, small bodies and exoplanets*, *J. Quant. Spec. Radiat. Transf.*, 217, 86–104.
- Waite J. H. J., Lewis W. S., Magee B. A. et al. (2009) *Liquid water on Enceladus from observations of ammonia and ⁴⁰Ar in the plume*, *Nature*, 460, 487–490.
- Watanabe N. and Kouchi A. (2002) *Efficient formation of formaldehyde and methanol by the addition of hydrogen atoms to CO in H₂O-CO ice at 10 K*, *The Astrophysical Journal Letters*, 571, L173.
- Weaver H. A., Chin G., Bockelée-Morvan D. et al. (1999) *An Infrared Investigation of Volatiles in Comet 21P/Giacobini-Zinner*, *Icarus*, 142, 482–497.
- Weaver H. A., Mumma M. J., and Larson H. P. (1987) *Infrared investigation of water in Comet P/Halley*, *Astron. Astrophys.*, 187, 411–418.
- Wedlund C. S., Kallio E., Alho M. et al. (2016) *The atmosphere of comet 67p/churyumov-gerasimenko diagnosed by charge-exchanged solar wind alpha particles*, *Astronomy & Astrophysics*, 587, A154.
- Weiler M. (2012) *The chemistry of C₃ and C₂ in cometary comae. I. Current models revisited*, *Astron. Astrophys.*, 538, A149.
- Wierzchos K., Womack M., and Sarid G. (2017) *Carbon Monoxide in the Distantly Active Centaur (60558) 174P/Echeclus at 6 au*, *Astron. J.*, 153, 230.
- Wirström E., Geppert W. D., Hjalmarsen Å. et al. (2011a) *Observational tests of interstellar methanol formation*, *Astronomy & Astrophysics*, 533, A24.
- Wirström E., Geppert W. D., Persson C. M. et al. (2011b) in *The Molecular Universe, Posters from the proceedings of the 280th Symposium of the International Astronomical Union held in Toledo, Spain, May 30-June 3, 2011*, # 384, vol. 280.
- Womack M., Sarid G., and Wierzchos K. (2017) *CO in Distantly Active Comets*, *PASP*, 129, 031001.
- Wright I., Barber S., Morgan G. et al. (2007) *Ptolemy—an instrument to measure stable isotopic ratios of key volatiles on a cometary nucleus*, *Space Science Reviews*, 128, 363–381.
- Wurz P., Rubin M., Altwegg K. et al. (2015) *Solar wind sputtering of dust on the surface of 67p/churyumov-gerasimenko*, *Astronomy & Astrophysics*, 583, A22.
- Wyckoff S., Kleine M., Peterson B. A. et al. (2000) *Carbon Isotope Abundances in Comets*, *Astrophys. J.*, 535, 991–999.
- Wyckoff S., Lindholm E., Wehinger P. A. et al. (1989) *The ¹²C/¹³C Abundance Ratio in Comet Halley*, *Astrophys. J.*, 339, 488.
- Wyckoff S. and Theobald J. (1989) *Molecular ions in comets*, *Advances in Space Research*, 9, 157–161.
- Yang B., Hutsemékers D., Shinnaka Y. et al. (2018) *Isotopic ratios in outbursting comet C/2015 ER61*, *Astronomy & Astrophysics*, 609, L4.
- Yang B., Jewitt D., Zhao Y. et al. (2021) *Discovery of Carbon Monoxide in Distant Comet C/2017 K2 (PANSTARRS)*, *Astrophys. J. Lett.*, 914, L17.
- Yao Y. and Giapis K. P. (2017) *Dynamic molecular oxygen production in cometary comae*, *Nature communications*, 8, 1–8.
- Zhang T., Xu K., and Ding X. (2021) *China’s ambitions and challenges for asteroid–comet exploration*, *Nature Astronomy*, pp. 1–2.
- Ziurys L. M., Savage C., Brewster M. A. et al. (1999) *Cyanide Chemistry in Comet Hale-Bopp (C/1995 O1)*, *Astrophys. J. Lett.*, 527, L67–L71.